FIBER-OPTIC INSTRUMENTATION
FINAL REPORT
TECHNICAL REPORT A001:
CRYOGENIC SENSOR MODEL DESCRIPTION

NASA CR-
160448

CONTRACT NO. NAS9-15454

25 NOVEMBER 1979

PREPARED FOR

NASA/JSC
HOUSTON, TEXAS

TRW
DEFENSE AND SPACE SYSTEMS GROUP

FIBER-OPTIC INSTRUMENTATION
FINAL REPORT
TECHNICAL REPORT A001:
CRYOGENIC SENSOR MODEL DESCRIPTION

CONTRACT NO. NAS9-15454

25 NOVEMBER 1979

PREPARED FOR

NASA/JSC
HOUSTON, TEXAS

PREPARED BY:

M.M. SHARMA ____________
PROJECT MANAGER,
FIBER-OPTICS INSTRUMENTATION

APPROVED BY:

P. STAUDHAMMER Peter Staudhammer
MANAGER,
ADVANCED TECHNOLOGY LABORATORY

TRW
DEFENSE AND SPACE SYSTEMS GROUP

CONTENTS

CONTENTS (Continued)

ILLUSTRATIONS

ILLUSTRATIONS (Continued)

TABLES

1. INTRODUCTION AND SUMMARY

The development of fiber-optic systems and of passive optical sensors appropriate for measurement of conditions in cryogenic liquid propellant tanks in accordance with requirements of NASA/JSC Contract NAS9-15454 entitled "Fiber-Optic Instrumentation" has been completed. The purpose of this report is to outline the overall program undertaken by TRW, to document the research, development, and testing performed under this contract, and to identify recommendations for subsequent development programs.

1.1 BACKGROUND AND PURPOSE OF STUDY

United States space programs use launch-vehicle engines requiring highly explosive propellants. For example, the Space Shuttle, the current launch vehicle of the space program, incorporates main engines that are fueled by liquid oxygen and liquid hydrogen - both of which are extremely explosive liquids. Every effort is made to reduce the potential hazards associated with handling and using these propellants. However, a large portion of the cost of using hazardous materials such as LOX is reflected in the necessary safety measures that must be implemented. Therefore, a small improvement in increasing safety results in a large reduction in cost.

In the case of the Space-Shuttle LH_2 and LOX tanks, the instrumentation that performs liquid-level gauging principally consists of point electrical sensors, which are a proven and common method for gauging tanks. Capacitance gauges are also employed, particularly when a continuous reading is required. Although from the engineering standpoint point sensors and capacitance guages can be made to work well in a LOX or LH_2 tank, from the safety standpoint, both techniques are undesirable because the power and signal leads to the sensor must penetrate the tank, thus presenting the possibility cf an electrical anomaly capable of causing an explosion.

When a hazardous condition exists, such as that of point sensors within LOX tanks, the risk has been controlled by very careful quality control and extensive testing to reduce the possibility of a failure to an extremely low number. The result of this special handling and additional record keeping has been imposition of a significant increase in the overall cost of inexpensive hardware. Obviously, if current-carrying wires can be eliminated from tanks that contain material susceptible to ignition, then both increased safety and lower costs are realized.

Recent advances in fiber-optic technology are leading to wider application of such systems, including use in passive optical-sensing devices. The purpose of present TRW programs in fiber-optic instrumentation has been to develop applicable technology to replace current-carrying signal and power wires of point-sensors, temperature sensors, and presure sensors with fiber-optic systems.

1.2 SUMMARY OF STUDY AND RECOMMENDED SENSOR CONCEPTS

In the Concept Study, general sensor concepts initially were examined to classify types of sensors which would be applicable to the cryogenic regime. Subsequently, specific sensor concepts were studied in detail, in some cases with special laboratory measurements made to facilitate choosing of the best concepts. Library and literature surveys were conducted, and concentrated efforts to generate new and novel concepts and/or adaptations of older ones were undertaken.

Final TRW recommendations were based on a scoring procedure devised to reflect the contractual objective of "developing the technology to replace current-carrying signal and power wires of point sensors, temperature, and pressure sensors with fiber optics." Simplicity and reliability were particularly emphasized in this evaluation because sensor operation will occur within the stringent, cryogenic temperature range. Sensor concepts recommended by TRW were the following:

- Liquid-Level Point Sensor — Bare-fiber concept used as "ON-OFF" level indication.
- Temperature Sensor — Semiconductor bandedge absorption shift used with instrumentation concept of matching bandedge location with a temperature-cycled reference.
- Pressure Sensor — Movement of a pressure-sensitive deflecting membrane sensed via an optical readout device.

Criteria used in evaluating the sensor concepts considered and details of rankings assigned to the various sensors considered are identified in Section 2, selected sensors are described in Section 3, and test results for the completed sensor system are given in Section 4. Principles of fiber-optic systems are summarized in a previous report (Ref. 1).

1.3 OBJECTIVES

Objectives of this investigation were directed towards achieving the following critical goals:

- Assessment and determination of technology requirements for developing a demonstration model to evaluate feasibility of practical cryogenic liquid-level, pressure, and temperature sensors.
- Construction of a demonstration model to measure characteristics of the selected sensor and to develop test procedures.
- Development of an appropriate electronic subsystem to operate the sensors.

These goals were achieved by review of prevailing concepts, matching requirements with available concepts to develop evaluation criteria, and design, development, and test of selected concepts, with modification of basic approaches where necessary.

Because the main consideration during this effort was to design practical gauging systems suitable for use in actual systems, the complete experimental system is housed in a suitable cabinet. The electronic display panel consists of pressure and temperature readouts, indicating lights for the liquid-level sensors, and calibration controls. The liquid nitrogen Dewar is installed on the side of the cabinet.

1.4 CONCLUSIONS

Completed study efforts have led to the following conclusions:

- Available fiber-optic sensor technology pertains to sensing of high-refractive-index liquids at or near room temperature.
- Concepts developed in this program indicate definite feasibility of applying fiber-optic instrumentation to practical usage.
- Development of the demonstration model has identified several areas of beneficial modifications to the present practical designs.

- Because the sensing systems based upon measuring the amplitude of the return signals are prone to drift, the systems that depend upon measurement of "time" as the readout, such as the present temperature-gauge concept, are more appropriate.
- The present liquid-level and pressure sensors exhibit large insertion loss, thereby imposing need for rather complex electronics.

Subsequent study of this project has revealed several possible improvements capable of further enhancement of fiber-optic instrumentation feasibility.

1.5 RECOMMENDATIONS

The demonstration model reflects careful consideration of evaluated concepts, and associated electronics have been built using low-noise and noise-discrimination techniques. However, the additional improvements discussed in Sections 1.4.1 through 1.4.3 are also recommended:

1.5.1 Liquid-Level Sensor

Although much more efficient than previous ones, the newly designed sensors can be further modified by incorporation of improved mounting methods also developed by TRW (Ref. 2).

1.5.2 Pressure Gauge

The housing and the diaphram design should be modified to minimize the effect of temperature shock. Also, the design can be modified to incorporate a reference system to cancel drift effects. The reference is identical to the measuring system except that it measures the displacement of the diaphram near its circumference where pressure-induced diaphragm displacement is minimal. This would be a differential system in which the extraneous drifts are cancelled.

Future modification may incorporate a technique called the "Geode" system, or "Sign Around." These are essentially distance-measuring systems capable of measuring displacements as small as one micron. Because these are based on time-of-flight measurements, they are accurate and are devoid of extraneous drifts.

1.5.3 Temperature Sensor

The basic design of the temperature gauge is based upon the intrinsic transmissive properties of commonly available crystals. The readout of the present system measures the time taken by the power pulse to elevate the laser-diode temperature when the emission wavelength of the laser diode matches that of the sensing crystal. However, a better technique would be to measure the temperature of the junction of the emitting laser diode at the instant when wavelength matching takes place. The technique used for measuring instantaneous junction temperature of the laser diode is based upon the dependence of band-gap voltage of the forward-biased laser diode at a specific current, say 10 mA, or of one certainly less than the threshold current of the laser diode (Refs. 1-5).

2. SENSOR SELECTION

Many sensor concepts were considered briefly, but almost immediately rejected because they were judged to be inappropriate for use in the cryogenic tank environment. An example is the concept of sensing liquid level via a float that is somehow connected to an optical readout system. Although it should be possible to devise a float system suitable for dealing with this problem, the mechanical complications appear to make this concept impractical and not worthy of serious consideration.

Because an exhaustive list of such "automatically" rejected concepts would not add to the clarity of this report, no such summary has been developed because the rejected concepts were not considered in any depth. Rather, the practical sensor concepts that were evolved from the early part of the Concept Study were evaluated in detail, as discussed in Sections 2.1 through 2.4.

2.1 SPECIFIC CONCEPTS CONSIDERED

2.1.1 Liquid-Level Sensor

Table 2-1 identifies the liquid-level sensor concepts considered, together with brief descriptions, the total evaluation score, and some pertinent comments. Table 2-2 lists details of the individual evaluations of each concept. The **bare-fiber** concept is clearly the performer choice, achieving the only perfect score of all the sensors. The main virtues of the **bare-fiber** level sensor are its extreme simplicity and its nondependence on absolute light levels due to the fact that the detector signal will either be on (when the fiber is not immersed) or off (when the fiber is immersed). Figure 2-1 is a sketch of the principle of the **bare-fiber** level sensor. The wetting response time is less than the time required to cover the fiber. The unwetting response time is slightly longer because of film effects, but laboratory tests on a model of this sensor have shown this effect to be minimal.

Table 2-1. Liquid-Level Sensor Concepts Considered

Concept Description	Evaluation Score*	Remarks
BARE FIBER (Light refracted from fiber when in in contact with liquid)	180	Extremely simple; residual film no problem
PRISM (Light ray reflected back to return fiber until liquid reaches prism and refracts beam into tank)	155	Good concept; residual film wetting would be a problem
NOTCHED CLADDING (Part of light refracted from notch when liquid is at notch level)	0	Dirt and residual droplets cause erratic behavior, causing elimination from further consideration

*Maximum Score Possible = 180

Table 2-2. Evaluations of Point Level-Sensor Concepts

Requirement/Goal	Evaluation of Point Level Sensors			
	Scoring Basis	Bare Fiber	Prism	Notched Cladding
MANDATORY REQUIREMENTS				
Electrically Passive at Sensor	0, 10 (Yes, No)	10	10	10
Operates at Cryogenic Temperatures	0–10 (Judgment)	10	10	10
Can Perform Present Sensor Functions	0, 10	10	10	10
Can Operate Immersed or Nonimmersed	0, 10	10	5?	0**
Mechanically Simple and Rugged	0–10	10	5	
PERFORMANCE REQUIREMENTS				
Operating Range OK?	0–10	10	10	
Sensitivity/Resolution OK?	0–10	10	5	
Response Time OK?	0–10	10	5	
Insensitive To				
Connector Reconnects?	0–10	10	10	
Source Intensity Variations?	0–10	10	10	
ΔT for Press Sensor?	0–10	—	—	
ΔP for Temp Sensor?	0–10	—	—	
Stability (over 200 cycles)?	0–10	10	10	
Remote Indication (100 ft) OK?	0–10	10	10	
ADDITIONAL CONSIDERATIONS				
Cost	0–10	10	5	
Weight	0–10	10	10	
Size	0–10	10	10	
Power Consumption	0–10	10	10	
Simple Data Processing and Readout	0–10	10	10	
Interchangeability	0–10	10	10	
TOTAL SCORE*		180	155	0

*Maximum Score Possible = 180
**Automatic Elimination.

CONCEPT: With fiber cladding totally removed, external liquid "shorts out" transmitted light, thus indicating presence of liquid at fiber level.

REMARKS: Concept is point sensor, (i.e., On-Off indicator). Extremely simple sensor and readout.

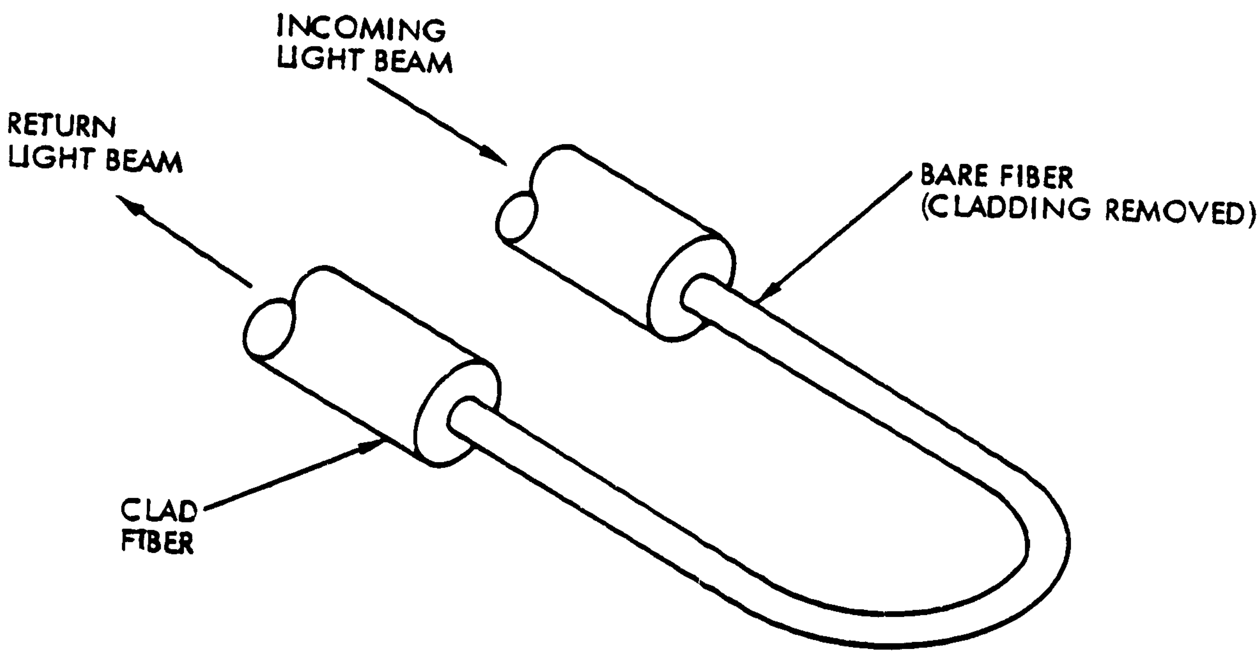

Figure 2-1. Recommended Liquid-Level Point Sensor Concept

2.1.2 Temperature Sensor

Table 2-3 shows the temperature-sensor concepts considered and Table 2-4 the details of the individual evaluations. The semiconductor absorption bandedge-shift concept is the most attractive sensor concept primarily because of its simplicity, which results from the fact that the sensor is a small chip inserted between the input and output fibers. Figure 2-2 illustrates the principles of the recommended temperature-sensor concept, and Figure 2-3 shows the temperature dependence of the absorption bandedge location for GaAs, given here as an example of the principle utilized.

Possible instrumentation concepts to implement the absorption bandedge concept for temperature measurement are shown in Figures 2-4(a) through 2-4(c), which correspond to the concepts listed under the semiconductor bandedge shifts addressed in Tables 2-3 and 2-4. All three instrument concepts were considered in detail, with the concept illustrated in Figure 2-4(a) the one chosen for the final instrumentation package.

2.1.3 Pressure Sensor

Pressure-sensor concepts considered are noted in Table 2-5 and details of the evaluations in Table 2-6. Because of their basic mechanical simplicity the concepts utilizing optical indication of the position of a pressure-sensitive diaphragm or bellows are preferred. Although, as indicated in Table 2-6, the digital encoder instrumentation concept was favored originally, a simpler system which senses the variations in light reflected from a pressure-deformable bundle ultimately was implemented. Variations in the output of the source light are sensed and normalized in accordance with obtained readings.

Table 2-3. Temperature-Sensor Concepts Considered

Concept Description	Evaluation Score*	Remarks
SEMICONDUCTOR BAND-EDGE SHIFT:		
Wavelength of Absorption Cut-Off is Temperature Dependent		
Match with Cut-Off of Reference Device;	176	Mechanically Simple;
Spectral Analysis of Output;	172	Simple But Higher Cost;
Ratio of Outputs From 2 Led's.	172	Requires 2 Sources.
PHOSPHORESCENCE:		
Time Decay of Light Pulse.	145	Inefficient?; Phosphorescence Into 2π Ster.
VIBRONIC ABSORPTION:		
Ratio of Absorption In 2 Sidebands (Phonon Creation/Destruction).	144	Little Known Interaction; Good Potential, Requires More Research.
TWO-COLOR INTERFERENCE COUPLER:		
Spacing Varies With Expansion; Ratio of 2-Color Signals Temperature Dependent.	138	Difficult To Match Fiber N.A., Surface Finish, etc.
FABRY-PEROT:		
Spectral Analysis of Transmitted Intensity.	136	Requires High Spectral Resolution, Therefore High Cost.
THERMOSTAT BIMETAL:		
Optical Readout of Motion	110	Expansion Coefficient Low at Cryogenic Temperatures; Many Fibers In Liquid.

*Maximum Score Possible = 190

Table 2-4. Evaluation of Temperature-Sensor Concepts

Requirement/Goal	Scoring Basis	Semiconductor Bandedge Shift: Match Cut-off of Reference Device	Semiconductor Bandedge Shift: Spectral Analysis of Output	Semiconductor Bandedge Shift: Ratio Outputs from 2 LED's	Phosphor-escence	Vibronics Absorption	Two-Color Interference Coupler	Fabry-Perot	Thermostat Bimetal
MANDATORY REQUIREMENTS									
Electrically Passive at Sensor	0, 10 (Yes, No)	10	10	10	10	10	10	10	10
Operates at Cryogenic Temperatures	0-10 (Judgment)	10	10	10	5	5	8	5	5
Can Perform Present Sensor Reactions	0, 10	10	10	10	5	5	5	5	5
Can Operate Immersed or Nonimmersed	0, 10	10	10	10	10	10	10	10	10
Mechanically Simple and Rugged	0-10	6	6	8	10	10	2	5	2
PERFORMANCE REQUIREMENTS									
Operating Range OK?	0-10	8	8	8	5?	5?	8	8	5
Sensitivity/Resolution OK?	0-10	7	7	7	5?	5?	8	10	7
Response Time OK?	0-10	9	10	9	8	8	8	8	5
Insensitive to									
Connector Reconnects?	0-10	10	10	8	10	8	5	5	5
Source Intensity Variations?	0-10	10	10	8	10	5	7	7	5
ΔT for Press Sensor?	0-10	–	–	–	–	–	–	–	–
ΔP for Temp Sensor?	0-10	10	10	10	10	10	9	9	10
Stability (Over 200 Cycles)?	0-10	10	10	10	5?	10	5	8	5
Remote Dedication (100 Ft) OK?	0-10	10	10	10	2	5	8	8	5
ADDITIONAL CONSIDERATIONS									
Cost	0-10	5	5	8	8	5	5	5	5
Weight	0-10	10	8	10	9	9	9	88	5
Size	0-10	10	10	10	8	9	8	7	5
Power Consumption	0-10	8	8	8	9	8	8	5	5
Simple Data Processing and Readout	0-10	8	10	8	10	7	5	5	9
Interchangeability	0-10	10	10	10	8	10	10	8	2
TOTAL SCORE*		176	176	172	145	144	138	136	110

*Maximum Score Possible = 190

CONCEPT: Light absorbed by semiconductors or insulators dependent on intrinsic or impurity absorption; absorption bandedge a sharp cut-off and temperature-dependent.

REMARKS: Simple, small-size sensor; various instrument concepts available for indication.

EXAMPLE: Transmission and absorption of emission spectrum of HP HEMT-6000 LED at 25°C shown with selenium crystal, also at 25°C.

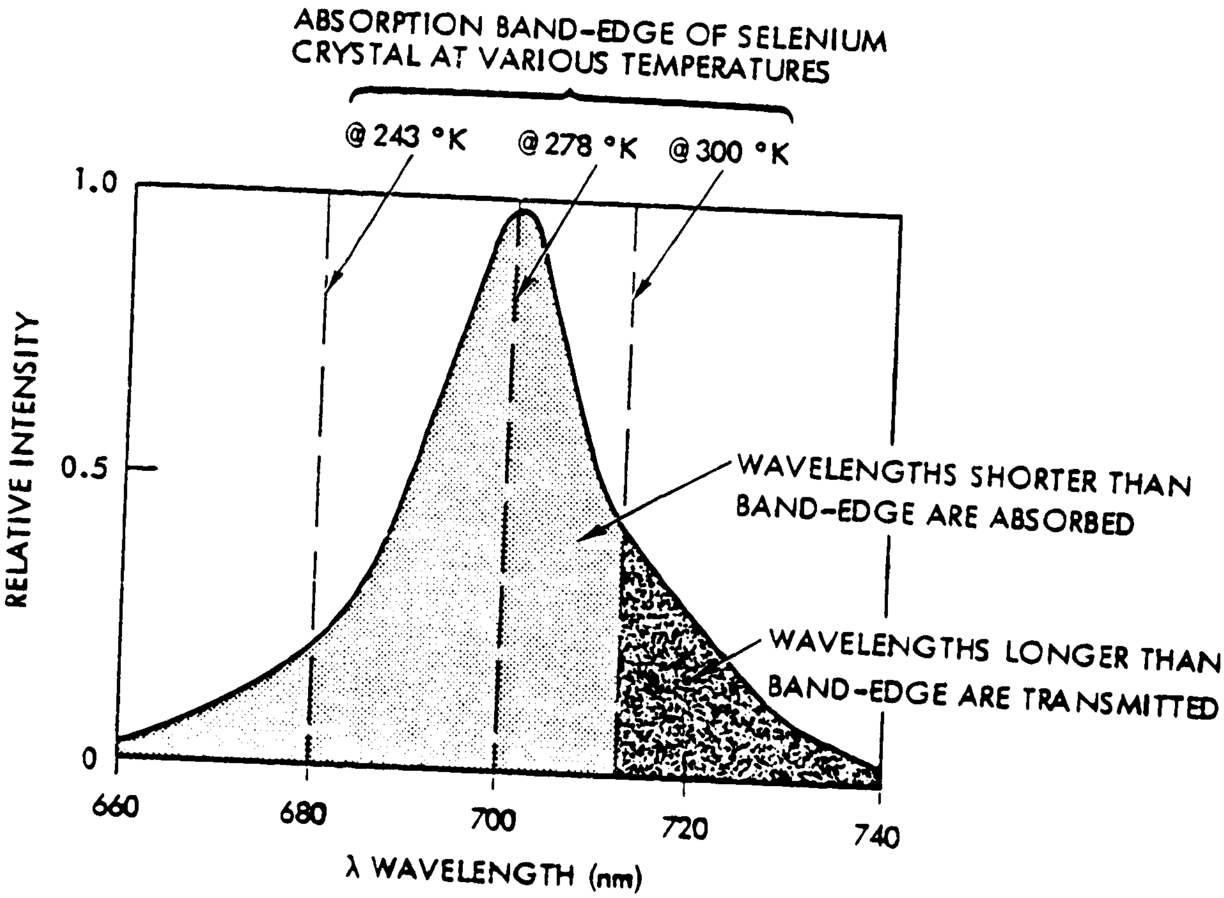

Figure 2-2. Recommended Temperature-Sensor Concept

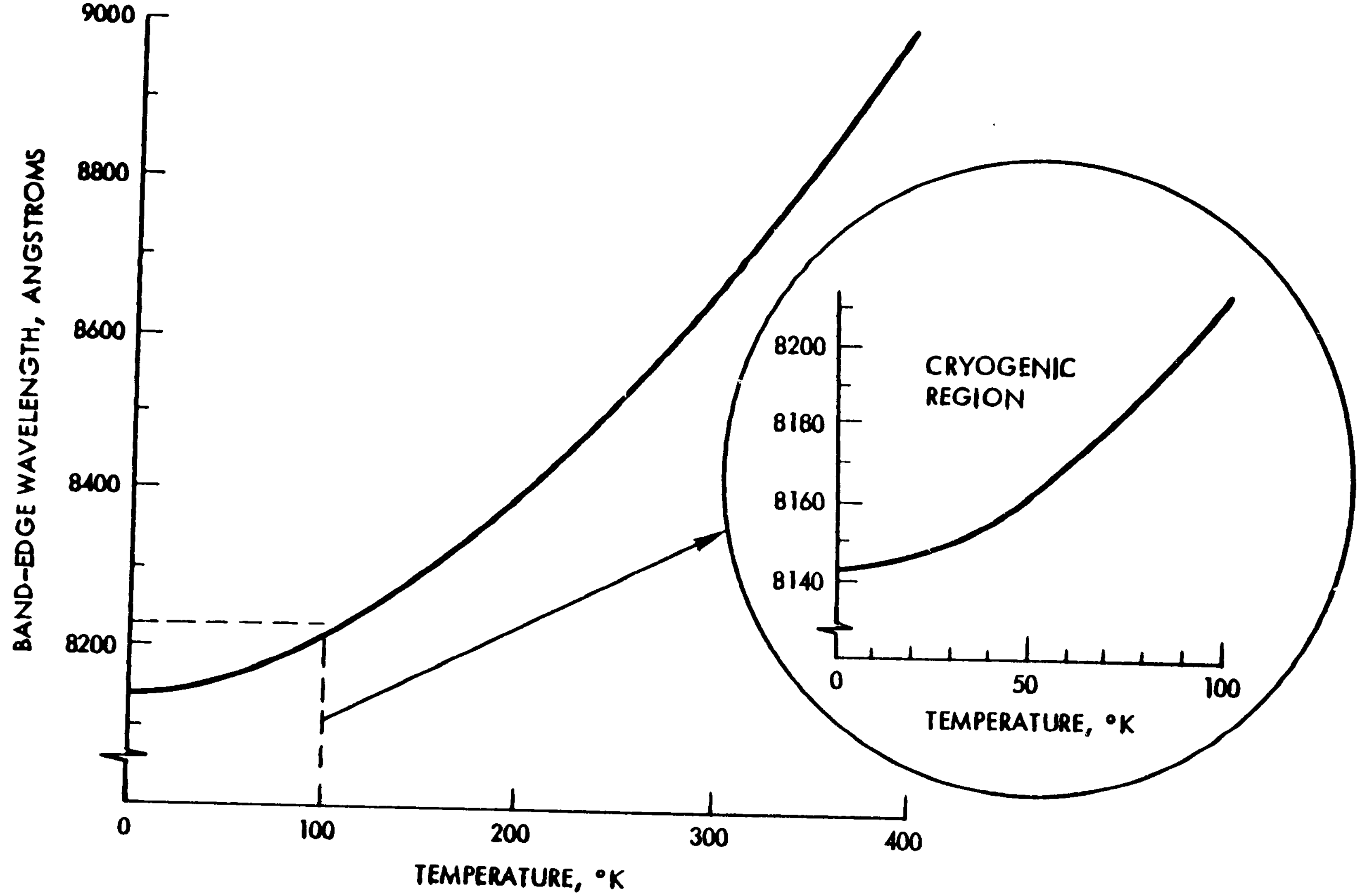

Figure 2-3. Temperature Dependence of Absorption Bandedge Location for GaAs

INSTRUMENT CONCEPT: LIGHT BEAM FROM LED IS PASSED THROUGH BOTH REFERENCE SEMICONDUCTOR (AT CALIBRATED, CYCLED TEMPERATURE T_R) AND SENSOR (AT T_S). WHEN $T_R < T_S$ ABSORPTION CONTROLLED BY SENSOR; WHEN $T_R > T_S$ ABSORPTION CONTROLLED BY REFERENCE. KNEE OF INTENSITY-TIME RESPONSE DETERMINES $T_S = T_R$.

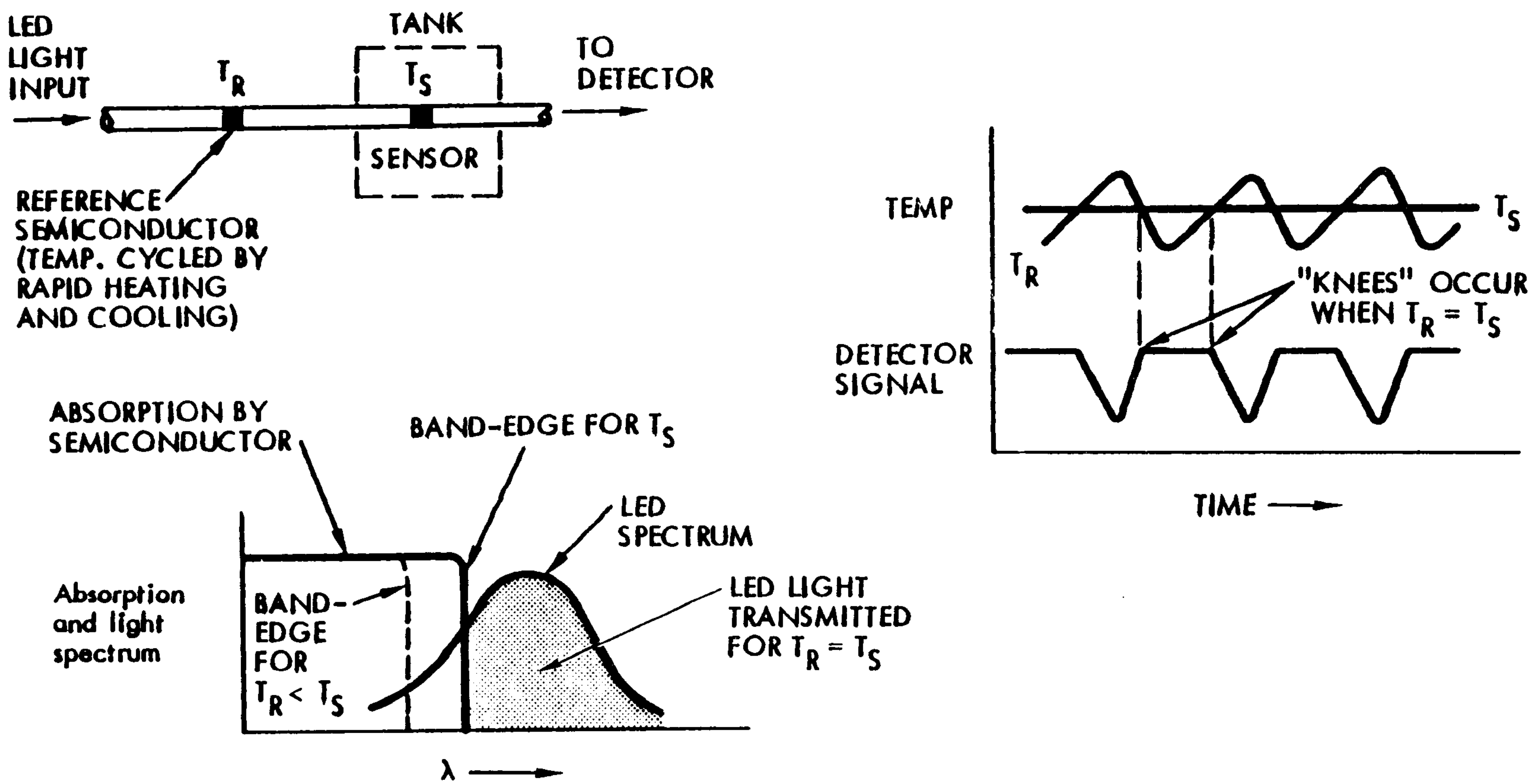

Figure 2-4(a). Instrument Concept for Semiconductor Bandedge Temperature Sensor: Reference Temperature Cycling

INSTRUMENT CONCEPT: TRANSMISSION OF LIGHT BEAM FROM LED IS CONTROLLED BY ABSORPTION BAND-EDGE OF SENSOR. WAVELENGTH OF TRANSMISSION CUT-OFF INDICATES SENSOR TEMPERATURE, T_S.

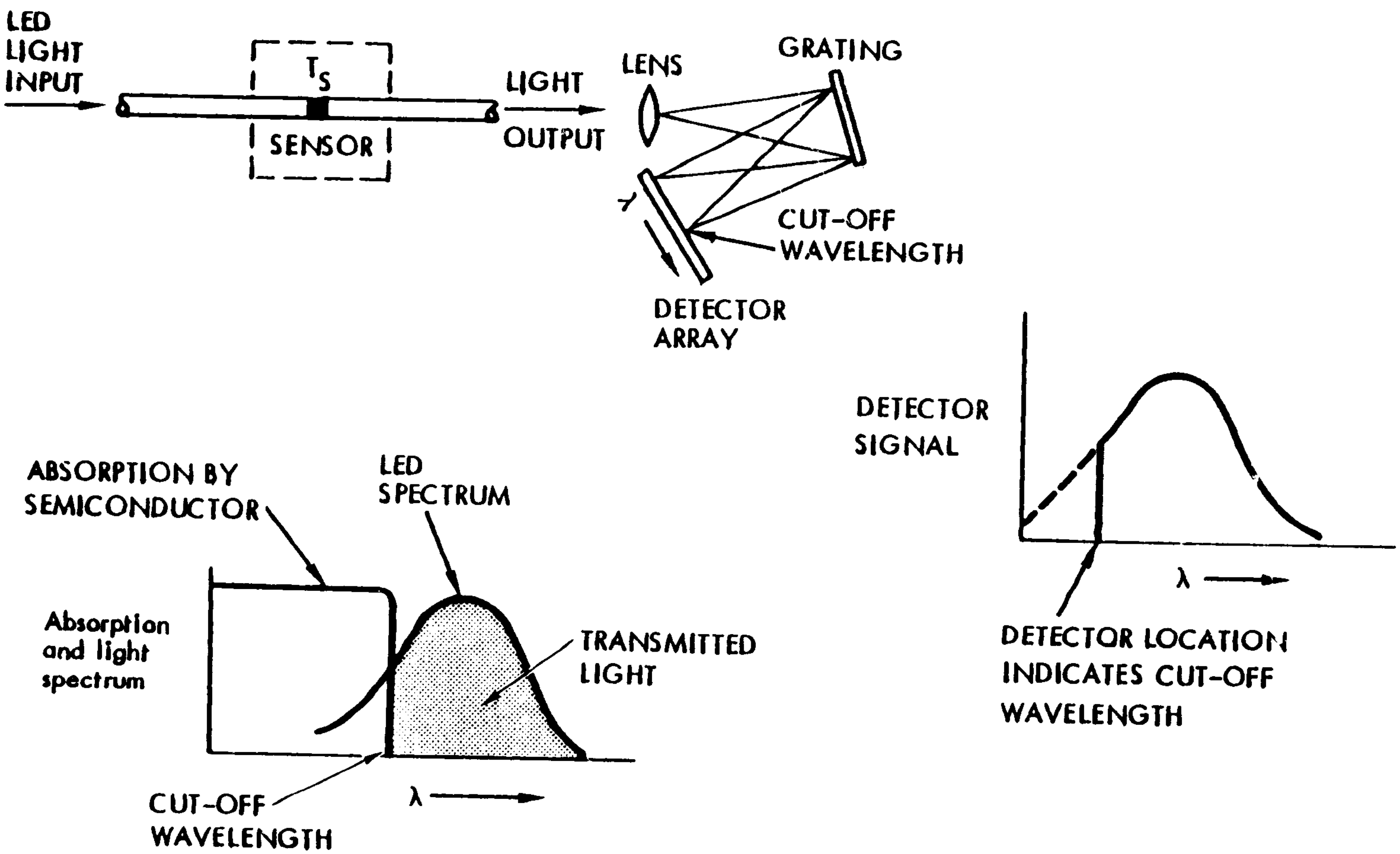

Figure 2-4(b). Instrument Concept for Semiconductor Bandedge Temperature Sensor: Spectral Analysis

INSTRUMENT CONCEPT: TRANSMISSION OF ALTERNATE BEAMS FROM 2 DIFFERENT-COLOR LED'S IS CONTROLLED BY ABSORPTION BAND-EDGE OF SENSOR.
RATIO OF TRANSMITTED LIGHT FROM LED'S INDICATED SENSOR TEMPERATURE

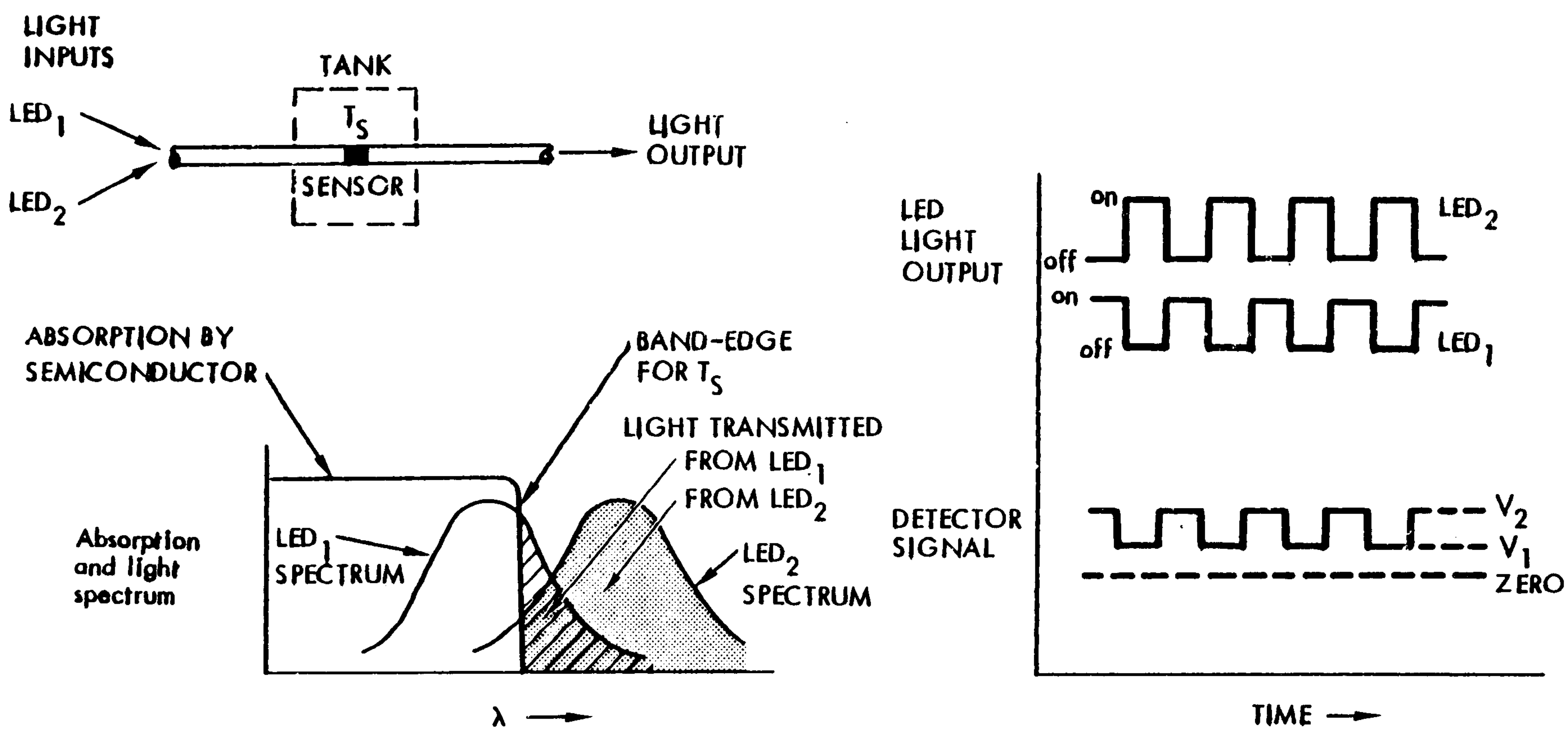

Figure 2-4(c). Instrument Concept for Semiconductor Bandedge Temperature Sensor: Ratio of 2-Color Outputs

Table 2-5. Pressure-Sensor Concepts Considered

Concept Description	Evaluation Score*	Remarks
MOTION OF DIAPHRAGM OR BELLOWS		All Motion Devices Simple and Rugged
Optical Indication of Position		
Digital Encoder	166	No Ratioing Needed; Sensitive
Fiber Ribbon	164	Requires Many Fibers
Variable Size Holes	162	Requires Intensity Ratioing
Linear Taper Absorber	157	Requires Intensity Ratioing
Linear Density Filter	156	Requires Intensity Ratioing
Moire Grid	151	Zero Point Uncertain
Fiber Bundle and Diaphragm	147	Requires Ratioing, Initial Calibration
PRESSURE ACTIVATED SPECTROMETER		
Location of Dispersed Beam Varies with Pressure	134	Spectral Variation of Fiber Ribbon Indicator; Temperature Sensitive
PHOTOELASTIC METHOD		
Variable Transmission Through Stressed Birefringent Crystals	93	Mechanically Complex; Temperature Sensitive

*Maximum Score Possible = 180

Table 2-6. Evaluation of Pressure Sensor Concepts

Requirement/Goal	Scoring Basis	Digital Encoder	Fiber Ribbon	Hole Indicator	Linear Taper	Linear Density Filter	Action of Diaphragm or Bellows: Moire Grid	Fiber-Bundle Diaphragm	Pressure Activated Spectro-meter	Photo-Elastic Method
MANDATORY REQUIREMENTS										
Electrically Passive at Sensor	0, 10 (Yes, No)	10	10	10	10	10	10	10	10	10
Operates at Cryogenic Temperatures	0-10 (Judgment)	10	10	10	10	10	10	10	10	5?
Can Perform Present Sensor Functions	0, 10	10	10	10	10	10	10	10	10	10
Can Operate Immersed or Nonimmersed	0, 10	–	–	–	–	–	–	–	–	YES**
Mechanically Simple and Rugged	0-10	9	10	10	5	5	5	5	5	2
PERFORMANCE REQUIREMENTS										
Operating Range OK?	0-10	10	10	10	10	10	10	10	10	5
Sensitivity/Resolution OK?	0-10	8	8	2	8	8	10	8	5	5
Response Time OK?	0-10	10	10	10	10	10	10	10	9	2
Insensitive to										
Connector Reconnects?	0-10	10	10	10	8	8	6	7	8	8
Source Integrity Variations?	0-10	10	10	10	8	8	8	7	8	5
ΔT for Press Sensor?	0-10	8	8	8	8	8	5	8	2	2
ΔP for Temp Sensor?	0-10	–	–	–	–	–	–	–	–	–
Stability (over 200 cycles)?	0-10	10	10	10	10	10	10	8	8	5
Remote Indication (100 ft) OK?	0-10	10	10	10	10	10	10	10	10	10
ADDITIONAL CONSIDERATIONS										
Cost	0-10	8	9	8	8	8	5	7	7	5
Weight	0-10	8	8	8	8	8	7	6	5	2
Size	0-10	9	7	9	9	9	7	5	5	2
Power Consumption	0-10	8	9	7	7	7	8	7	7	7
Simple Data Processing and Readout	0-10	8	5	10	8	7	5	6	5	3
Interchangeability	0-10	10	10	10	10	10	10	10	10	5
TOTAL SCORE*		166	164	162	157	156	151	147	134	93

*Maximum Score Possible = 180

**Only photoelastic method requires immersed sensor

2.2 OVERVIEW OF STUDY RESULTS

After an initial period wherein essentially all types of sensor concepts were considered, the range of concepts was narrowed to those identified in Figure 2-5. Final recommendations were based on the numerical scoring procedure indicated in Table 2-7, the evaluations being weighted strongly in favor of practical systems which operate in a cryogenic environment. The selected concepts have been incorporated in the demonstration model to permit further evaluation.

2.3 CONCEPTS SELECTED

This section identifies sensors selected for final development from the various sensor concepts previously considered in Section 2.1. Specific test data that have been accumulated on the developed sensors are summarized in Section 4.

2.3.1 Liquid-Level Sensor

The selected fluid-level sensor concept is based upon measuring optical attenuation through a glass rod used as the level sensor, as shown in Figure 2-6. Attenuation through the sensor is a function of the refractive index of the material surrounding the glass rod. Because liquids generally have higher refractive index, attenuation through the sensor increases when the sensor is submerged in the liquid. This concept in its simplest form works very well for liquids having high refractive indices, such as water, gasoline, oil, etc. However, liquid-level sensors for low refractive indices such as those of LN_2 or LH_2 must be designed with several concepts given consideration. The anatomy of the present sensor design is elaborated below.

Figure 2-7 is a schematic of a system in which light is coupled from an input fiber to an output fiber through a straight unclad coupling rod. In the following discussion it is assumed that the index of refraction of the fiber-optic core is the same as that of the rod, that there are no reflection losses, and that $n_3 < n_2$. The latter is true for all fibers and fuels of interest to this program.

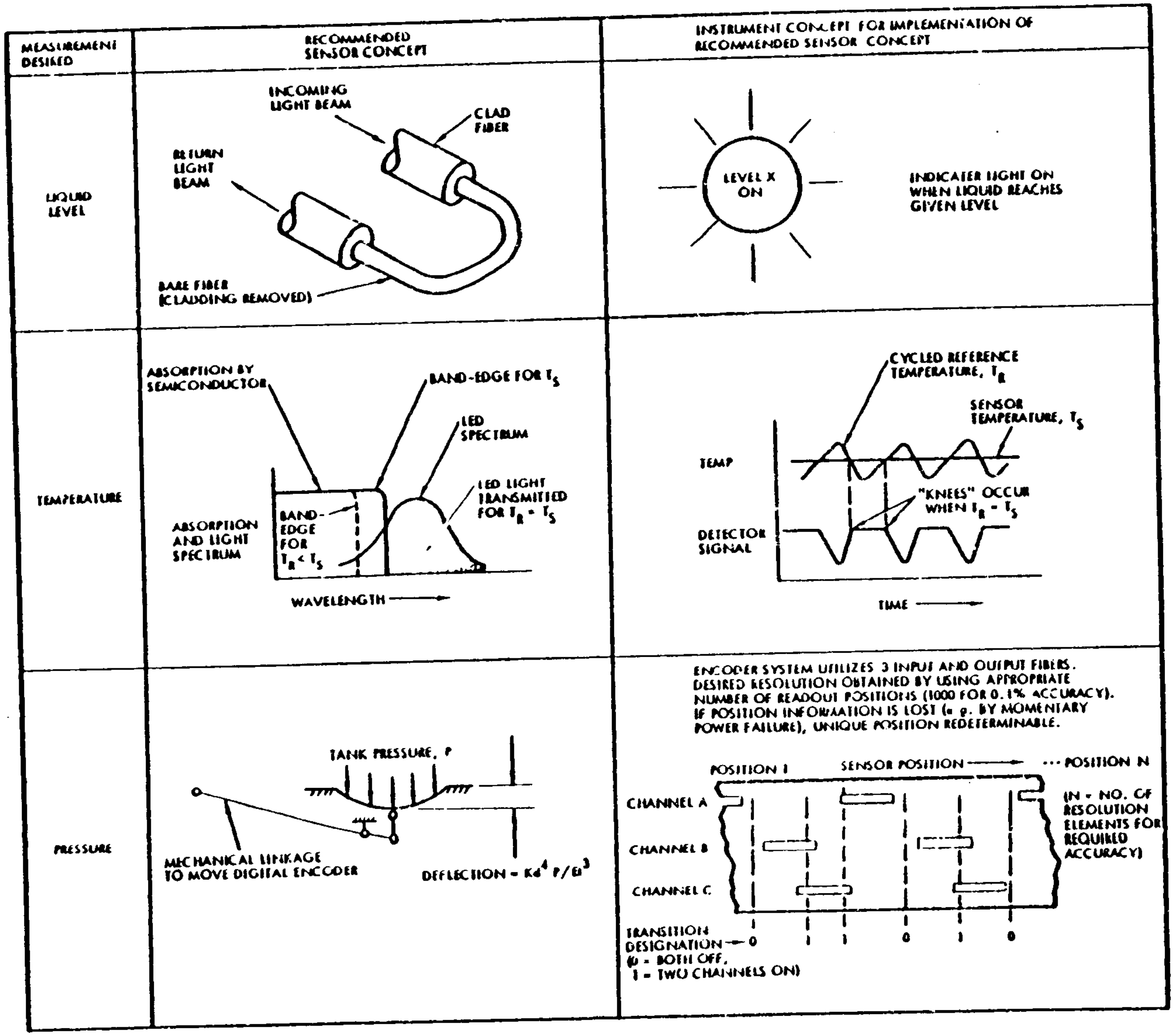

Figure 2-5. Summary of Recommended Sensor and Instrument Concepts

Table 2-7. Sensor Scoring Evaluation

Requirement/Goal	Scoring Basis*
MANDATORY REQUIREMENTS	
Electrically Passive at Sensor	0, 10 (Yes, No)
Operates at Cryogenic Temperatures	0–10 (Judgement)
Can Perform Present Sensor Functions	0, 10
Can Operate Immersed or Non-Immersed	0, 10
Mechanically Simple and Rugged	0–10
PERFORMANCE REQUIREMENTS	
Operating Range O.K.?	0–10
Sensitivity/Resolution O.K.?	0–10
Response Time O.K.?	0–10
Insensitive To	
Connector Reconnects?	0–10
Source Intensity Variations?	0–10
ΔT For Press Sensor?	0–10
ΔP For Temp Sensor?	0–10
Stability (Over 200 Cycles)?	0–10
Remote Indication (100 Ft) O.K.?	0–10
ADDITIONAL CONSIDERATIONS	
Cost	0–10
Weight	0–10
Size	0–10
Power Consumption	0–10
Simple Data Processing and Readout	0–10
Interchangeability	0–10

*Maximum Score Possible = 200

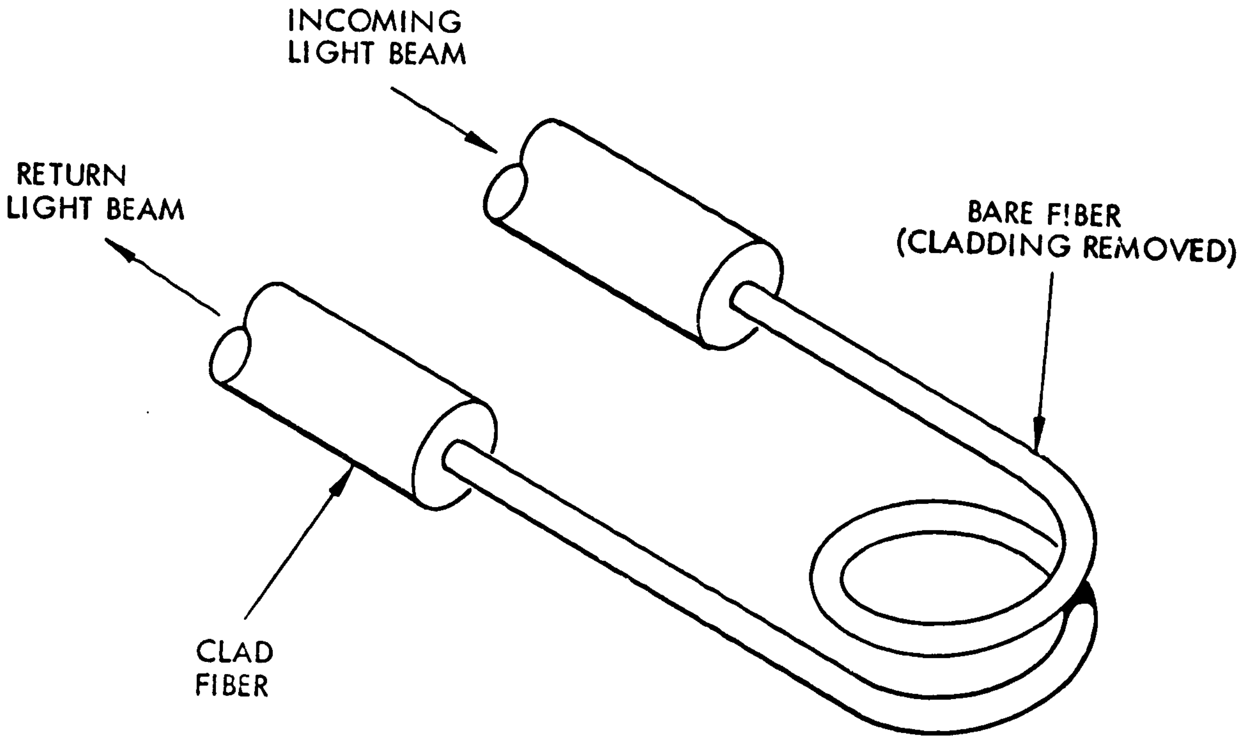

Figure 2-6. Selected Fluid-Level Sensor Concept

The light entering the rod will have a numerical aperture given by

$$\sin\theta_1 = (n_1^2 \cdot n_2^2)^{1/2}$$

where θ_1 is the angle between the extreme ray propagated by the fiber and the fiber axis (Ref. 1). Since N_3, the refractive index of the medium surrounding the rod, is less than n_2 for all cryogenic fuels, the numerical aperture of the rod, or

$$\sin\theta_2 = (n_1^2 - n_3^2)^{1/2} > \sin\theta_1$$

is greater than that of the fiber. Therefore if the rod is aligned to the fiber it will transmit all of the incoming light without loss whether or not it is surrounded by the liquid. If the diameters of the fibers and

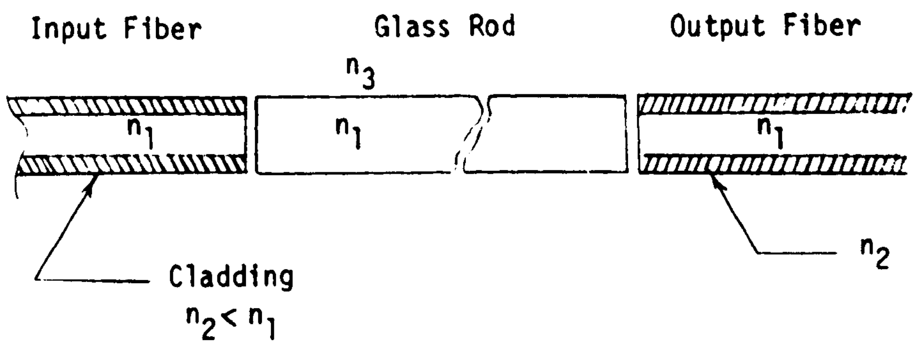

Figure 2-7. Schematic of Light Coupling Between Input and Output Fibers

the rod are not matched there will be coupling losses associated with the system, but these losses will be independent of the medium surrounding the sensor rod. Consequently, a straight in-line sensor as shown in Figure 2-7 cannot be used as a liquid-level gauge.

It also would be possible to introduce a scattering center within the rod to induce higher-order modes, whereby the fraction of input light that is transmitted by the rod would be a function of the index of refraction of the medium because the higher-order modes created by the scattering center would be cast through the walls of the rod. However, when $n_3 < n_2$, as is always the case here, the final solution of the amount of light transmitted to the receiver would be governed by the numerical aperture of the output fiber (which is smaller than that of the rod), and the signal received would again be independent of the medium surrounding the sensor rod. Therefore this scheme also cannot be used to detect the presence or the level of a fluid.

A multiplicity of scattering centers of course would serve to couple energy between modes, so that the amount of light accepted and transmitted by the output fiber would be a function of the index of refraction of the medium surrounding the rod. However, in practice it is difficult to fabricate rods with the proper number and distribution of scattering centers, and TRW experience indicates that commercial glass, poor as it is, does not have a sufficient number.

It thus is necessary to produce in a controlled manner effective means of inducing higher-order modes as well as of coupling energy between modes. The simplest technique for accomplishing this is to form a number of bends in the rod, each bend serving to mix incoming modes, to outcouple high-order modes, and to induce new modes. The amount of light exiting from the rod within the numerical aperture of the return fiber then will be a function of the index of refraction of the medium surrounding the rod.

The optimum number of bends and the radii of curvature of the bends must be determined experimentally. The closer the index of refraction of the liquid is to that of air, the greater are the number of bends required to accentuate the difference between air and the liquid. TRW has found through a number of experiments on a variety of level-sensor configurations that the configuration shown in Figure 2-6 is optimal for the present system.

Insertion loss of this sensor in air is 18 db. When immersed in liquid nitrogen the signal loss is 28 dB, yielding a 10-dB change in the signal in going from no-fluid to fluid environment. The signal loss in liquid hydrogen is estimated to be 22 dB, or a 4-dB change in signal due to the presence of the fluid. Such change magnitudes are readily detected and indicated by the recommended system. Figure 2-8 is a schematic of the entire level-sensing system.

2.3.2 Pressure Sensor

Figure 2-9 is a sketch of the recommended pressure-sensor configuration. The fiber-optic cable has been bifurcated so that some (about one-half) of the fibers are used for input and the remainder for output. Light is coupled from the input fibers to the output fibers by reflection off the thin-end plate diaphragm. The curvature of this diaphragm is determined by the pressure external to the sensor (i.e., flat at atmospheric pressure and concave inward at higher pressures). This change in shape of the reflecting surface with pressure changes the coupling between input and output fibers, thus producing a signal change as a function of pressure. Locations of the fiber end faces relative to the diaphragm are set and locked during assembly and test. The entire sensor is made of Invar to minimize thermal effects. Figure 2-10 is a schematic of the electronic circuitry associated with this sensor.

2.3.3 Temperature Sensor

This sensor is the most sophisticated of the three in that its operation is based upon the fact that the position of the optical absorption (or transmission) edge of the semiconductor crystal is a well-defined function of temperature. A schematic of this phenomenon is shown in Figure 2-11, wherein T is the temperature of the LED and t is the

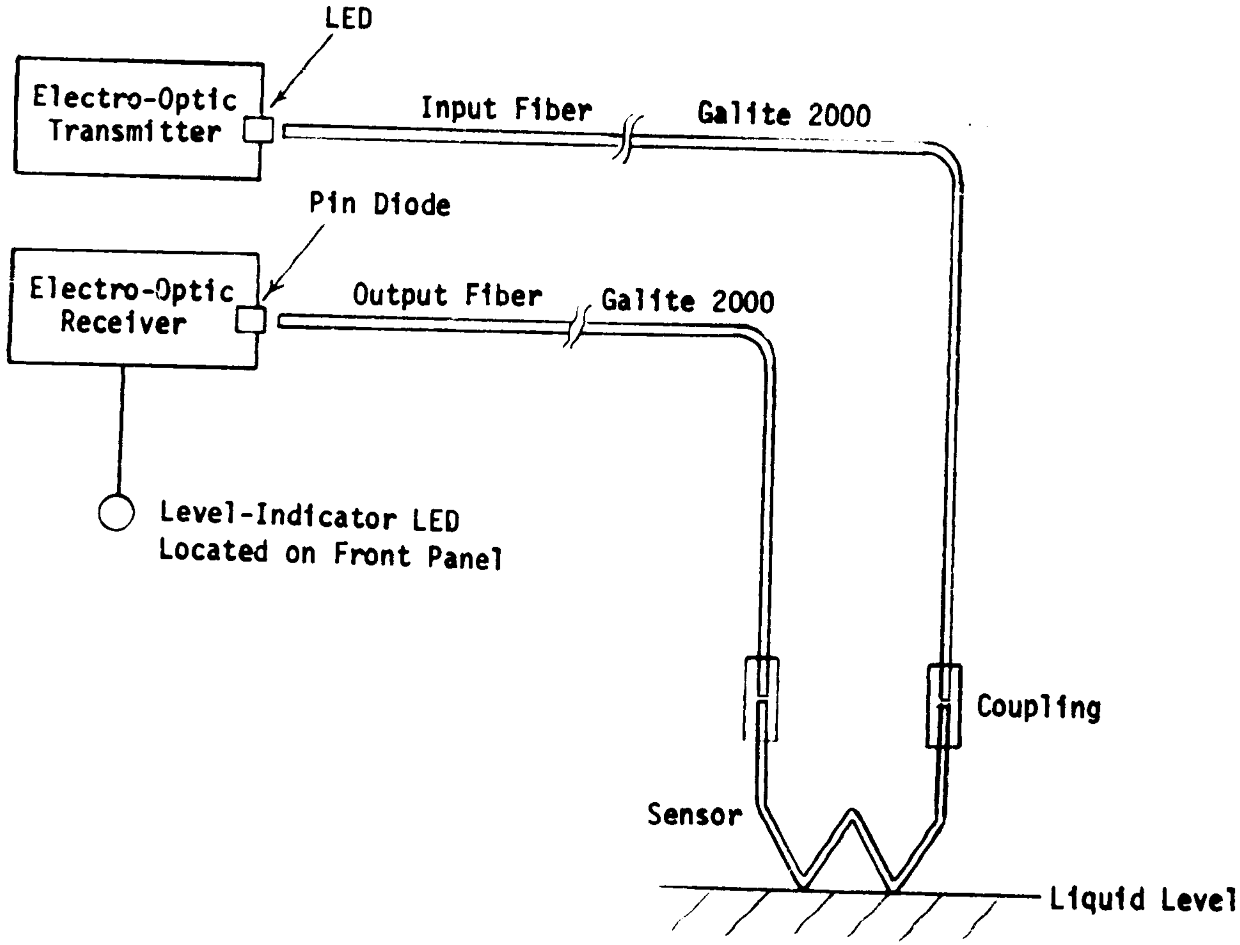

Figure 2-8. Schematic of TRW Level-Sensing System

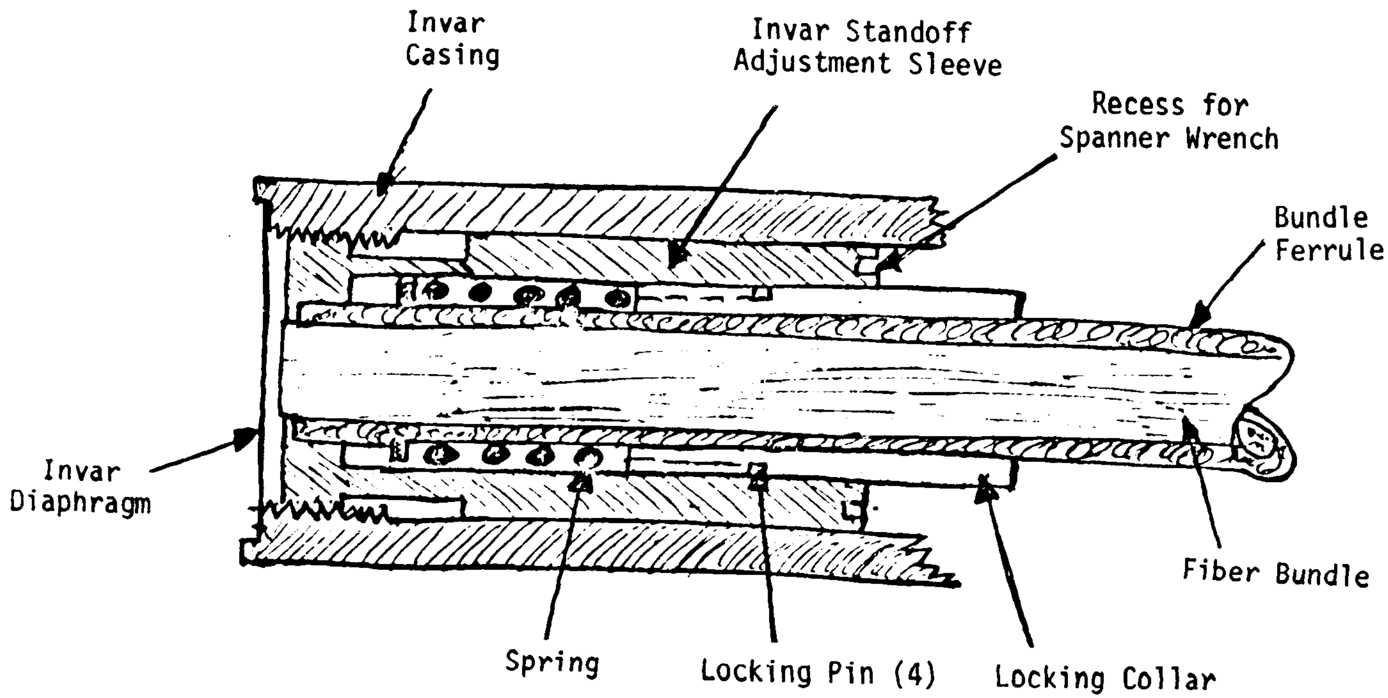

Figure 2-9. Recommended Pressure-Sensor Configuration

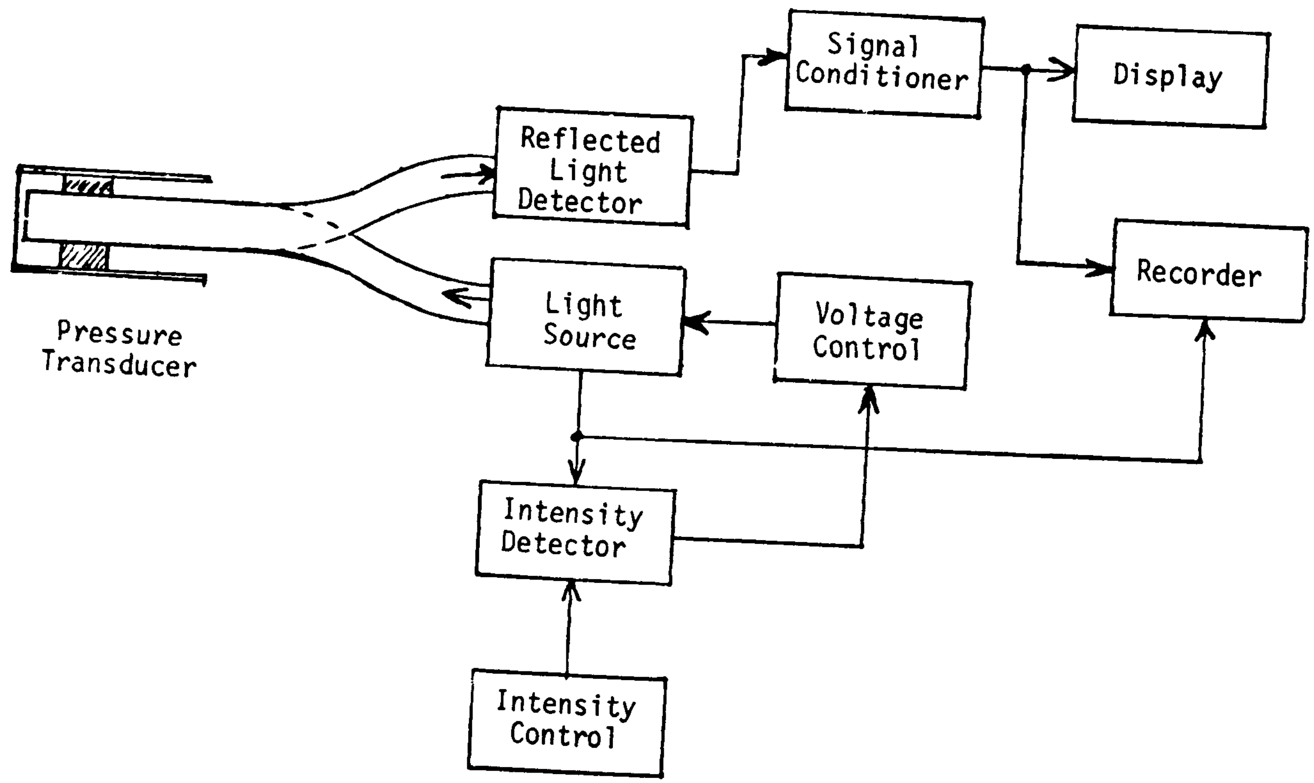

Figure 2-10. Electronic Circuit Associated with Pressure Sensor

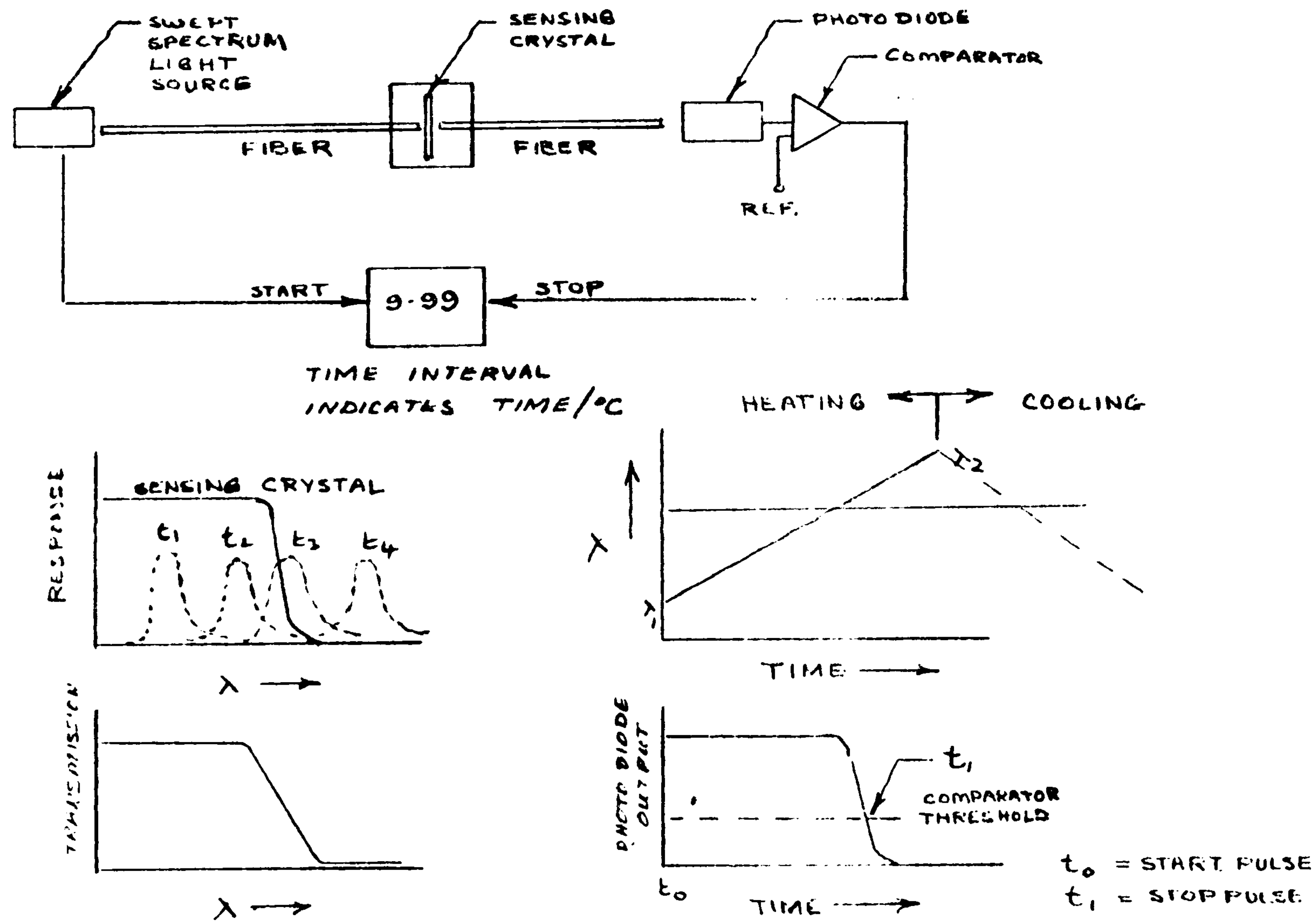

Figure 2-11. Temperature-Tuned LED Output Sweeping Through Absorption Edge of Sensor Crystal

length of time after the sensor crystal has turned on and begins to heat up due to the electrical energy dissipated within it. Thus, if an appropriate crystal is immersed in the fluid of interest and the wavelength of the absorption edge determined, the temperature of the crystal (and hence of the fluid) is known.

A number of techniques for locating the position of the absorption edge use an optical source to sweep through the wavelengths of interest. TRW chose to measure the optical transmission of the sensor crystal using a narrow-band tunable optical source. The wavelength at which there is a rapid change in the transmission is the cutoff wavelength which is directly analogous to the crystal temperature.

Gallium arsenide (GaAs) laser diodes satisfy applicable requirements, and they may be operated at room temperature. Because room-temperature GaAs lasers emit around 0.87 microns (exact wavelength depends upon doping) the sensor crystal must have an absorption edge near that wavelength when it is at cryogenic temperature. Indium phosphide (InP) is such a crystal, as is evident from comparing the GaAs data with the InP data of Figure 2-12. It should be noted that at 300°K the output of a GaAs laser is at a wavelength slightly shorter than the bandedge wavelength of InP at cryogenic temperatures, which makes it possible to tune the GaAs output through the InP absorption edge by heating the laser. Heating is highly preferred over cooling because heating can be accomplished by the laser drive current itself.

The simplest tunable optical approach is to use a pulsed laser diode driven in such a manner that during its ON pulse it heats up, causing its output wavelength to increase. Figure 2-13, which shows this process schematically, is a sketch of the complete temperature-sensing system and of associated input and output signals.

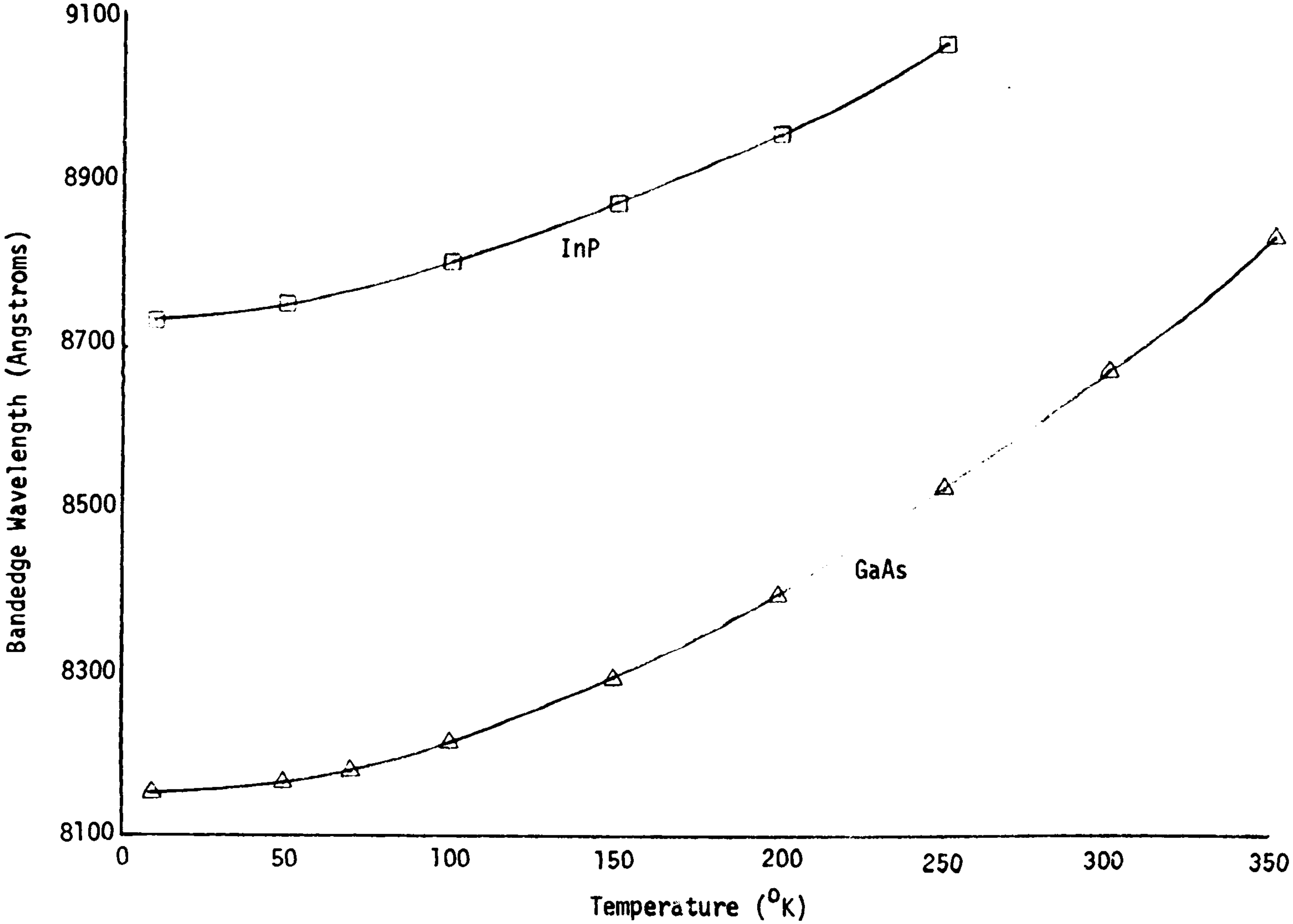

Figure 2-12. Data Bandedge of Indium Phosphide and Gallium Arsenide vs. Temperature

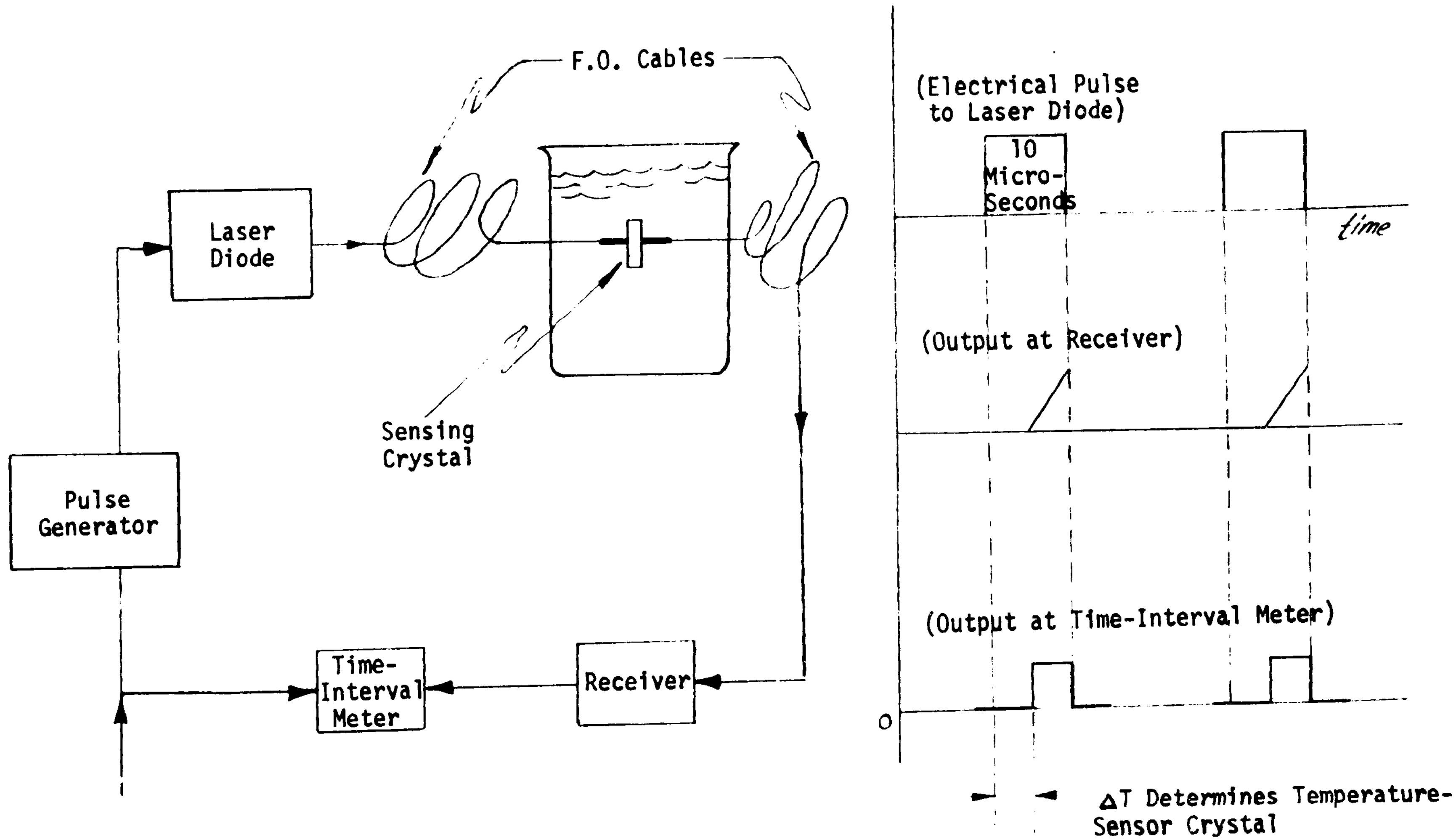

Figure 2-13. Schematic of Temperature-Sensing System and Associated Input/Output Waveforms

3. EXPERIMENTAL MODEL

An experimental model was built to demonstrate and evaluate the performance of all three sensors. As shown in Figure 3-1, the model consists of a console cabinet with a cryogenic Dewar affixed to its side. The necessary electronics is behind the panels mounted in the sloped cut-out. The Dewar can be detached and operated as far away from the cabinet as 30 feet. The only connection between cabinet and Dewar is via fiber cables. The experimental model is self-contained, however, and therefore helium gas and liquid nitrogen must be applied during test. The electronics, self-contained with internal power supplies, can be operated by a 120V line. The total power required is less than 120 watts. Various test jacks located on the rear panel of the electronics module are connected to a standard oscilloscope to monitor applicable signals. To operate the demonstration model the following items are required:

- Helium gas cylinder with two pressure control valves
- Liquid nitrogen cylinder with stop valve
- Standard triggered oscilloscope

3.1 PERFORMANCE REQUIREMENTS

Sensor performance requirements were dictated principally by the test procedures specified in a previously issued TRW document identifying test plans and procedures for fiber-optic instrumentation (Ref. 3).

In accordance with Section 2.1 of the above document, the three sensors are mounted on a sensor chamber attached to a 2-ft section of galvanized tubing (sting assembly) as shown in Figure 3-2. This tube can be lowered into and out of the Dewar to allow three sensors to be inserted into a quiescent bath of LN_2 contained in the cryogenic Dewar. The Dewar is designed to withstand pressures of 40 psig, which is higher than the required test pressure of 15 psig. For safety purposes, a 15-psig limit valve has been incorporated.

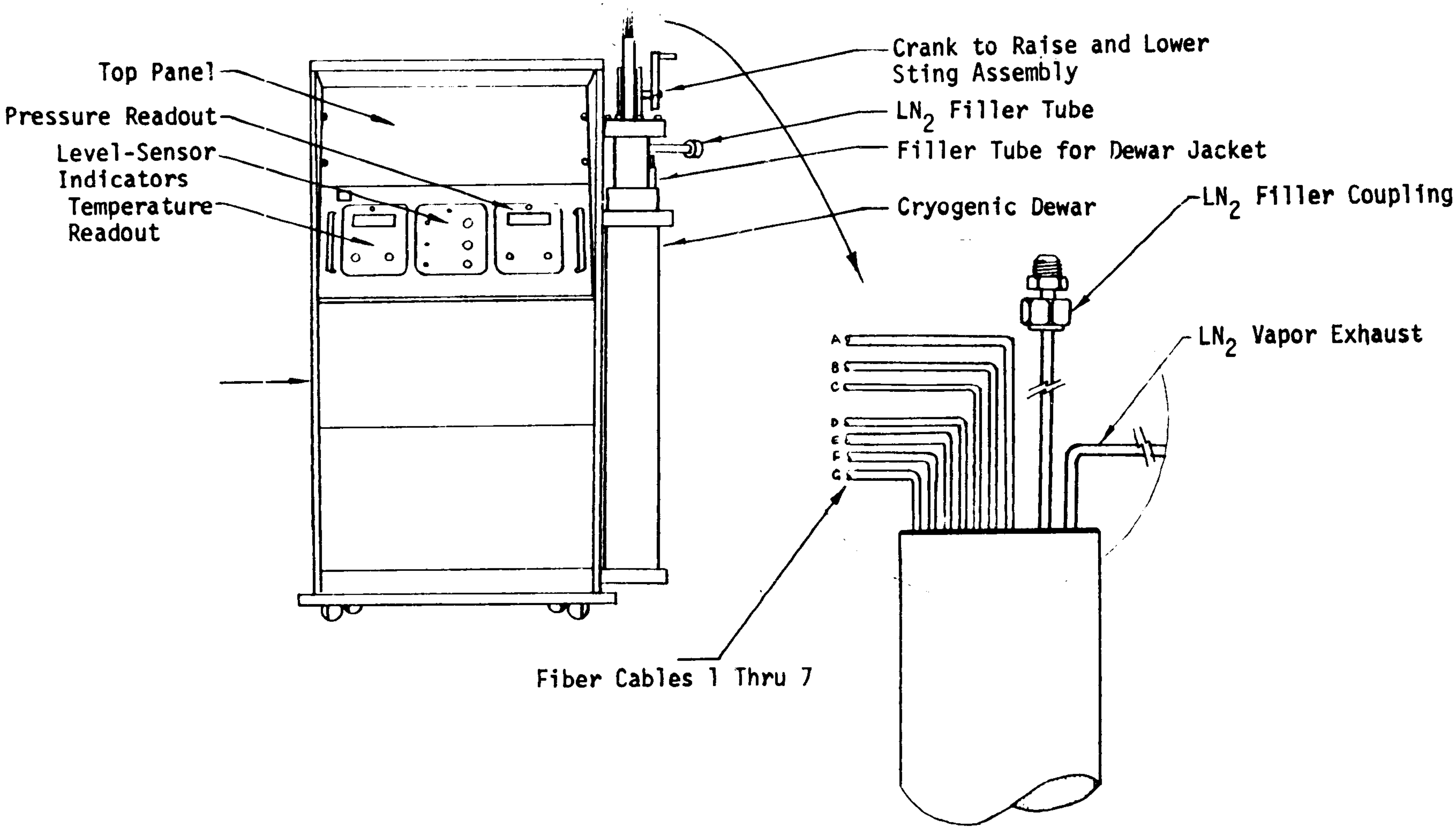

Figure 3-1. Experimental Model

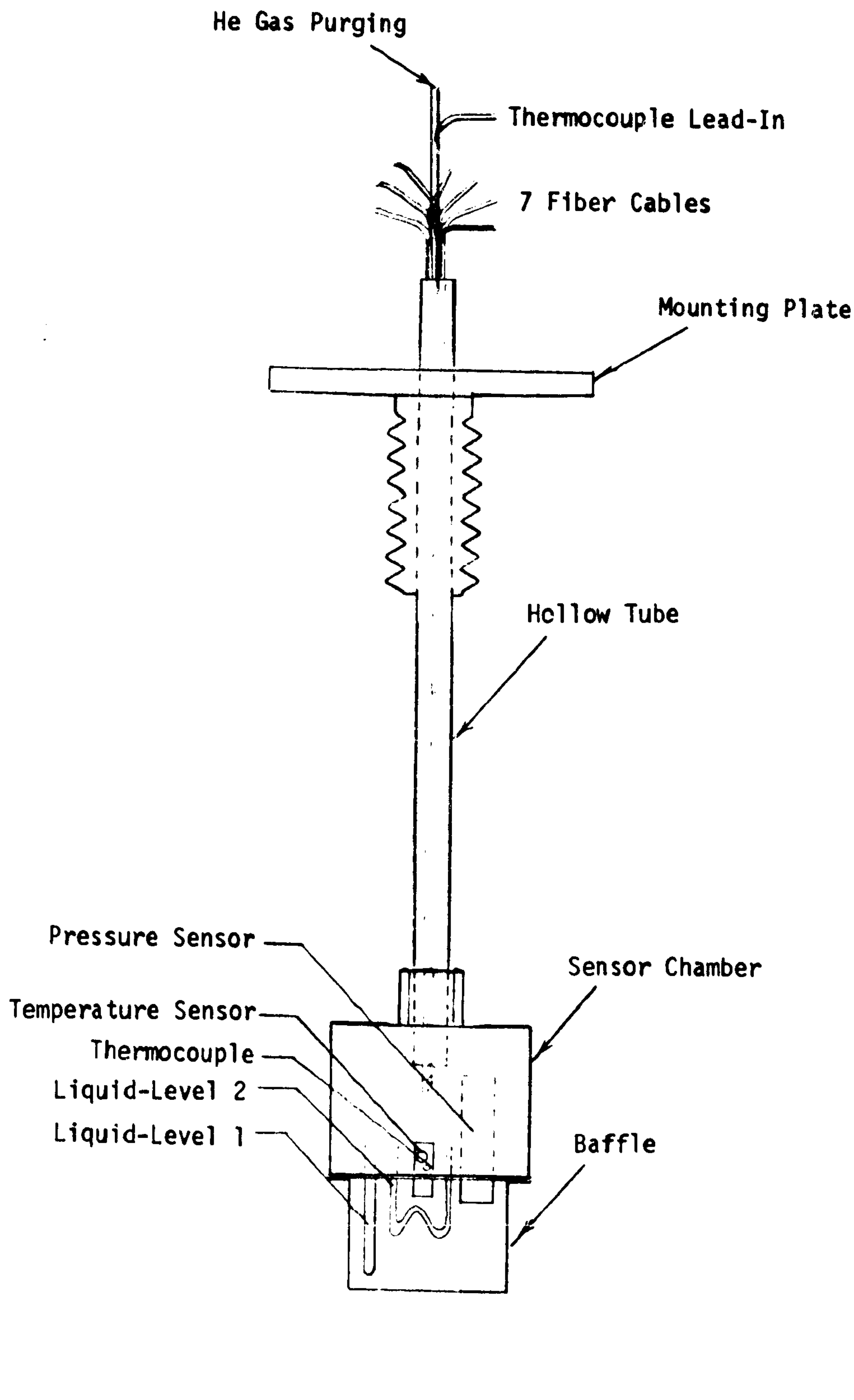

Figure 3-2. Sting Assembly

Sensor performance goals versus achieved performance of the experimental model are noted in following Sections 3.1.1 through 3.1.11.

3.1.1 Environment

The cryogenic Dewar of the experimental model allows testing of the sensors at 77°K.

3.1.2 Operation Mode

The sensor chamber and the sting assembly can be lowered or raised five inches. This provides sufficient height variation to cover and uncover the sensors during dry-to-wet or wet-to dry operation.

3.1.3 Level Accuracy

As discussed under level-sensor design methodology, the decision height-of-level indication is less than the diameter of the glass rod used to construct the liquid sensor. In the experimental model the sensors are of 1-mm diameter rod. Therefore the level accuracy is 1 mm or less. The diameter of the smallest tank that can provide 0.1 percent level accuracy by volume would be 10 cm provided the tank is cylindrical.

3.1.4 Temperature Range

The experimental model operates at 77°K. Its design permits operation down to 20°K, although no tests have been performed to evaluate operation below 77°K.

3.1.5 Pressure Range

Although the Dewar is designed for 350 psig, no tests have been performed with pressures higher than 45 psig.

3.1.6 Time Response

- Level Sensor: "On" time is limited only by the time constants of the receive electronics, whereas "Off" time is dependent upon the time needed for the sensors to dry off. Care has been exercised in designing the shape of the sensor to preclude clinging of liquid. Assessment of success in meeting this requirement was accomplished by monitoring the output signal of the sensor on the scope while the Dewar was being jolted. Best estimate is the response time was approximately 150 msec "On" time and 300 msec "Off" time.

- Pressure Gage: The limiting factors for the pressure gage time response are the mechanical time constants of the diaphragm. With appropriate analysis it can be shown that the time response is less than 100 msec.

- Temperature Gage: In the present setup, the light source is a pulsed laser diode that is pulsed once every 750 msec (i.e., one reading every 750 msec). The response of the temperature gauge gauge therefore is 750 msec. This performance can be improved by selecting different laser diodes that would operate at pulsing frequency of greater than 10 Hz.

3.1.7 Sensor Installation Accuracy

All sensors are designed to be affixed by cyogenic epoxy onto the reference platform. A simple jig can be used to assure installation within an accuracy of 0.1 inch.

3.1.8 Sensor Location

The only factor limiting the distance between the location of the sensor and the electronics is the lineal attenuation of the fiber. The fiber bundle being used presently is Galite 2000, which has an attenuation of 650 dB/km. The worst-case power margin of only 15 dB of the level sensors includes the loss of 60 feet of fiber. Extra length of fiber will increase the system loss by 3 dB, which would leave 12 dB as an adequate power margion.

In the experimental model, one of the level sensors is fitted with 30 meters of fiber each way, which clearly demonstrates the capability of sensors operating at a distance of 100 feet.

3.1.9 Flow Location

This performance goal relates to mechanical strength of the various sensors. Mountings of the sensors are sufficiently sturdy to withstand 27 fps liquid flow. Sensors are further projected by a baffle that is installed around the sensors.

3.1.10 Sensor Lifetime

- Sensor lifetime is principally dependent upon the following moving mechanical parts:

  - Bellows on the sting.

  - Rack and pinion installed on the sting to raise and lower the sensors in the Dewar.

  - Crank handle mounted on the Dewar.

  - Rubber gasket between the Dewar and the cover.

  - Tube joints connecting LN_2 and helium to the Dewar.

- The steel bellows can fail due to any puncture in it. Therefore, unless it is punctured accidentially, it can last for 200 cycles and fatigue failure can be precluded for 200 cycles.

- Rack and pinion can be damaged if the sting is moved forcibly while frozen due to frozen-water moisture in the sting guides. Correct procedure would be application of heat with a small heat gun until the sting frees itself. If accidentially damaged before 200 cycles, the rack and pinion can be repaired using very ordinary mechanical components.

- Crank handle is sufficiently sturdy to last for 200 cycles. Rubber gasket should be replaced as necessary.

- Tube joints should be replaced as necessary.

3.1.11 Lifetime of Electronics

Electronic components lifetime is estimated to be at least one year of continuous use. Degradation of LEDs and of the laser diode within one year have been considered in the design, and appropriate margins have been incorporated. However, periodic failures have not been precluded, and replacement parts are easily available.

3.2 TEST PROCEDURES

Setup and measuring procedures are complicated only by the two requirements that the Dewar must be free of moisture and that the pressure gauge must be calibrated differently at different temperatures. It must be noted that presence of moisture in the Dewar interferes with operation of the liquid-level sensor because of moisture condensation.

3.2.1 Initial Setup

The demonstration model is broken down for shipment into two major elements consisting of the console and the sting assembly. For reassembly, the Dewar should first be mounted on the side of the cabinet, using the brackets and hardware that are provided. Proper care must be exercised in handling of the Dewar because the fiber cables emerging from the Dewar and from the sensor assembly within the Dewar are relatively fragile.

After the Dewar has been installed, the seven fiber cables together with the thermocouple lead-in can be passed through the hole on the side of the cabinet. The surplus lengths of the cables can then be coiled and stowed outside the cabinet in the manner indicated in Figure 3-3. All fiber connections should be installed as shown. Because the fiber-optic connectors are made of plastic and are therefore fragile, particular care must be taken to avoid misalignment of connections and resulting stripped threads. Proper installation of Dewar and of the fiber cables may require as much as four to five hours.

After all fiber connections have been made the ac power cord may be plugged into any 117-Vac outlet and the electronics turned on by actuating the power switch on the front panel. The two digital meters should then light up.

The final step is to purge and to cool down the Dewar.

3.2.2 Cool-Down and Moisture-Purging Procedure

1. Inspect empty test Dewar interior for moisture droplets. Wipe Dewar walls and floor if any visible moisture is present.
2. Insert sensor module into test Dewar. Secure cap with screws provided.
3. Open test Dewar exhaust valve.
4. Purge test Dewar with gaseous helium via its fill tube for about 15 minutes.
5. Simultaneously purge sensor module interior with gaseous helium via the Optical Cable Access tube. Reduce gas flow to a "trickle" after 15 minutes and continue the "trickle purge" throughout

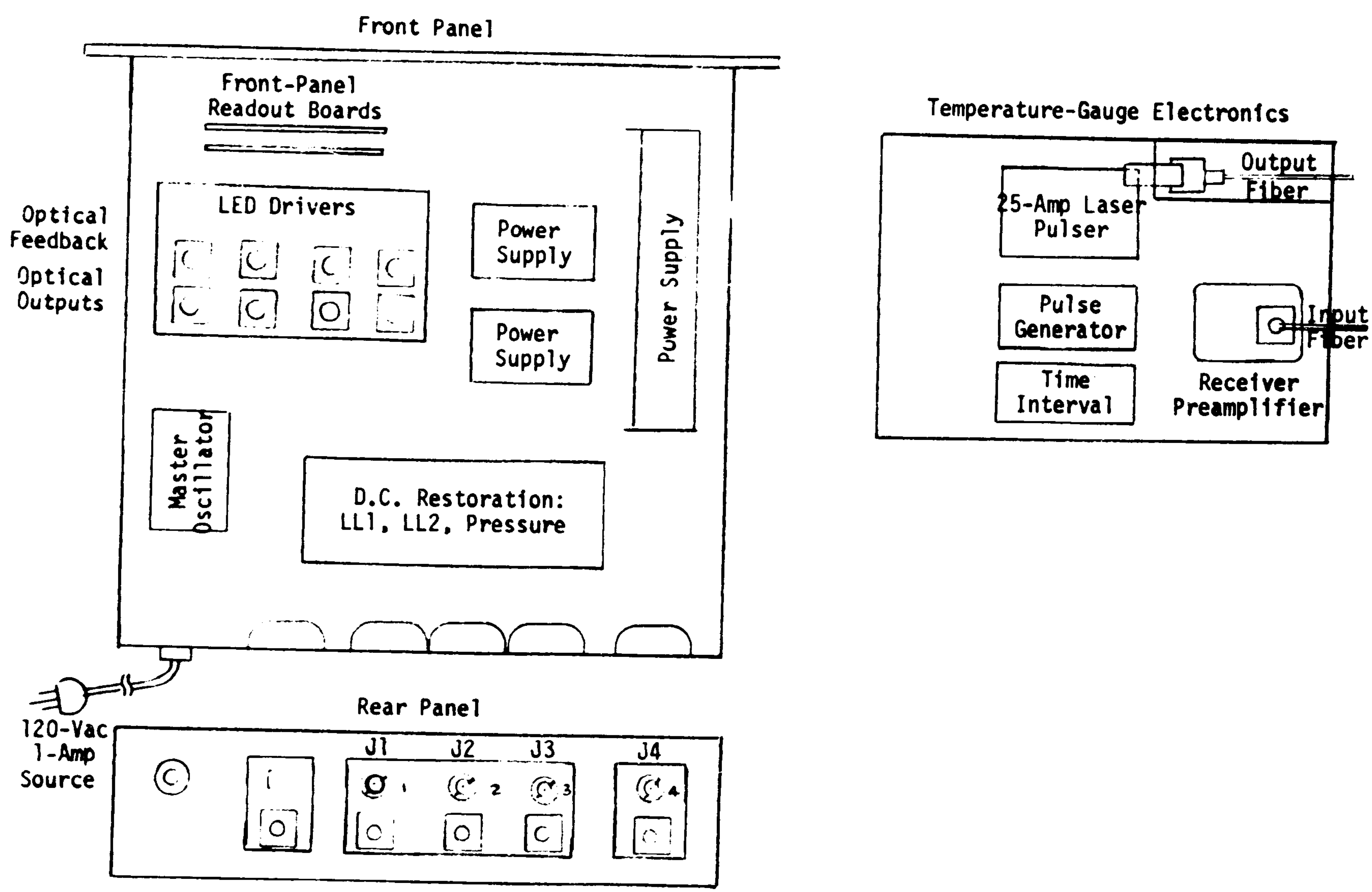

Figure 3-3. Experimental-Model Fiber-Optic Connections

demonstration. When testing temperature sensor withdraw purge tube to within 3 inches of top of access tube to prevent spurious heating signal from helium flow.

6. Close test Dewar exhaust valve and built up 5 psig in test Dewar, and then shut off helium flow to fill tube.

7. Remove helium input line from fill tube and connect liquid nitrogen transfer tube.

8. Crack nut on transfer tube at supply Dewar, re-open test Dewar exhaust valve, and purge transfer tube by directing helium back through the test Dewar exhaust line. (For this operation the helium input line can be hand-held to exhaust port.) After purging re-tighten nut on transfer tube.

9. Position sensor module about midway on the gear rack positioning mechanism.

10. Open test Dewar exhaust valve.

11. Fill test Dewar "slowly" with liquid nitrogen to desired level, as indicated by level sensors.

12. Insert sensor module about 2-1/2 inches into liquid nitrogen and allow about <u>60</u> minutes to achieve thermal equilibrium. Top off liquid nitrogen as required during equilibration. It will be necessary to top off three or four times.

13. Proceed with all demonstrations. Refill as necessary.

SPECIAL NOTES ON COOL-DOWN PROCEDURE

Item 1: If LN_2 is left in Dewar ice will form inside.

Item 2: GN_2 is satisfactory for initial purge, but after liquid nitrogen is in Dewar any further purging should be done with GHe because of its lower freezing point.

Item 6: Positive pressure inside Dewar keeps moisture out.

Item 11: Filling takes approximately 9 minutes.

3.2.3 Calibration Procedures

Calibration procedures consist mainly of adjusting the output levels of the LEDs that provide optical power to the sensors. The criterion of proper adjustment is to ensure particular voltage level at the output of the receiver preamplifier, which in this case is 1-V peak. The liquid-level sensors and the pressure-gauge detection circuits then are adjusted to operate properly with 1-V signals. Once these levels are set no future adjustments are necessary because all the LEDs incorporate an optical feedback arrangement which keeps LED output constant. However, readjustment will become necessary whenever the fiber optic connectors are remated. Calibration can be accomplished using a triggered oscilloscope. A 3-channel oscilloscope unit would be most appropriate in order to allow the two level sensors and the pressure sensor to be adjusted simultaneously. The temperature gauge does not require any calibration. The oscilloscope should be connected as shown in Figure 3-4. With the levels of each output set at a 1-V peak with the trimpots located on the front panel, the pressure linearity pot should be adjusted to cause the pressure meter to read zero with zero pressure. The temperature gauge requires no adjustment because it is dependent upon time measurements rather than on voltage measurements.

A thermocouple is attached to the fiber-optic temperature gauge for calibration purposes. The thermocouple leads should be connected to a dc millivolt meter. The output of the fiber-optic temperature gauge can also be monitored on an oscilloscope, but should be done on a different unit because the repetitition rate of the temperature gauge is approximately 1 pps whereas those of the other gauges are 1 kHz. Scope connections to monitor the temperature gauge also are shown in Figure 3-4. It is advisable although not necessary to leave the oscilloscopes connected while demonstrating operation of the experimental model.

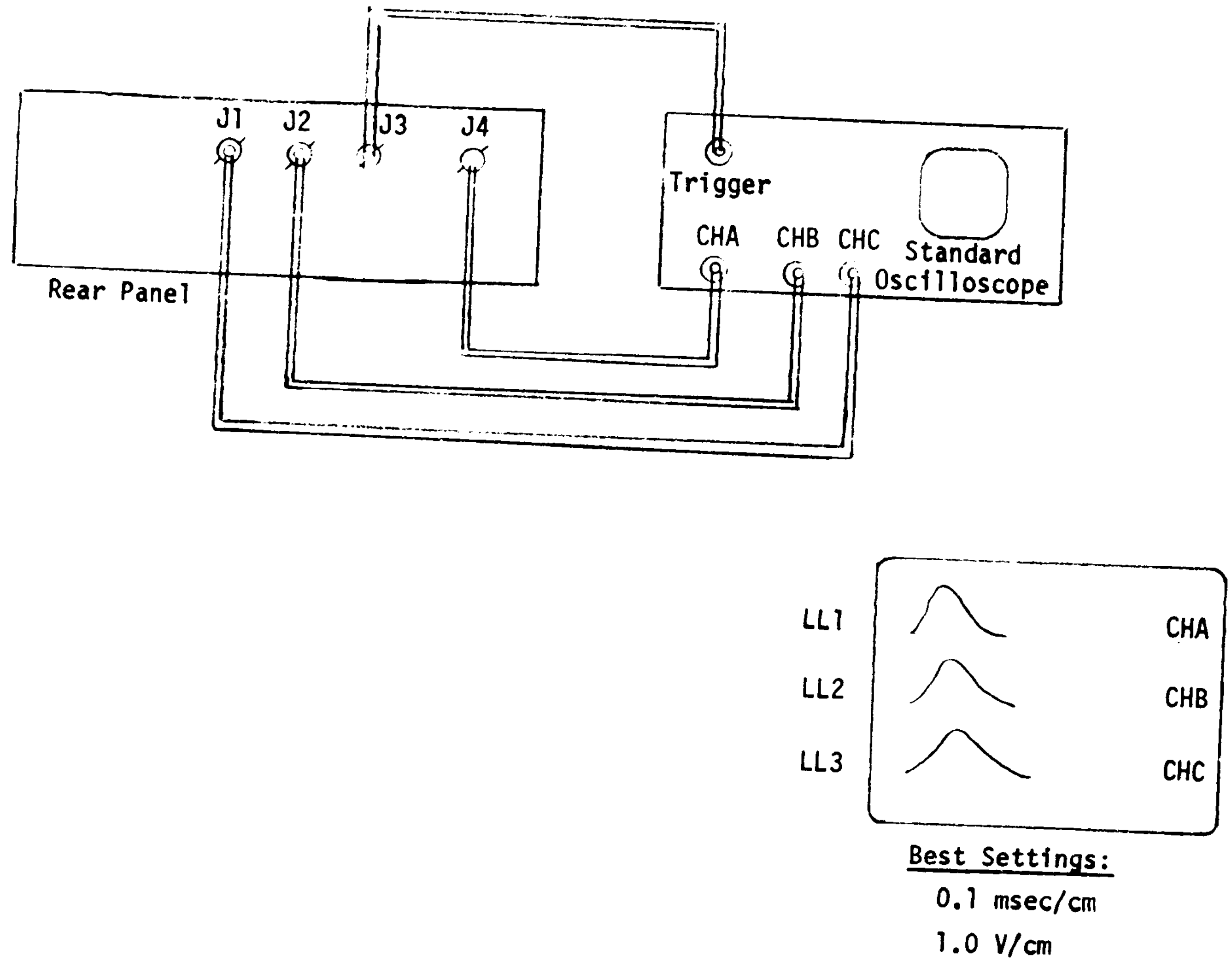

Figure 3-4. Oscilloscope Connections for Experimental-Model Electronics Calibration

3.2.4 Demonstration Procedure

Liquid-level sensor operation is demonstrated by moving the sting assembly up and down (in and out) of the stabilized LN_2. The sensing lights should come on when the sensors are immersed in the liquid.

The pressure sensor may be demonstrated by applying pressure at the LN_2 input line. This is most effectively accomplished by replacing the LN_2 bottle with a helium gas bottle. After closing the relief valve on the Dewar, pressure is applied by opening the valve of the helium gas container. Readings of the fiber-optic gauge are then compared with those of the mechanical pressure gauge at the helium bottle. Experimental data and a lookup table are included in Section 4. Temperature-gauge demonstration is accomplished by lowering the sting sufficiently to immerse the temperature sensor in the liquid helium. Because the temperature sensor is mounted approximately 1 inch higher than the No. 2 liquid-level gauge, the sting therefore must be lowered 1 inch past the indication of that liquid-level sensor. At this point both the fiber optic sensor and the thermocouple should read $77^{0}K$. Operation of the temperature gauge can be demonstrated by raising the sensor assembly out of the liquid and observing the temperature rise. The two gauges should always agree with each other, although any thermal lag between the two can result in some difference in the readings.

3.3 ELECTRONIC SUBSYSTEM

Figure 3-5 is the block diagram of the total electronic subsystem of the experimental model. The electronics for the two level sensors and for the pressure sensor are located behind the main panel and the temperature-gauge electronics are located behind the other panel. Electronics for the two liquid-level sensors are shown in Figure 3-6(a). The master 1-kHz pulser serves as an approximately 10-percent-duty-cycle pulser to all four transmitting LED drive circuits (i.e., both level sensors, pressure sensor, and spare channel). Each of the drive circuits apply power to its corresponding LED while also responding to the feedback circuit to keep the optical power of the LED at a constant level. The receive circuit of the level sensors is comprised of a

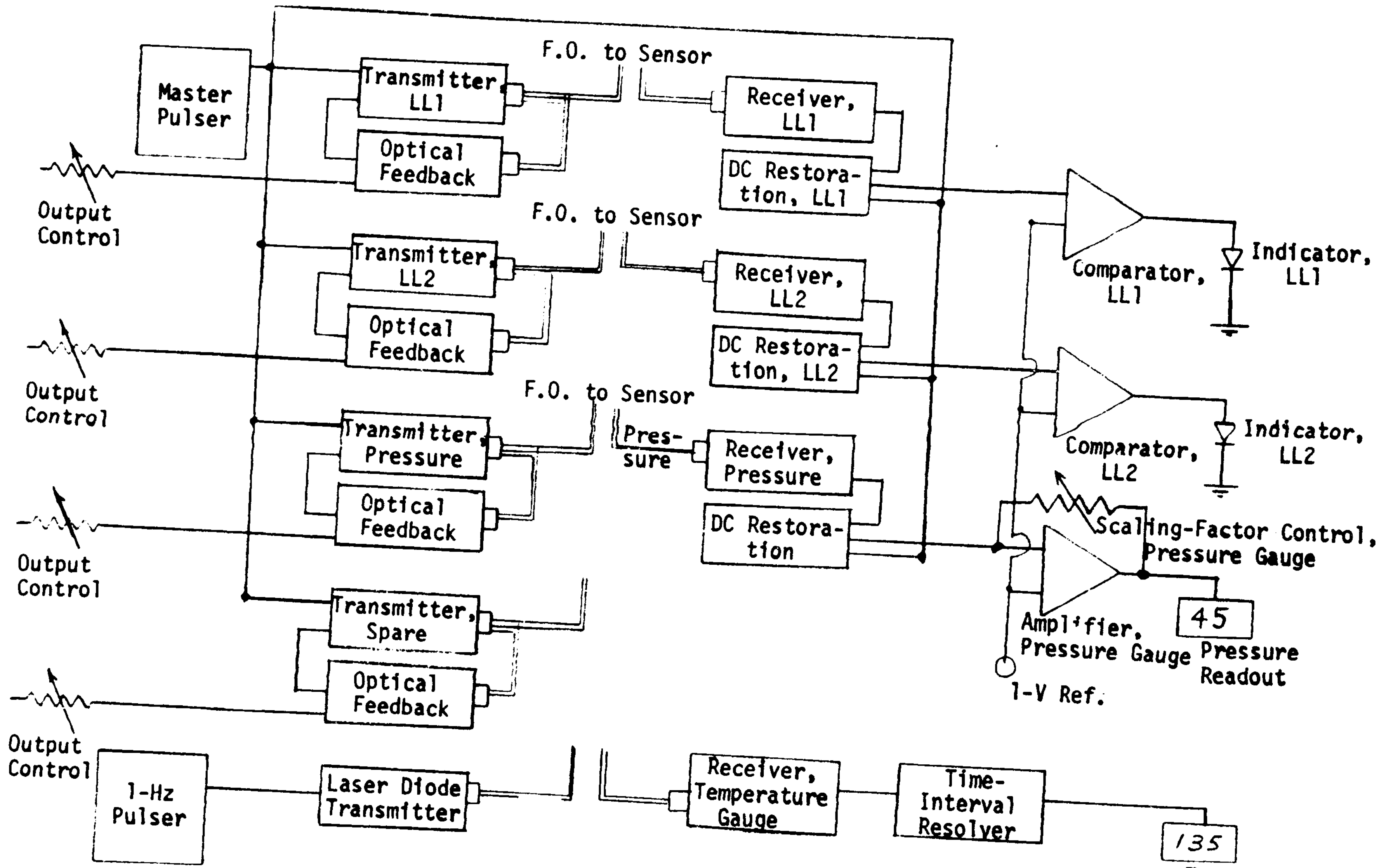

Figure 3-5. Block Diagram of Experimental-Model Electronic Subsystem

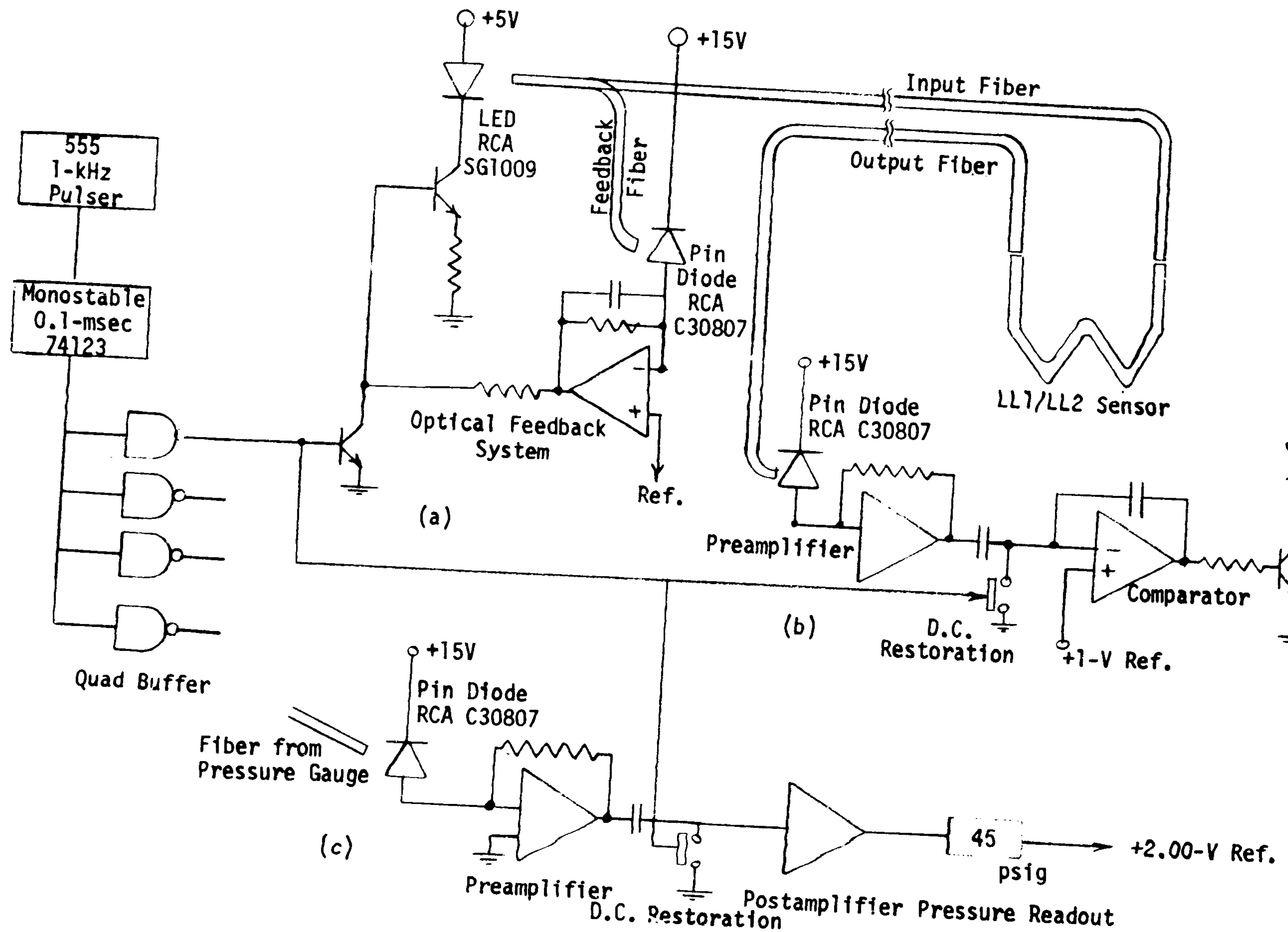

Figure 3-6. Block Diagrams for Liquid-Level, Pressure, and Temperature Gauges

high-gain low-noise transimpedence bandpass amplifier, a dc restorer circuit, a threshold detection circuit, and the indicating LED drive circuit. The block diagram is shown in Figure 3-6(b), and a complete schematic is included in Section 4. Although that block diagram details operation of the level-gauge electronics, a few specific characteristics particularly should be noted. For example, a pulsed signal rather than a dc signal was selected in order to minimize dc drifts in the receiver, and a 10-percent rather than a 50-percent duty cycle in order to obtain most peak power from the LED.

The pressure-gauge electronics as shown in Figure 3-6(c) obviously is very similar to the level-gauge electronics, except that the threshold-detection circuit has been replaced by a linear amplifier which drives the front-panel pressure readout.

Conversely, the temperature-gauge electronics differs greatly from the level-sensor electronics, as shown in Figure 3-7, in that the transmitter is comprised of a pulse generator that produces pulses at a repetition rate of approximately 1 Hz, with a pulsewidth of 10 microseconds. The pulse generator drives a 25-amp laser diode pulser which in turn drives a RCA SG 2007 laser diode. The optical power output of the associated laser is approximately 7 watts peak. The receive electronics also shown in Figure 3-7 is comprised of a low-noise high-gain wide bandwidth transimpedence preamplifier. The temperature-resolving electronics essentially is a time-interval-measuring circuit which measures the time between initiation of a laser power pulse and passage of the corresponding receiver pulse through the sensor. A detailed circuit diagram also is included in Section 4.

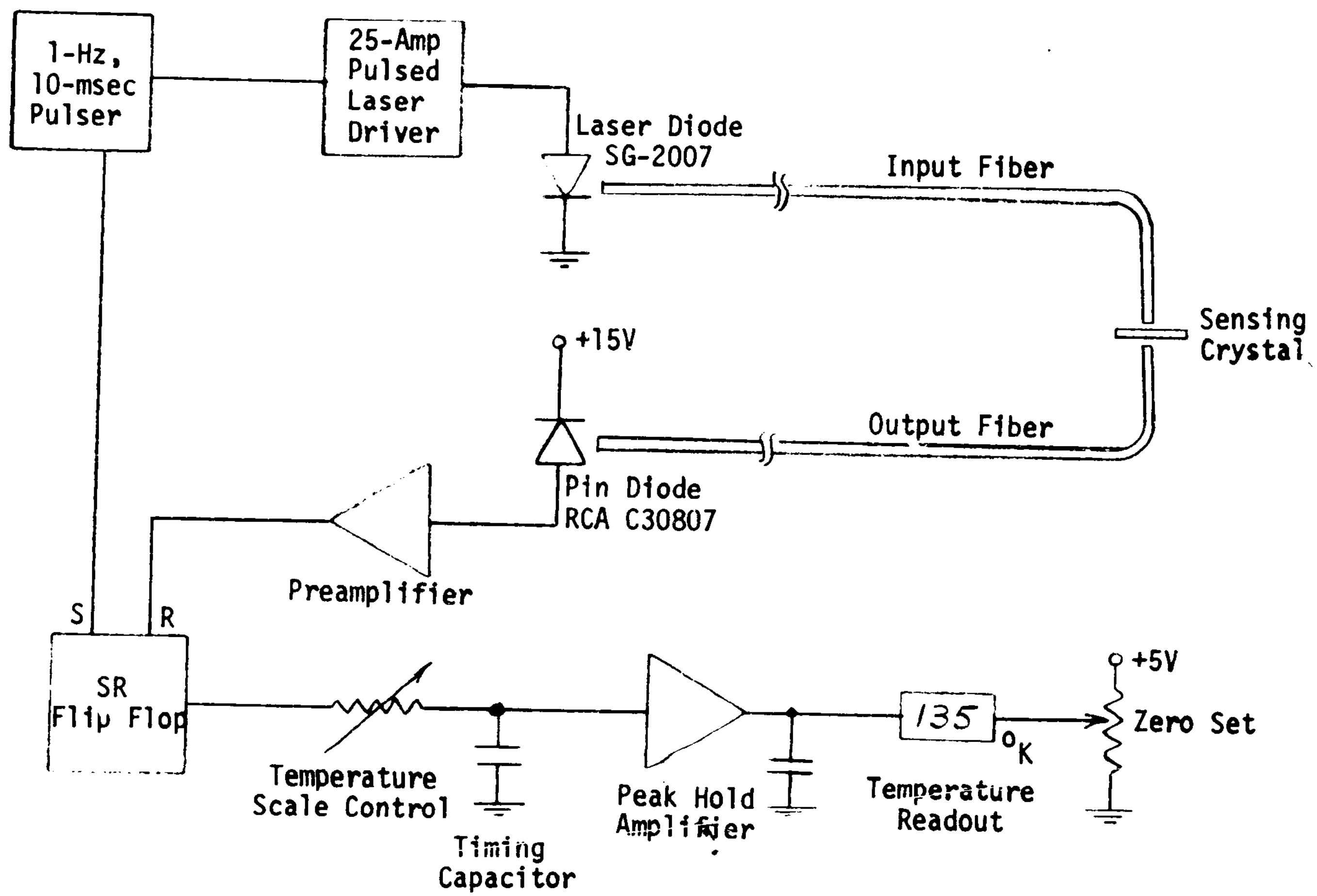

Figure 3-7. Block Diagram of Temperature-Sensor Resolving Electronics

4. SENSOR DEMONSTRATION MODEL DESIGN DESCRIPTION

This section summarizes design details, final data, and schematics of the TRW experimental cryogenic sensors demonstration model. Presented information reflects resolutions to problems recognized following other conceptual and sensor-selection phases of this project, during which it was found necessary to obtain various pertinent data that additionally were required for successful design of the final sensors.

Because the prevailing approach to level sensing proved in various ways to be inappropriate within cryogenic environments, it was found necessary to introduce many modifications in order to assure satisfactory level detection of cryogenic liquids having very refractive indices. Similarly, the pressure gauge required appropriate redesign to properly adapt it to its intended usage. On the other hand, the temperature gauge is essentially new, and several aspects of its operation had to be validated experimentally before its final design could be implemented.

4.1 LIQUID-LEVEL SENSOR

In the conceptual study the bare-fiber concept was selected. Although some of the preliminary experimentation clearly showed excellent feasibility (Ref. 2), these experiments were conducted with a HeNe laser without incorporating the signal-conveying fibers, fiber-optic connectors, and practical electronics. Consequently, practical level sensors based on the conceptual model suffered enormous loss, and the return optical signal was too small to be processed.

Several liquid-level sensors that were fabricated yielded the loss and sensitivity measurements itemized in Table 4-1. These data served to identify the approach to the final sensor shown in Figure 4-1. The new sensor has a throughput loss of 22 dB, sensitivity of 8 dB in LN_2, calculated sensitivity of 2 dB in LH_2, and a decision height of 0.25 mm. Further design work also was necessary to determine the most desirable adhesive for attaching the sensor to the sensor head. This was found to be "Scotchcast" XR-5241 material manufactured by 3-M Company, the only material that works satisfactorily in a cryogenic environment and that also has a high refractive index. This epoxy has been used to mount the sensor

Table 4-1. Liquid-Level Sensors Insertion-Loss and Sensitivity Data

LL Sensor Test Configuration	Insertion Loss (dB)	Sensitivity (dB)
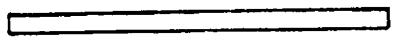	0.3	N/A (LN_2)
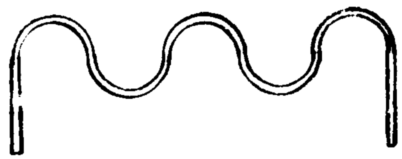	-36	6 (LN_2)
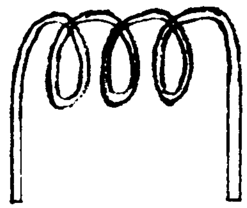	-32	4
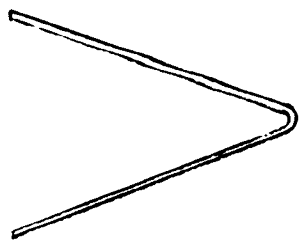	-10	6
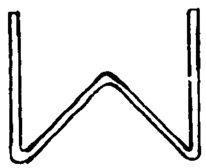	-18	8

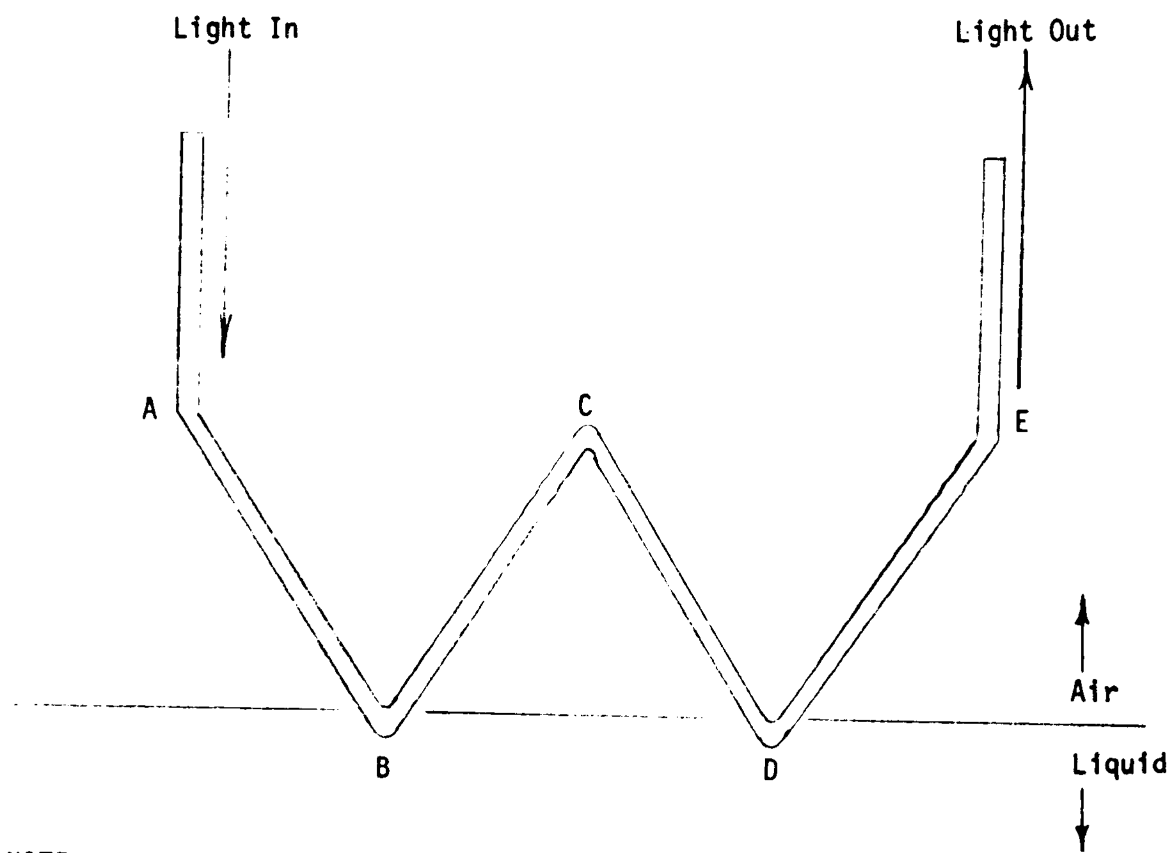

NOTE: Bends A, B, C, and D are scattering centers. Bends B and D are the bends where detection occurs. Bend E has no effect on sensing but is incorporated to provide symmetery.

Figure 4-1. Final Liquid-Level Sensor

to the sensor chamber while providing a cryogenic seal between the liquid and the dry environment inside the sensor chamber. Because use of epoxy increases the throughput loss, such loss was avoided by applying a coating of platinum at the point where epoxy would be emplaced. Measurements of losses of various configurations are given in Table 4-2.

In the final design a special bushing has been used together with glass windows to minimize loss due to attachment of the sensor. The arrangement now being used, and also a newer technique which has not been incorporated in the present experimental model have been described in detail in a current TRW publication (Ref. 2). A schematic diagram of level-gauge electronics is presented in Figure 4-2.

4.2 PRESSURE GAUGE

The pressure gauge of the experimental model resembles the conceptual design, and no modification was found necessary. However, the present design manifests a thermal shock effect which results in a thermal drift, whose effect can be minimized using proper calibration techniques. As noted in the discussion of the conceptual phase, the pressure gauge is based upon the known technology of measuring the distance of a reflective diaphragm from a sensing bifurcated fiber bundle by determining the amount of light that is reflected through the bundle. Figure 4-3 evaluates the function of reflected light versus distance. It should be noted that this curve displays two slopes, which represent the behavior of the reflected light as the diaphragm moves away from the fiber. The reflected light increases up to a certain peak and then starts to decrease. The zero-pressure diaphragm placement is at the point indicated in Figure 4-3, and as pressure increases the reflected light decreases.

Pressure-gauge electronics are arranged in such a manner that a certain voltage level (1-V peak in this case) designates zero pressure. Any output voltage less than zero then is indicated on the meter as a pressure reading. In the experimental model the gain values of the pressure-gauge receive electronics translate to 1 millivolt per pound of pressure.

Table 4-2. Signal Loss Due to Epoxy

Sensor Configuration	Insertion Loss (dB)
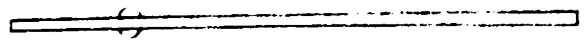 (1 Epoxy Ring 1.5 mm Wide)	10
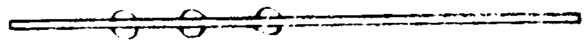 (3 Epoxy Rings Each 1.5 mm Wide)	14
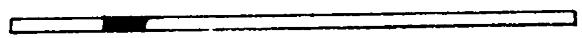 (Platinum Coating 0.2 in Wide)	7
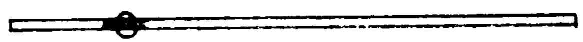 (Platinum Coating 0.2 in Wide Plus Epoxy Band)	9

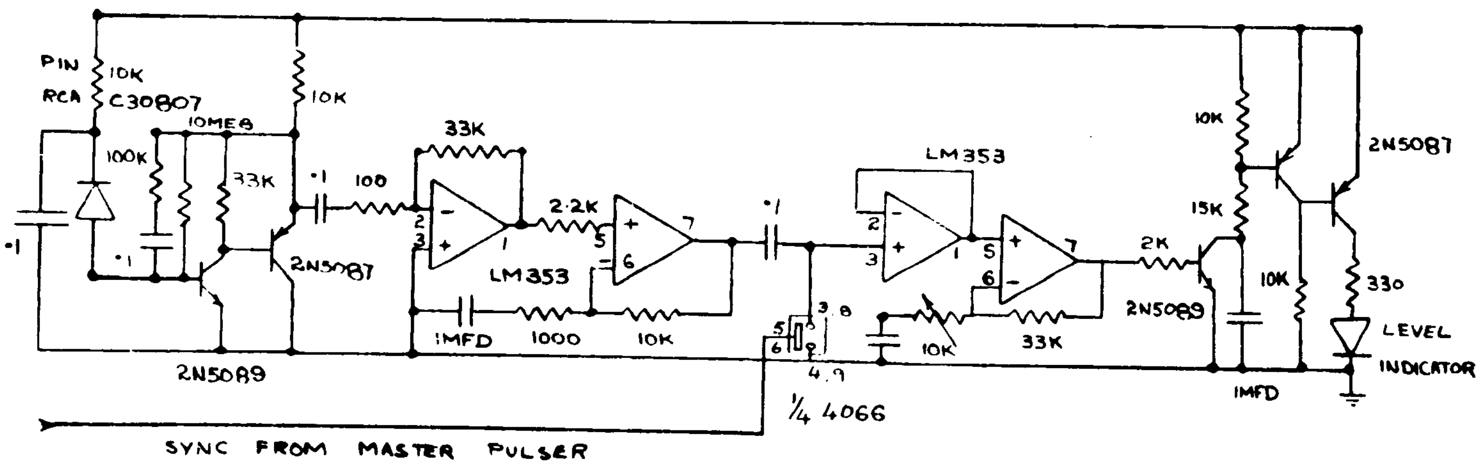

Figure 4-2. Level-Gauge Electronic Schematic

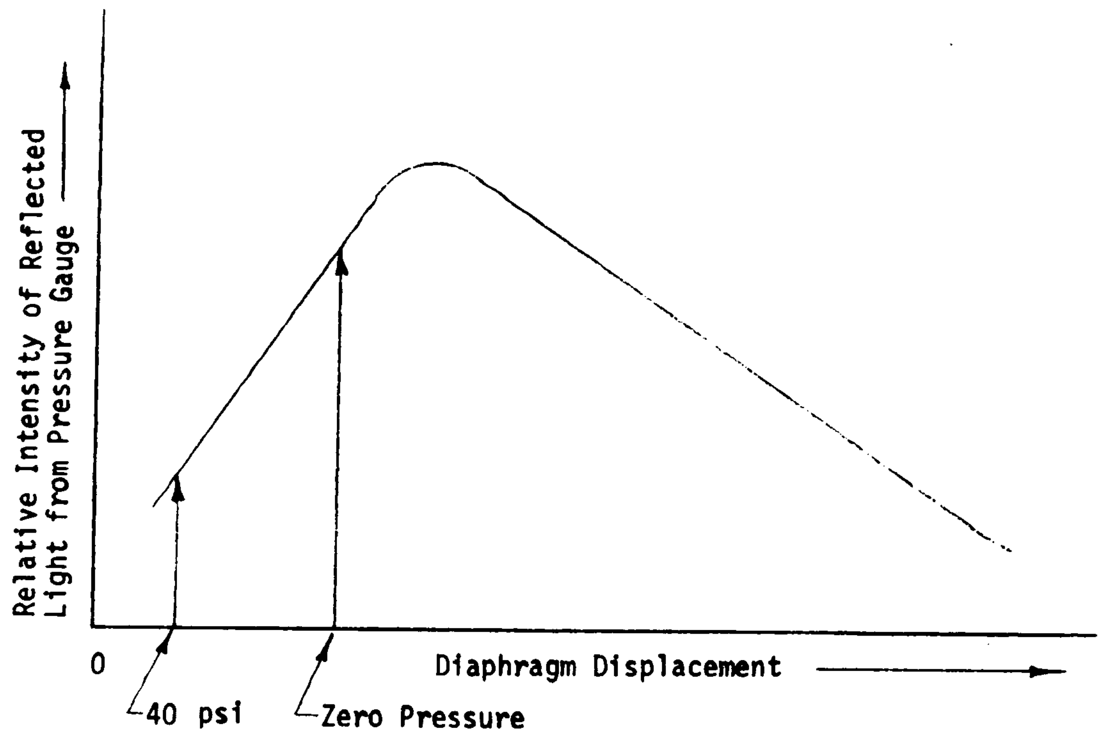

NOTE: Zero pressure adjustment shown at portion of curve yielding best linearity in pressure readings. A 0.006-mil diaphragm was selected to cover range of 0-40 psi.

Figure 4-3. Diaphragm Displacement vs. Reflected Light

Table 4-3 summarizes measured data up to 40 psi, within which range the pressure gauge is fairly linear. However, care must be taken while calibrating the pressure gauge in order to avoid effects of thermal shock. Table 4-4 is the associated lookup table. Pressure-gauge construction details and electronic schematics are shown in Figures 4-4 through 4-7.

4.3 TEMPERATURE GAUGE

An InP crystal was selected as the sensing crystal to accommodate the desired temperature range of $4^{O}K$ to $135^{O}K$. The bandgaps of InP and of GaAs are offset from each other roughly $300^{O}C$ and the sensitivities of crystals operating at room temperature and at cryogenic temperatures are in the ratio of 1:10. Therefore, the temperature of the GaAs laser diode must be swept from room temperature to 25^{O} above room temperature to cover the desired range of temperature measurement.

The basic premise of temperature measurement for present purposes is to measure bandedge shift. Also, the key issue in designing the temperature gauge is to develop simpler methods of measurement. Some of the suggested methods incorporated use of complicated and delicate optical components, and the effect of bandedge shift was measured in terms of amplitude. However, measurement of amplitude always includes drifts that cause inaccuracies in measurement. Also, resolution of the prevailing method is poor because the slope of the bandedge curve from 10 to 90 percent of the slope is $55^{O}C$ wide, as shown in Figure 4-8 for a GaAs crystal. The swept-spectrum method of measuring bandedge shift has been developed and incorporated in the experimental model. Full description of this technique has previously been published (Ref. 5). The light source is an RCA SG 2007 pulse laser diode. Although several other diodes also were considered, this wavelength and the thermal time constants of the SG 2007 diode were most suitable for this experiment. An elaborate setup including a spectrophotometer was used to measure the emitted wavelength shift as well as its range. Figure 4-9 presents oscillograms of this experiment, with results showing that the output wavelength of an SG 2007 diode shifts by 130 Å within 10 microseconds of the applied pulse.

Table 4-3. Pressure-Gauge Calibration Readings for Gauge Operating in LN_2

Pressure (psig)	Reading
0	00
5	07
10	11
20	20
30	29
40	38
60	56

Table 4-4. Pressure-Gauge Lookup Table for Gauge Operating in LN_2

Reading	Pressure (psig)
0	00
5	04
10	10
20	20
30	31
40	41
60	68

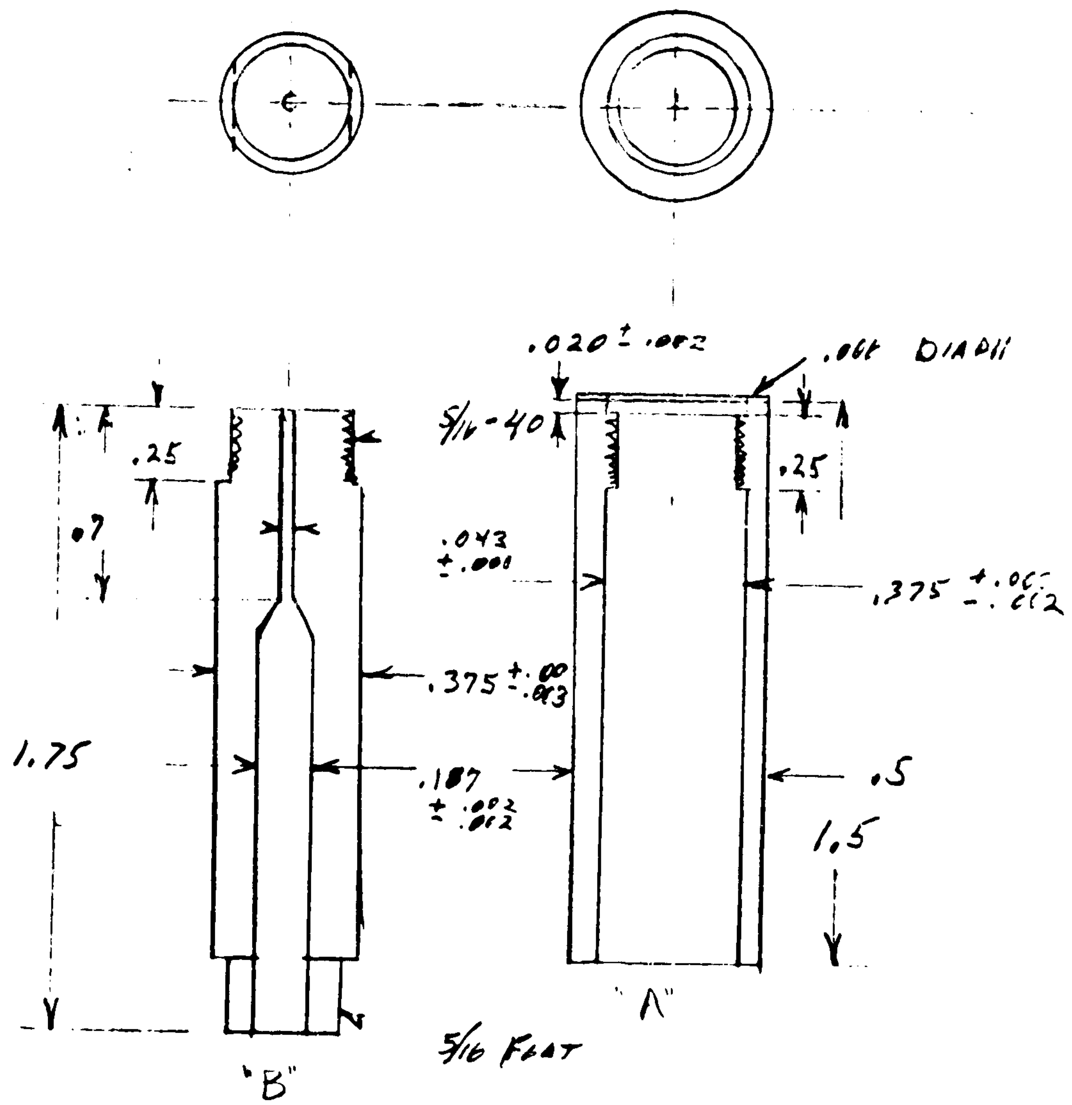

Figure 4-4. Pressure-Gauge Construction Details

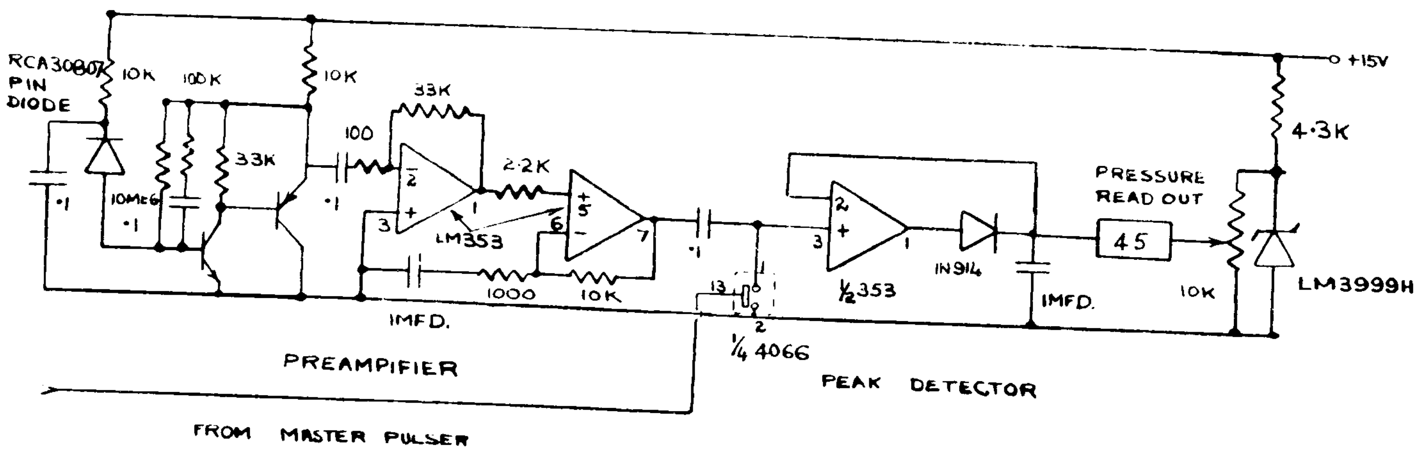

Figure 4-5. Pressure-Gauge Electronic Schematic

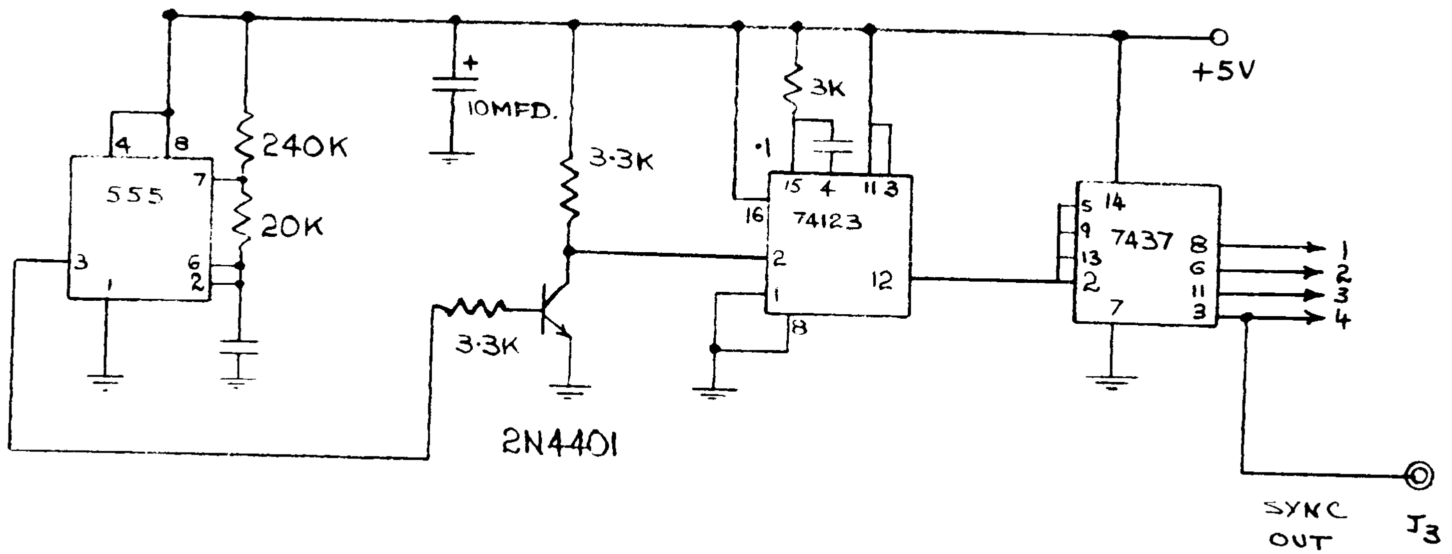

Figure 4-6. Schematic of Master Oscillator

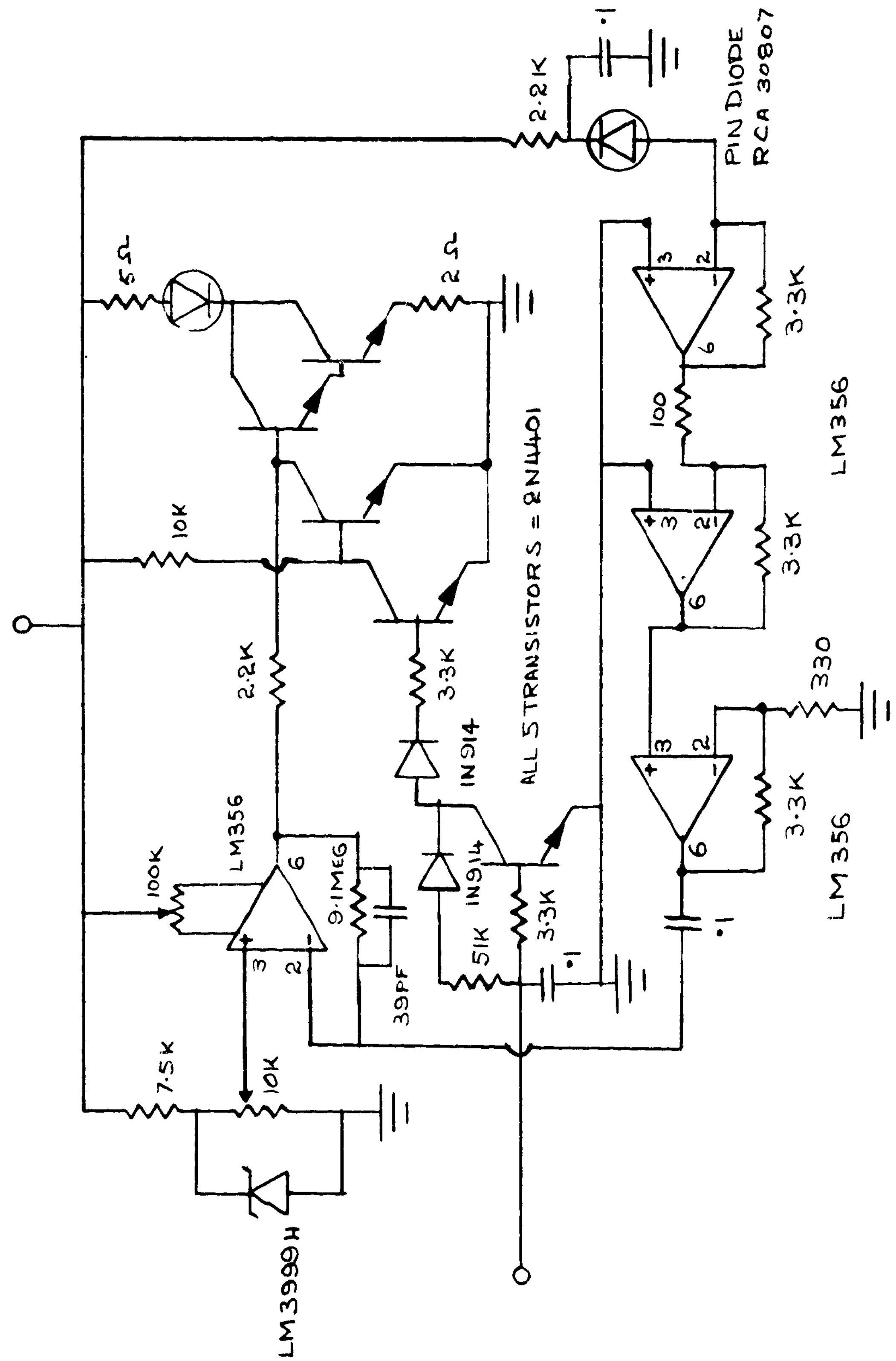

Figure 4-7. Schematic of LED Drivers with Feedback Control

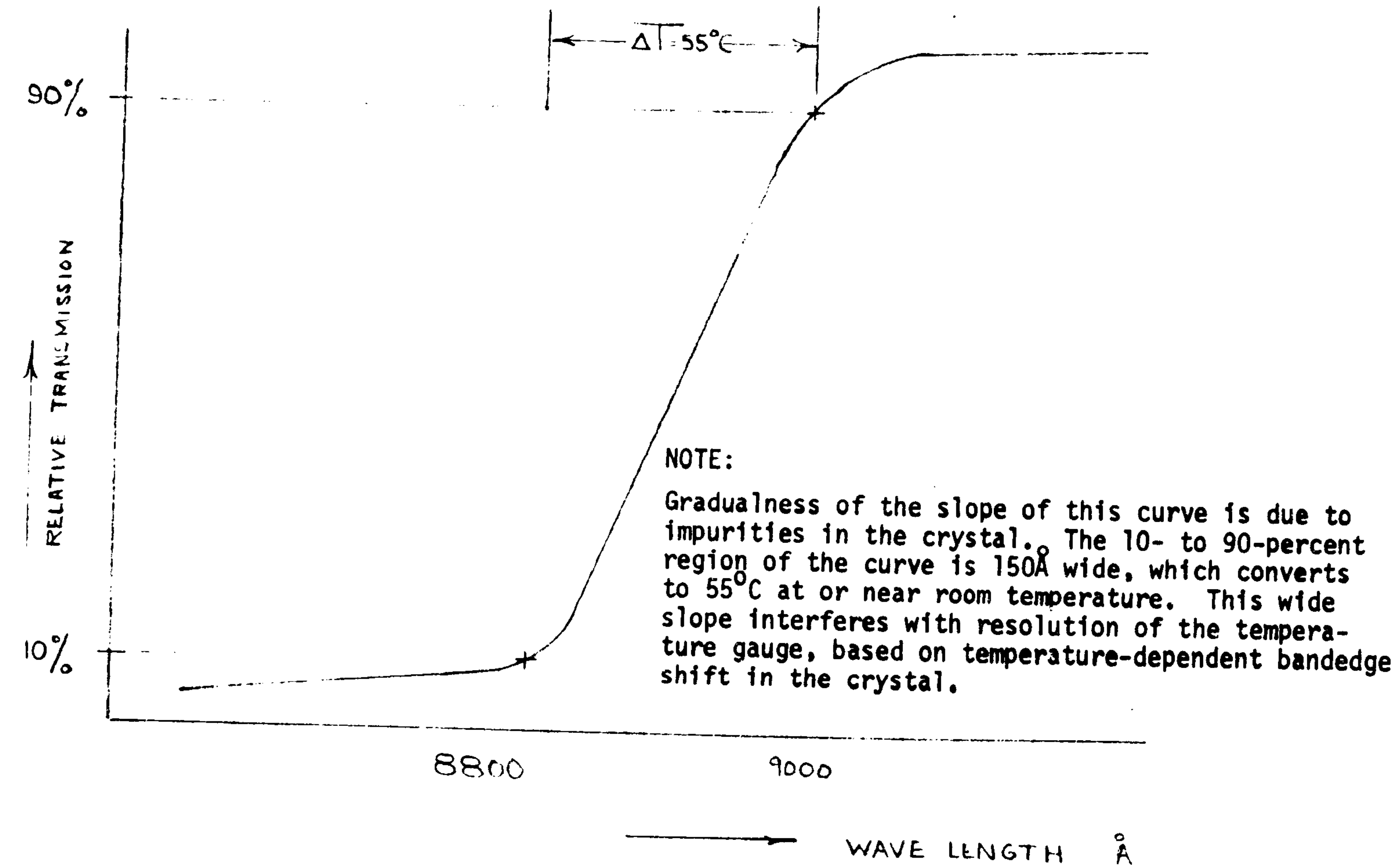

Figure 4-8. Bandedge Curve of GaAs Crystal

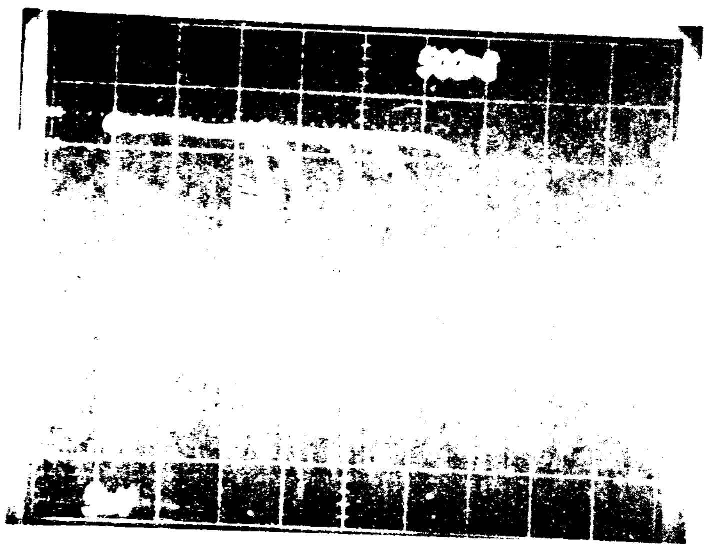

(a) Emission with Laser Diode at Room Temperature

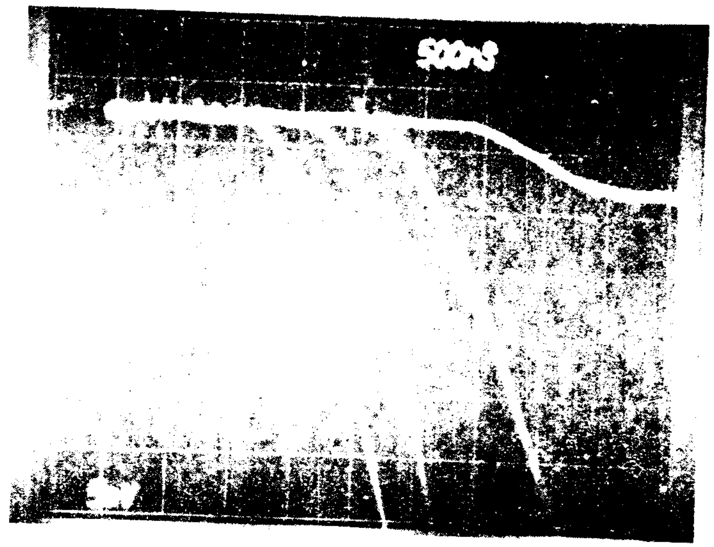

(b) Emission with Laser Diode at $-30^{o}C$

Figure 4-9. Oscillograms Showing Bandedge vs. Temperature for GaAs Laser Diode

Figures 4-9(a) and 4-9(b) illustrate emission wavelengths of an RCA SC-2007 laser diode at various junction temperatures. These exposures were obtained while the laser was being energized with 3-μsec 25-Amp pulses. The light was monitored through a monochromator tuned at various wavelengths. The time delay between initiation of a laser pulse and appearance of light is the time required for the laser-diode junction to heat sufficiently to emit wavelengths to which the monochromator is tuned. In Figure 4-9(a) the laser diode at room temperature has generated five wavelengths of 9050Å, 9060Å, 9070Å, 9080Å, and 9090Å. Figure 4-9(b) shows results of the same experiment with the laser junction cooled to -30^{o}C, producing wavelengths from left to right of 8970Å, 8980Å, 8990Å, and 9000Å.

These data were used to design required temperature-gauge electronics, for which a block diagram is shown in Figure 4-10. The transmitted pulse is 10 microseconds long and has a repetition rate of 1 Hz. Temperature is measured in terms of the time interval between initiation of the laser pulse and pulse arrival at the sensing crystal. The temperature gauge indicates the 77^{o}K (LN_2 temperature) reading by a time interval of approximately 4.5 microseconds.

Obtained experimental data of temperature versus temperature-gauge readings and the associated lookup table are given in Tables 4-5 and 4-6. Mechanical arrangement of the temperature gauge is depicted in Figure 4-11. Electronic schematics of the temperature gauge and of the associated 25-Amp laser-diode pulser are given in Figures 4-12 and 4-13 respectively.

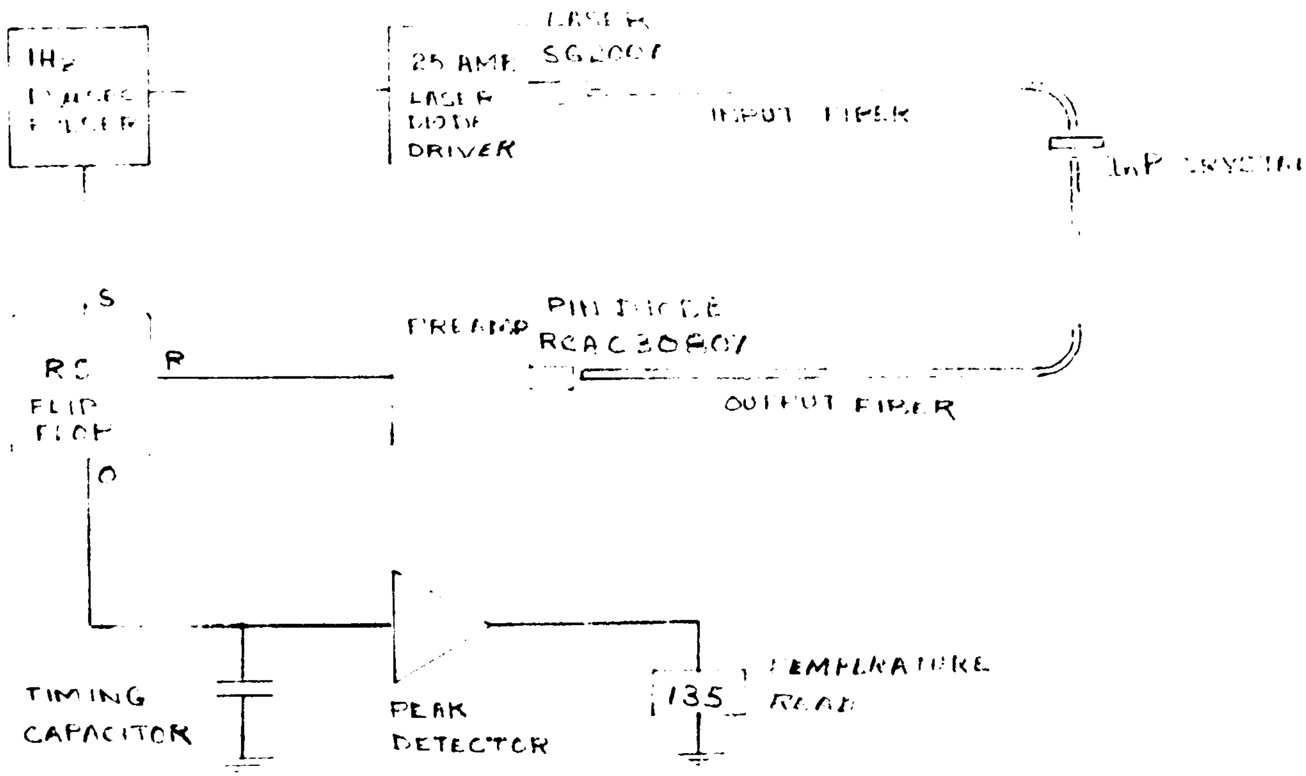

Figure 4-10. Block Diagram of Temperature-Gauge Electronics

Table 4-5. Temperature-Gauge Calibration Readings for Gauge Operating in LN_2

Temperature (^oK)	Reading (^oK)
78	78
80	81
85	89
90	96
95	99
100	112
105	115
110	130
115	150
120	170
125	198
130	OFL

Table 4-6. Temperature-Gauge Lookup Table for Gauge Operating in LN_2

Reading (^oK)	Temperature (^oK)
78	78
80	79
85	83
90	84
95	92
100	96
105	97
110	103
115	105
120	107
125	108
130	110

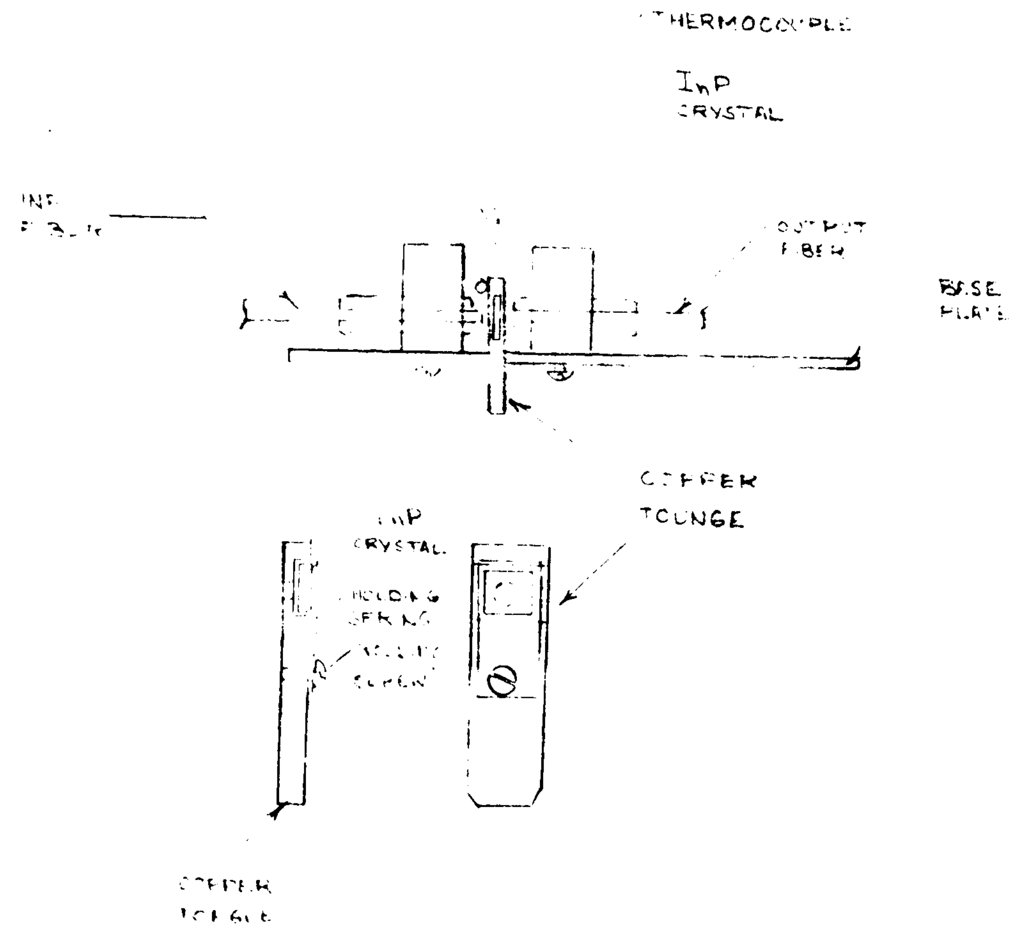

Figure 4-11. Temperature-Gauge Mechanical Arrangement

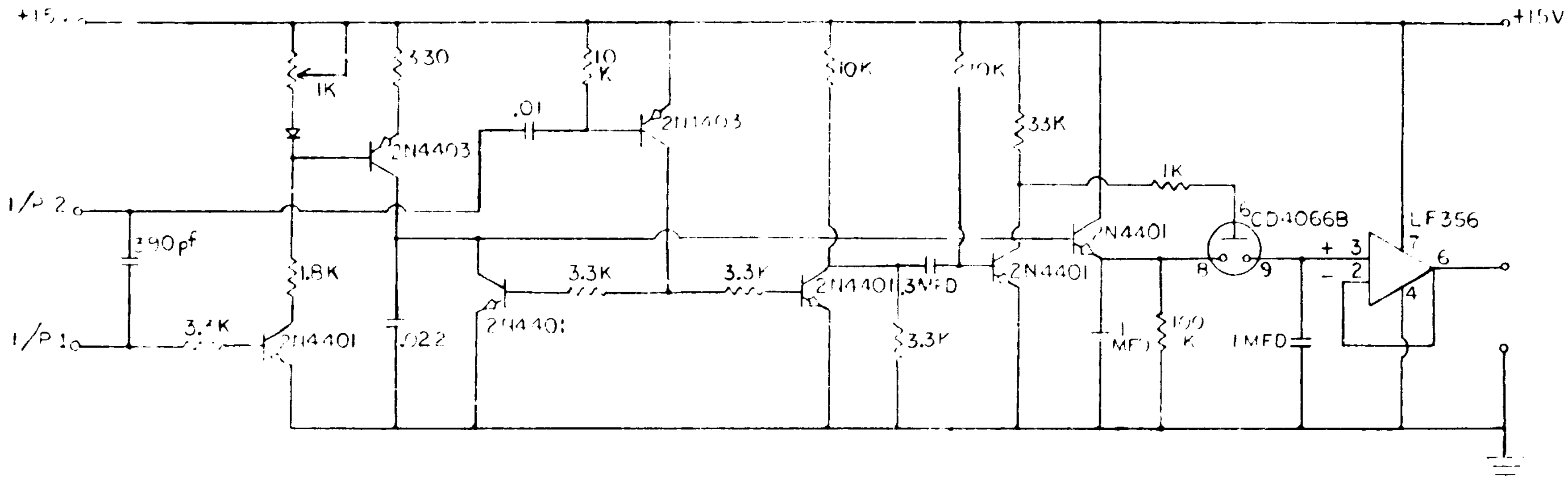

Figure 4-12. Temperature-Gauge Electronic Schematic

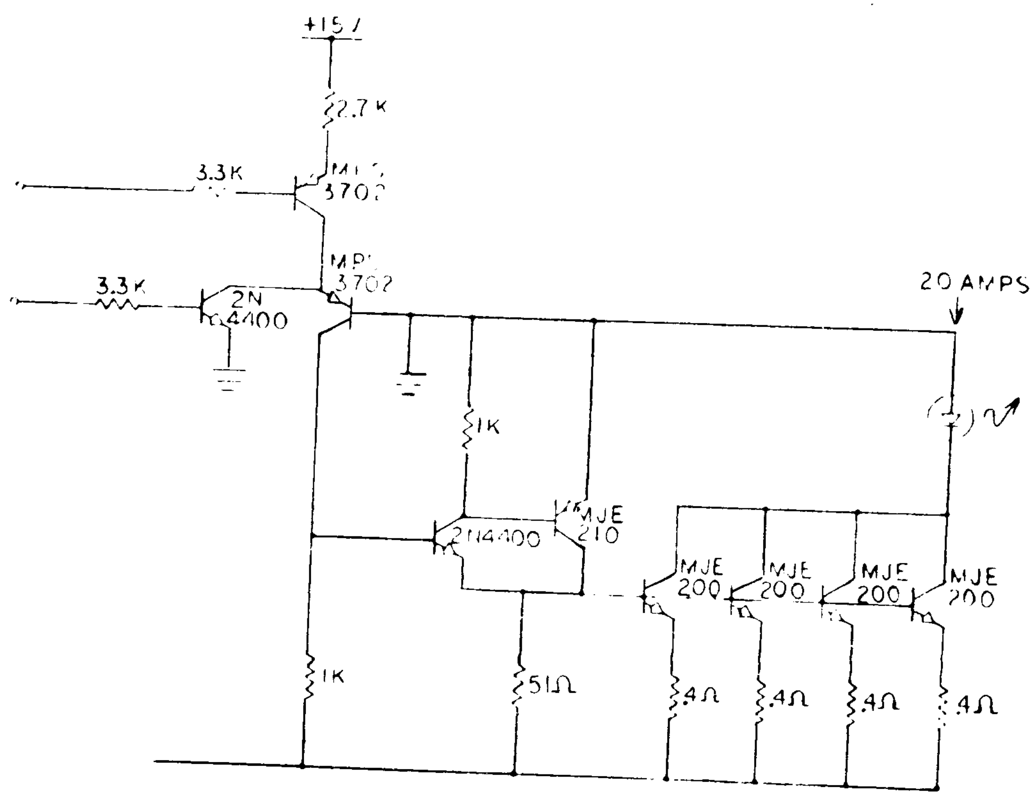

Figure 4-13. 25-Amp Laser-Diode Pulser Electronic Schematic

REFERENCES

To facilitate most convenient review, facsimile copies of the following references also are included among the technical material presented in Appendix A of this report.

1. "Principles of Fiber-Optic Systems." Informal unnumbered description of fiber-optic system elements and technology. TRW/DSSG, One Space Park, Redondo Beach, California.

2. "Fiber-Optic Liquid-Level Sensor New Technology Report." TRW patent description Report No. 11-182, TRW/DSSG, One Space Park, Redondo Beach, California (17 Oct 1979).

3. "Test Plan and Procedures for Fiber-Optic Instrumentation." Report No. 31262-6002-RU-00 prepared for NASA/JSC, TRW/DSSG, One Space Park, Redondo Beach, California.

4. "The Bandgap and the Temperature Coefficient of the Bandgap of GaAs Between 0° and 300° K." TRW/DSSG Memorandum 78.4351.2-021, TRW/DSSG, One Space Park, Redondo Beach, California (10 Feb 1978).

5. "Swept Spectrum Temperature Gauge." TRW/DSSG Memorandum 78.4351.8-013, TRW/DSSG, One Space Park, Redondo Beach, California (9 Feb 1979).

APPENDIX A

CONTENTS

PRINCIPLES OF FIBER OPTIC SYSTEMS

Basic Instrumentation Elements

The basic elements of any fiber optic instrument system are as shown in Figure 1. The system functions more or less as a communication link. Optical signals from a light source are transmitted via a fiber optic cable to a remote sensor which then "conditions" the transmitted light beam according to the measurement being made (in our case, the temperature). The resulting, modified light output from the sensor is returned to the optical receiver through another fiber optic cable, the signal output of the receiver thus furnishing the information about the sensed conditions through appropriate calibrations.

In the following sections, we present some detailed discussion of the principles of optical fibers and the associated components of a fiber optic system. Some of the material is more general in nature than required for the instrument and control systems of concern here, but is included as an overview of the basic principles.

The Source: LED's or Avalanche Diodes

The light source (or emitter) for the system must be capable of modulation at a rate sufficiently fast to handle the information flow. It can be externally modulated by a fast light shutter or light modulator, but this is usually much more complicated and costly than controlling the intensity directly by means fo the current flow. Second, the wavelength of the light from the source must be within a part of the spectrum that allows efficient transmission through the fiber. Third, the emitter area should be such that sufficient optical power can be coupled into the small diameter optical fiber or bundle. This last requirement rules out most conventional light sources, such as incandescnet lamps, where the light is dispersed over a large area. Thus the source must have high radiance and a small effective source diamter; otherwise, most of the light will be lost.

There are two kinds of light sources compatible with optical fibers: light emitting diodes (LED's) and the closely related injection laser. Both LED's and injection lasers are solid state devices, and can be made small enough to work well with fiber optic cables; in addition, their unit costs are typically low, of the order of a few dollars.

Light Emitting Diodes

LED's for fiber optic communications are p-n diodes made from crystals of aluminum-gallium-arsenide (AℓGaAs). Forward biasing of the junction causes the injection of electrons from the n-region where they recombine with holes, causing photons of light to be emitted. The emitted light is incoherent (random phase) and isotropic (nondirectional) and has a lower radiance than that from injection lasers. LED's not specifically designed for fiber optic use, e.g., display and sensor applications, generally have a low radiance and at best work only with fiber bundles that offer a large cross-section (typically 0.045 inch diameter) to capture the light.

For single fiber applications, higher radiance is needed and special devices have been designed for the purpose. Figure 2 shows one of these, the Burrus diode, named for its invetor at Bell Laboratories. This LED has low thermal resistance, high current density, and provides a "well" for the optical fiber so that coupling losses are minimized. Its useful power output is typically about one-tenth that of an injection laser but is adequate for many fiber-optic applications.

LED's can be directly modulated at rates up to a few hundred megahertz, and they have fairly linear power-drive characteristics, making them useful for analog applications. At the present time they also are less expensive, more reliable, and have a longer operating lifetime than injection lasers. Their big disadvantage is their lower radiance, which means lower coupled power and more repeater stations in long-haul fiber optic communication links.

Injection Lasers

Injection lasers are similar to LED's in that they use the same material, AℓGaAs, to form a p-n junction. The light producing mechanism is also the same; however, in the injection laser the p-n junction is perpendicular to the two cleaved ends of the crystal which form the reflecting mirrors of an optical cavity. Laser action occurs when the optical gain in the recombination region exceeds cavity losses. The emitted light is therefore coherent (in phase) and directed, and has a high radiance. The spectral distribution is narrower than that of the LED, about 0.002 μm.

Laser action in this type of device was first achieved in 1962, about two years after the first ruby laser. These early minature semiconductor lasers were simple p-n junctions (so-called "homojunctions" since a single material--gallium-arsenide--was used. To trigger the laser action, extremely high current densities were required (typically 50,000 amperes per square centimeter), so that they could only be operated in a pulse mode at reduced temperatures (liquid nitrogen). Even then, their operating lifetimes were measured in minutes.

Fortunately for fiber optics applications, significant advances have been made, and continuous injection laser operation at room temperature is now common. The development that made this possible is the double heterostructure (DH) injection laser shown in Figure 3. In this device, the thin recombination region is bounded by two heterojunctions, p-p and n-n, formed by changing the aluminum-gallium ratio. These heterojunctions serve two functions. First, waveguiding of the radiation occurs because the recombination region is bounced by material with a lower refractive index. Second, replacing gallium by aluminum increases the energy band gap outside the recombination region, causing minority carrier containment within the recombination region. Also, because the active region is confined to a narrow strip, typically about 13 μm wide, the device provides a high concentration of injected carriers (high optical gain). The required current density is greatly reduced--to a few hundered amperes per square centimeter--and the threshold current to cause laser action is typically 100 mA. By proper choice of the aluminum-gallium ratio, the recombination band gap and therefore the wavelength of the emitted radiation can be varied.

The Medium: Optical Fibers and Cables

The basic fiber lightguide consists of a transparent core surrounded by a cladding material having a lower refractive index. The refractive index of quartz is 1.46 and for common types of glass ranges up to about 1.7. When light travels from a high index region to a low index retion at a sufficiently shallow angle (termed the critical angle for total internal reflection), it is completely reflected; at a steeper angle the light rays are partially transmitted into the low index region.

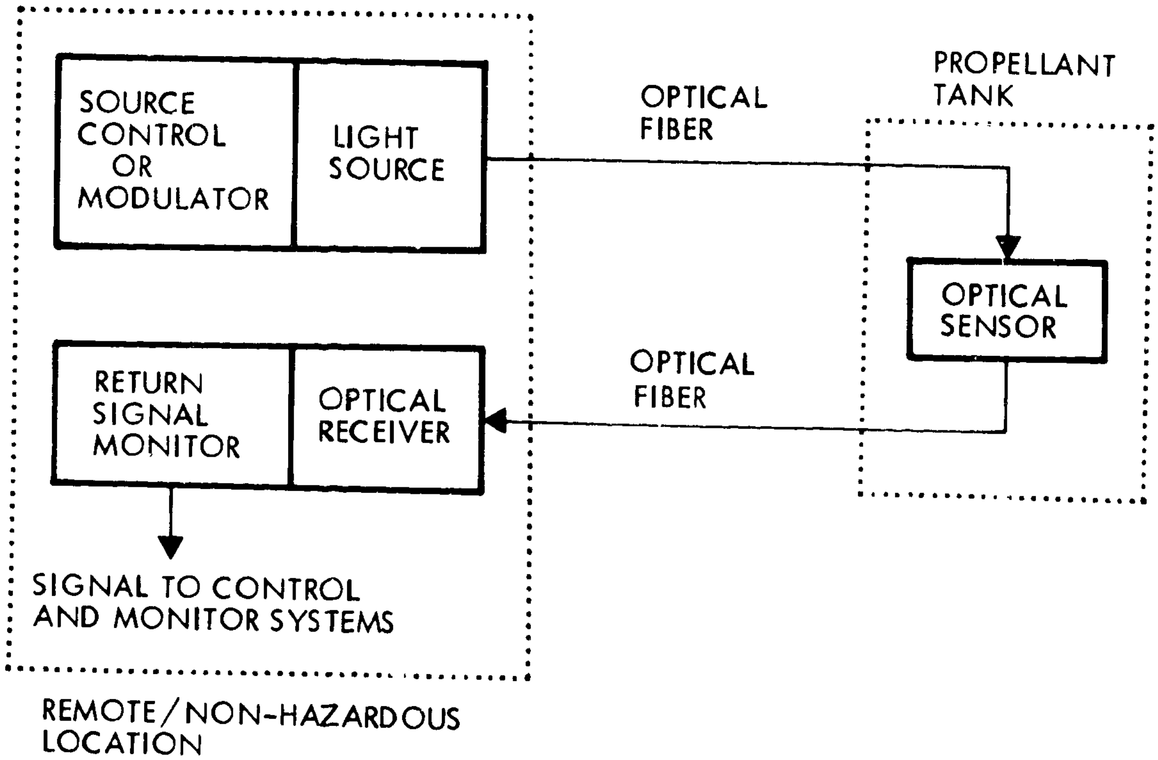

Figure 1. Basic elements of a fiber optic instrument system for remote measurements of propellant tank conditions.

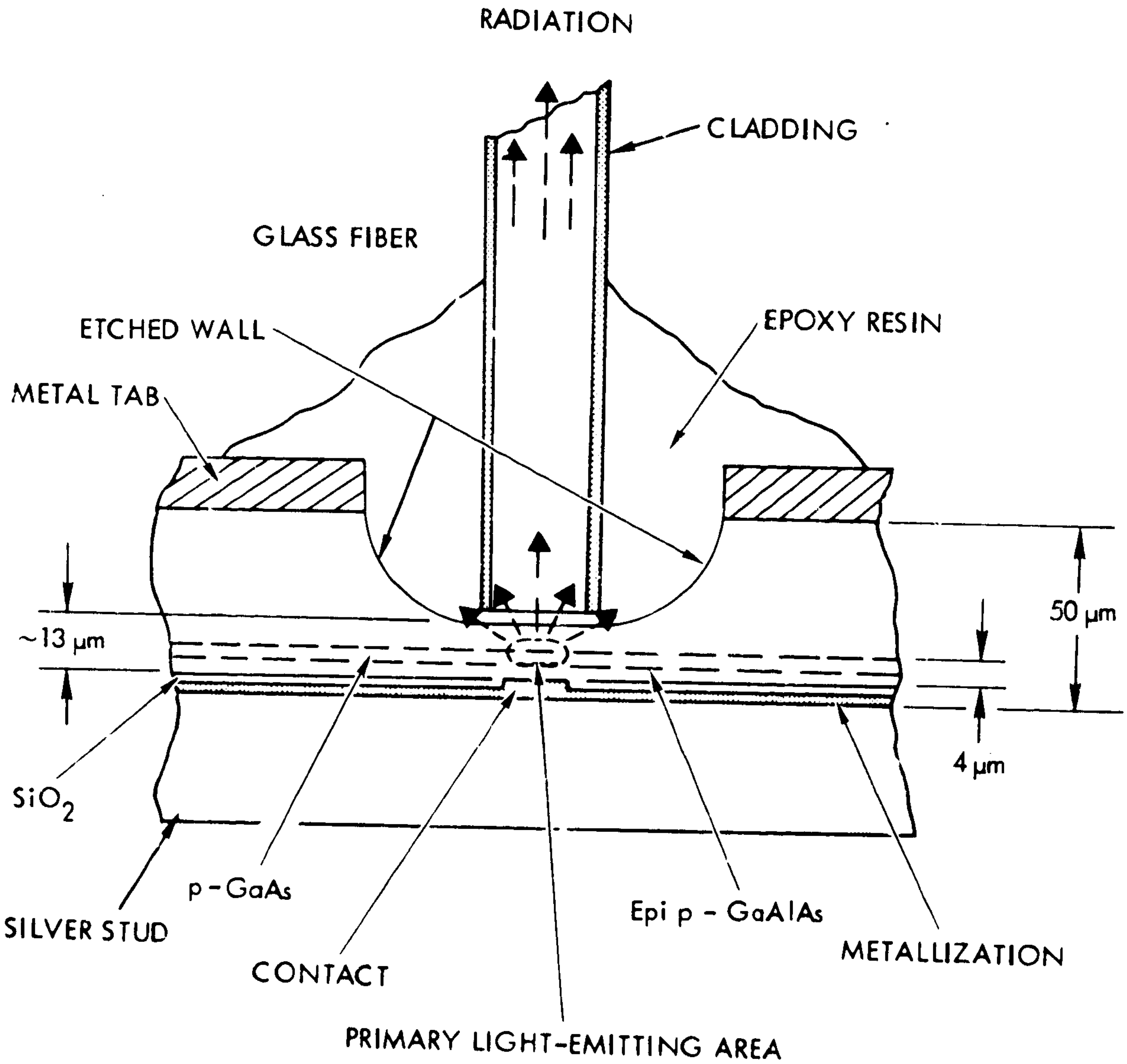

Figure 2. Construction of a Light-Emitting Diode (LED).

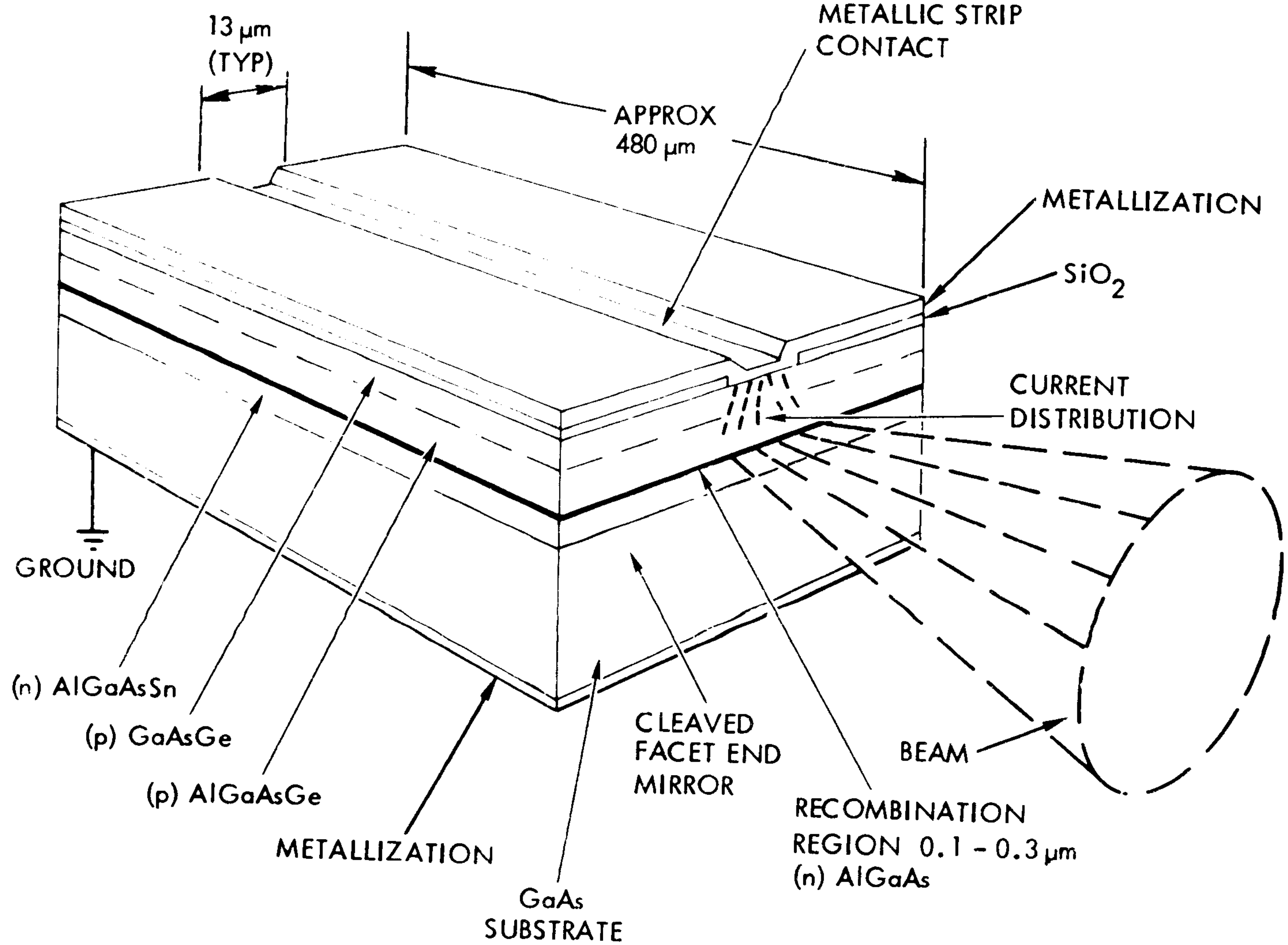

Figure 3. Double Heterostructure Injection Laser.

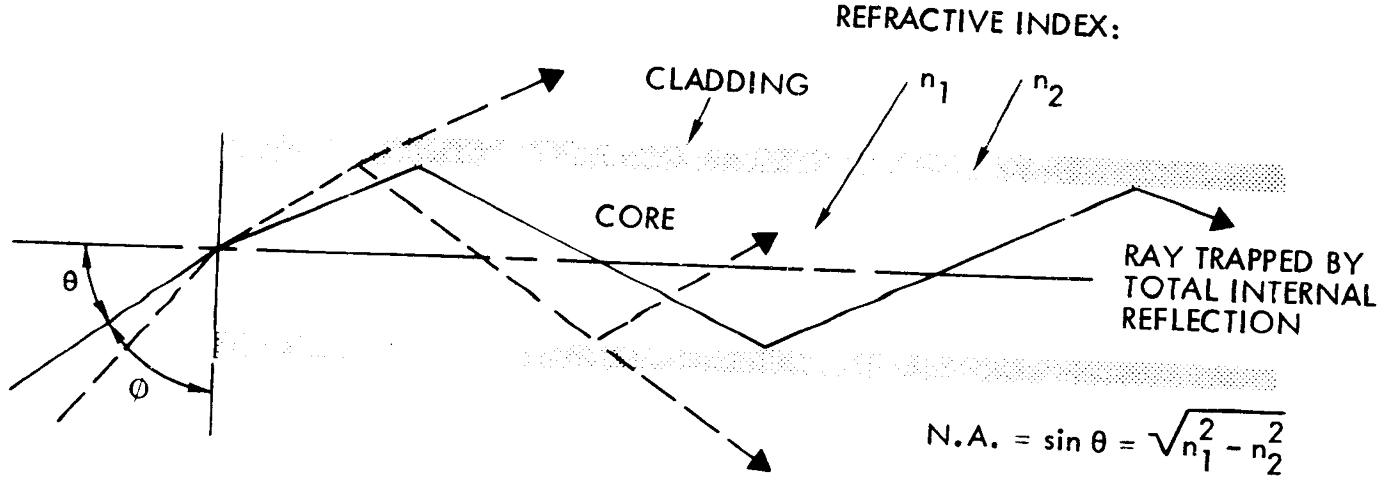

$$\text{N.A.} = \sin\theta = \sqrt{n_1^2 - n_2^2}$$

Figure 4. Cross-section of fiber optic waveguide with reflected light rays.

The simplest concept of light-guiding in an optical fiber is to visualize the light at being totally internally reflected by the core-cladding interface. In more detailed terms, the fiber acts as a dielectric waveguide which supports only a limited number of propagation modes. The modes (or eigenfunctions) are solutions to the wave equation, with boundary conditions dictated by the structure through which the energy propagates--in our case the optical fiber. There are guided modes and unguided or radiation modes. We are most interested in the guided modes since they are confined by the fiber and travel with minimum loss down it.

For a fiber waveguide of finite size, there are a finite number of guided wave modes for a given optical frequency that is a finite number of discrete solutions to the wave equation. Each mode exhibits a unique spatial distribution of energy across the fiber. Light guided by the fiber can be decomposed into the various permitted modes. The amount of energy in each mode depends on the optical emitter, coupling mechanisms, and irregularities in the fiber that can cause mode conversion. With smaller fibers, fewer modes are allowed. The single mode fiber, as its name implies, propagates only one mode.

An important characteristic of an optical fiber is its numerical aperture (N.A.), defined as the sine of the maximum half-angle of acceptance (θ) of the incoming light beam. Light entering the fiber at a larger angle will leak through the core-cladding interface and be lost. Thus, the theoretical extremes for the value of N.A. are 0 and 1, corresponding to half-angles of acdeptance of 0 and 90 degrees, respectively. When maximum light acceptance (large number of propagation modes) is important, high N.A. fibers are used, and values of 0.7 or higher are not uncommon. For fiber optic communications, lower values (typically 0.1 to 0.2) are used, since a large number of propagation modes leads to problems in modal dispersion, which produces pulse smearing in digital systems and frequency roll-off in analog systems, because different modes travel at different relative propagation velocities through the fiber. Figure 4 shows the relationship between the half-angle of acceptance and the refractive indices of core and cladding.

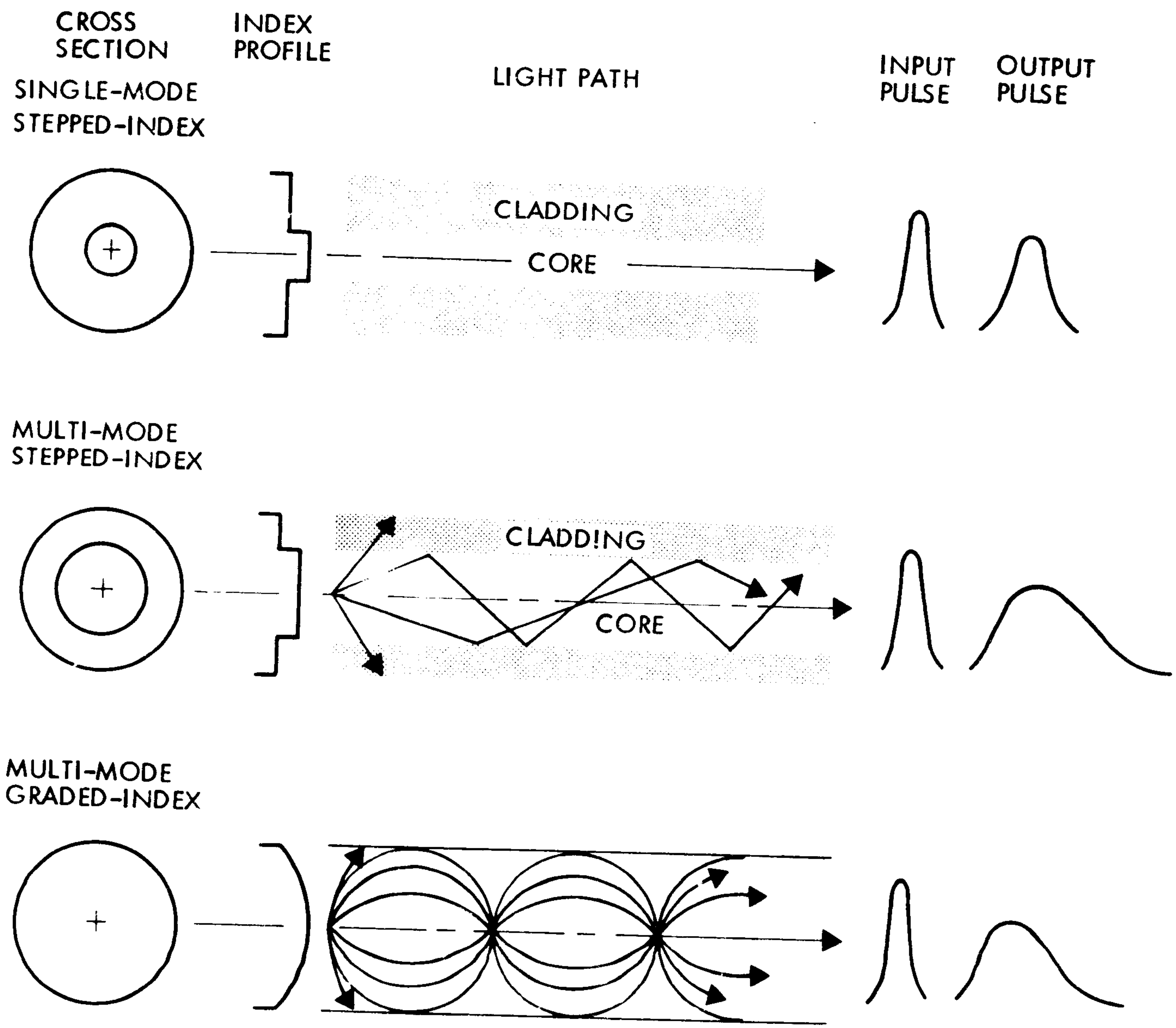

Figure 5. Three types of optical fibers.

II-182

FIBER OPTIC LIQUID LEVEL SENSOR

NEW TECHNOLOGY REPORT

PROBLEM

At least 12 patents have been applied for the bare fiber liquid level, most of these innovations pertain to: sensing of ordinary liquids such as water, gasoline and oil-liquids with refractive indeces much higher than that of the air and, operable at or near room temperature. To design the sensors for the low refractive indeces that operate at cryogenic temperature several new techniques have been employed.

The bare fiber sensors work on the principle that the optical throughput loss is dependent upon the material that surrounds the bare fiber. A practical sensor, therefore, is a glass rod connected to the fiber optic system that continuously monitors the throughput loss. When the sensor is immersed in the liquid, the loss increases indicating that the sensor is in contact with the liquid. A typical system is shown in Figure 1. Figure 2 shows some of the existing sensors; multiple bends are to increase the sensitivity.

For most efficient sensors, two factors are important: the change in the throughput loss due to the refractive index of the liquid (sensitivity) and, the insertion loss of the sensor. Usually these are opposing factors since the sensitivity can be increased by adding bends to the sensor which also increase the insertion loss.

[signature]	10/1/79	[signature]	10/1/79	[signature]	10/3/79
Madan Sharma	Date	C. Roychoudhuri	Date	R. E. Brooks	Date

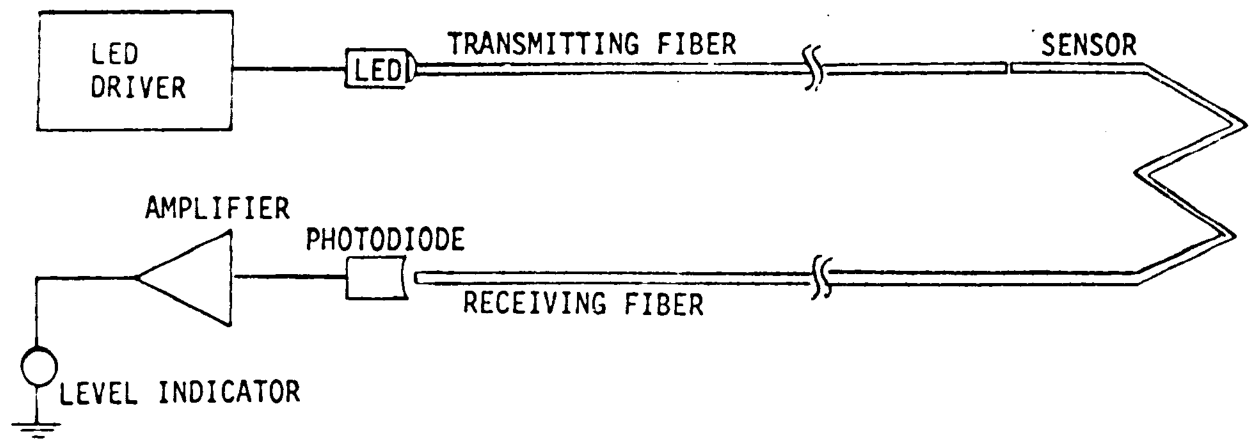

Figure 1. Shows the schematic of liquid level sensing system. The LED emits 200 micro second wide pulses at a frequency of 50 Hz. The receiver derives its timing signal from the transmitter for synchronous detection.

Madan Sharma	Date	C. Roychoudhuri	Date	R. E. Brooks	Date

11-182

Figure 2. Shows typical sensors. Premis used in designing these sensors is that the lineal attenuation changes when the sensor is immersed in the liquid.

Madan Sharma 10/16 Date C. Roychoudhuri Oct 16, '79 Date R. E. Brooks 10/16/79 Date

During initial evaluation of the sensor with techniques available at that time, it was found that to have a sensitivity of 2 dB for LH_2 would require 5 bends. The insertion loss of such a sensor was found to be 45 dB. This loss was enormous. Even using fairly expensive LED's the ouput of the sensor was too low to be measured. CW lasers and pulsed lasers were considered. CW lasers have not been tried. The pulsed lasers exhibited amplitude jitter and interferred with decision making threshold electronics.

OBJECTIVES

There are two problems to be considered: increase the sensitivity while keeping insertion loss down to 20-25 dB. and explore different means of attaching sensors to the fibers while maintaining a good pressure and liquid seal between the sensors and the signal conveying fibers.

PROCEDURE

To design more appropriate sensors, the phenomenon that does the liquid sensing must be examined. As often misquoted, the lineal attenuation of the glass does not change when immersed in the liquid, it is the numerical aperture which changes at the point of contact with the liquid. This can be explained with the aid of Figure 3. When the fiber is immersed in the liquid it is equvalent to two fibers. The one in the air has large exit numerical apertue while the portion in the liquid has small NA, since NA depends upon the refractive index of the surrounding material. The extra loss due to mismatch of the numerical aperture is in fact the sensing mechanism. This discussion clearly shows that the sensing is only at the surface of the liquid; no matter how long the fiber in the liquid the loss reading will be the same.

Madan Sharma 10/16 Date | C. Roychoudhuri Oct 16, 179 Date | R. E. Brooks 10/16/79 Date

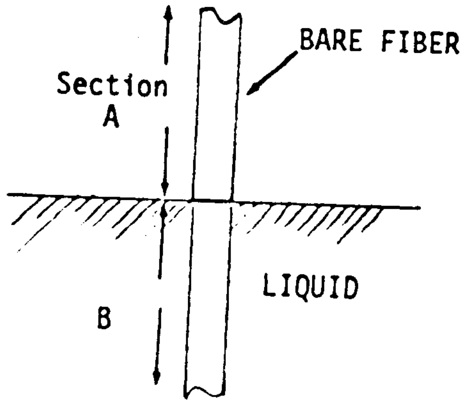

Figure 3. The liquid sensing is due to N.A. mismatch between the sections of fiber in the air and the section in the liquid.

Madan Sharma Date C. Roychoudhuri Date R. E. Brooks 10/16/75 Date

Another point worth considering is the contents of variety of optical modes present in the sensor. The loss due to mismatch of numerical aperture is dependent on the presence of oblique modes. An optical flux flowing through a long fiber sheds most of its modes along the length of the fiber. If well behaved modes are predominant the loss due to NA mismatch would be too small to detect - less sensitivity.

This discussion also points out that mismatch loss occurs only when the sensor goes from air to liquid but no sensing is done on its return trip if the sensor is u shaped. Mounting of the sensor is yet another problem. The configuration of this experimental system nessitates liquid and pressure cryogenic seal between the sensors and the signal conveying fiber optic cable. There are very few epoxies that are fit for this purpose. These epoxies have very high refractive index, any application of this results into heavy throughput loss.

Such constraints are the reason for applying new technology to the level sensors to be used in cryogenic environments when refractive index of the liquid not much higher than air.

PROGRESS

New liquid level sensors have been designed. Figure 4 shows the sensor being used in the experimental set-up. The total insertion loss is 20 dB and sensitivity is 8 dB in liquid nitrogen which means 2 dB in LH_2. The basic design approach was to achieve sensitivity with less number of bends. This was achieved by introducing scattering centers with sharp bends. A curve fiber has no good effect on the sensor, therefore, the legs of the sensor are kept straight. As has been discussed that the sensing loss is provided by a single point where the sensor touches the liquid, the final sensor detects the presence of liquid at its lowest points. The desired height

Madan Sharma	Date 10/16	C. Roychoudhuri	Date Oct 16, '79	R. E. Brooks	Date 10/16/79

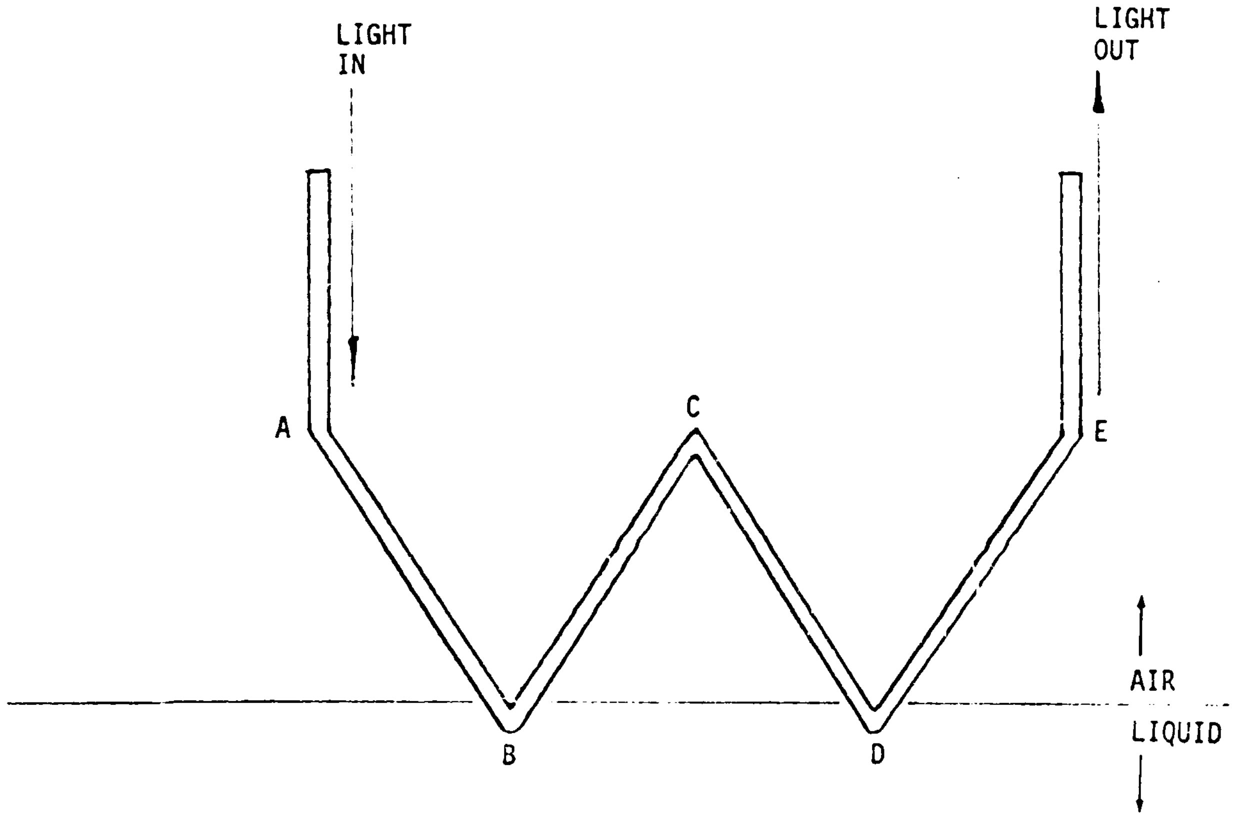

Figure 4. Shows the new sensor. The 5 bends A, B, C, D, are scattering centers B & D are bends where detection takes place. The bend E has no effect on sensing. It is there to provide symmetry.

11-182

Madan Sharma | Date | C. Roychoudhuri | Date | R. E. Brooks | Date therefore, is less than the diameter of the bare fiber which is in this case one millimeter.

The sensor is sealed with the appropriate epoxy using a special bushing which ensures a very fine band of point of contact with the sensor. The bushing also ensures that the seal is very near to the end of the sensor.

Figure 5 shows a modified sensor sealing arrangement. This method is being studied presently.

Madan Sharma	10/16	C. Roychoudhuri	Oct. 16, '79	R. E. Brooks	10/16/79
Madan Sharma	Date	C. Roychoudhuri	Date	R. E. Brooks	Date

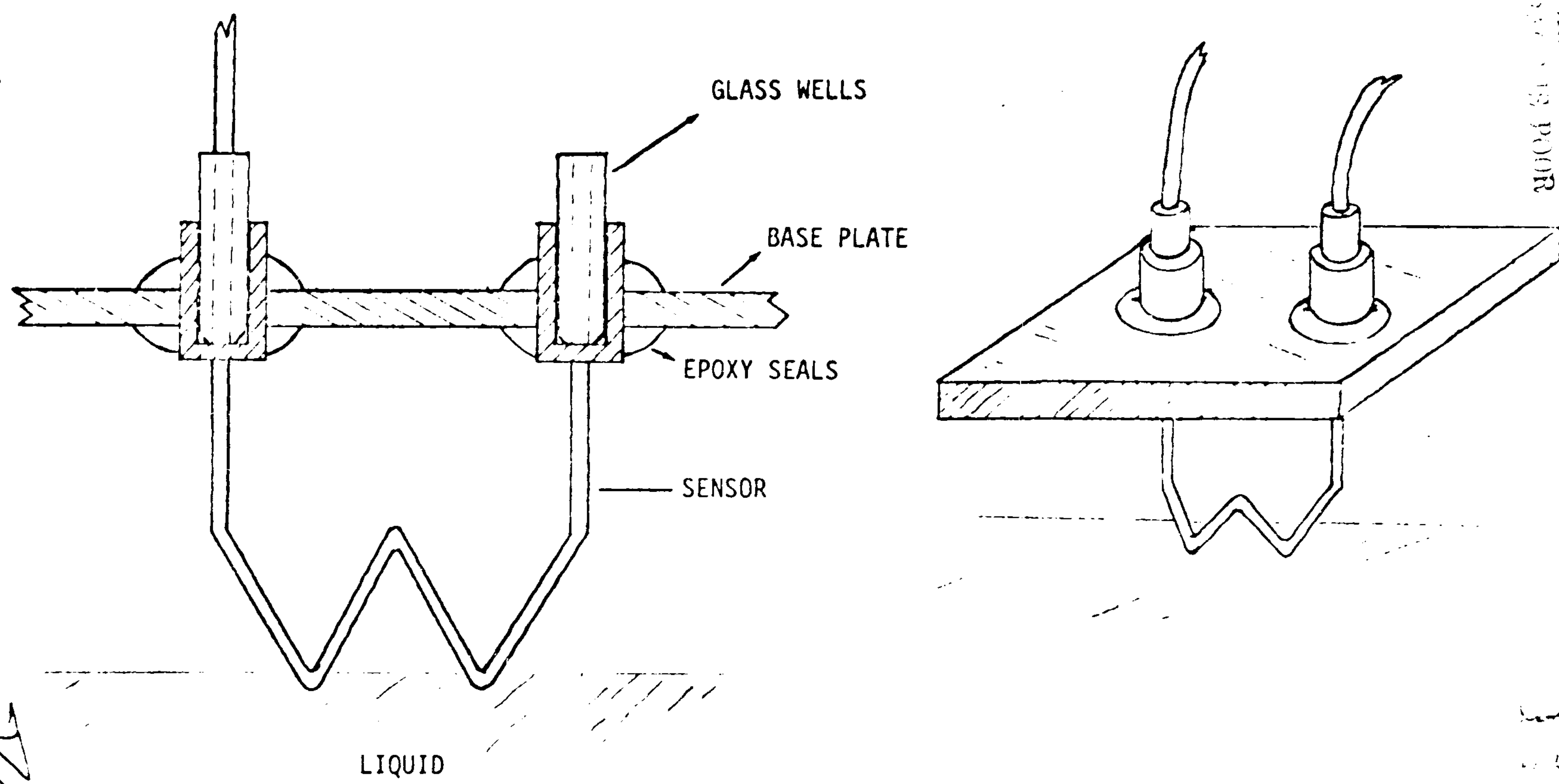

Figure 5. Glass wells have been attached to the sensor to avoid light leakage at the point where the sensors are sealed to the base plate.

Madan Sharma	Date	C. Roychoudhuri	Date	R. E. Brooks	Date

31262-6002-RU-00

"TEST PLAN AND PROCEDURES FOR FIBER OPTIC INSTRUMENTATION"

by

Ronald Watson

Prepared for
Contract NAS9-15454
NASA Lyndon B. Johnson Space Center

Approved by: R.S. Witte
R.S. Witte, Manager
TRW Electro-Optics
Department

Jack D. Alexander
Jack D. Alexander
Technical Manager
NASA/JSC

TRW Defense and Space Systems Group
One Space Park
Redondo Beach, California 90278

1.0 INTRODUCTION

The purpose of this document is to present the plan and procedures for testing the optical sensors developed for NASA Contract NAS9-15454. These sensors utilize fiber optic technology to provide passive sensing of liquid level, temperature, and pressure in cryogenic liquid propellant tanks.

The end product of the program is to be an engineering model, deliverable to NASA/JSC, with a set of working sensors to measure the level, temperature, and pressure in liquid nitrogen in a stainless steel (pressurizable) Dewar. Electronics components will be placed outside the LN2 tank, with measurements indicated on an instrument panel. Details of the program and sensor concepts are given in Reference 1.

Because the model tests do not involve operation in hazardous environments and are conducted at pressures below 15 psig (see Section 2.1 below), the test plan and procedures outlined here involve no special requirements beyond standard laboratory research methods.

2.0 TEST PLAN

2.1 Test Requirements

The sensor performance goals are given in Table 1.* Note that many of the goals listed are design goals only, associated with hazardous operation in LH2 and LOX and at high pressures; these design goals are not subject to test or demonstration on this program.

The tests to satisfy achievement of the demonstratable performance goals require insertion of the 3-sensor set into a quiescent bath of LN2 in a Dewar to contain no higher than 15 psig.

---

* Taken from the contractual statement of work, as amended February 23, 1979.

Table 1. Sensor Performance Goals

ENVIRONMENT:	Demonstrated operation in 77°K LN2 (system to be designed for LH2 and LOX operation*).
OPERATION MODE:	Demonstrated operation for LN2 covering and uncovering the sensors (dry-to-wet and wet-to-dry operation).
LEVEL ACCURACY:	Designed to obtain 0.1% by volume of the Shuttle tanks.*
TEMPERATURE RANGE:	Demonstrated measurements in 77°K (LN2) range (designed for measurements to 20°K/LH2 and survival to 150°F/launch-stand conditions*).
PRESSURE RANGE:	Demonstrated measurements in 0-15 psig range in LN2 (designed for measurements to 300 psig*).
TIME RESPONSE:	Demonstrated transient response in LN2 as follows: 50-100 msec for level sensor, 500 msec for temperature sensor (pressure sensor designed for 50-100 msec response*).
SENSOR INSTALLATION ACCURACY:	Designed for $\pm$ 0.1 inch*.
SENSOR LOCATION:	Demonstrated capability up to 100 feet from electronics.
FLOW LOCATION:	Designed to withstand up to 27 fps*.
LIFETIME:	Demonstrated to withstand over 200 cycles.

* These design goals can be satisfied by appropriate analyses and are not subject to test or demonstration on this program.

2.2 Test Hardware Configuration

The test hardware configuration shall consist of the following elements:

- Sensors (to measure level, temperature, and pressure) mounted on an extendable sting to insert into the LN2 bath,
- A stainless steel, pressurizable Dewar to contain the LN2, and the cover of which will support the sensor mounting sting,
- Associated electronics containing power supplies, light sources, and measuring and indicating systems,
- A console to contain all of the above.

2.3 Facilities and Test Equipment Requirements

The test facility is the LN2 Dewar, self-contained on the engineering model console, capable of maintaining the LN2 for a period of approximately four hours. Standard 110 V AC electrical power is required to operate the instrument electronics.

2.4 Test Schedule

The tests of the engineering model shall take place in the period of 15 March 1979 to approximately 6 April 1979.

2.5 Consumable Materials

The consumable materials are approximately 120 gr of LN2 (15 liters).

2.6 Minimum Quality Assurance and Reliability Requirements

Electronic and pressure indicating devices shall be calibrated as per TRW equipment pool procedures.

2.7 Special Safety Precautions

Standard procedures for handling LN2 shall be applied. Special automatic and manual pressure relief vent valves shall be provided to limit pressure in the Dewar to 15 psig.

2.8 Minimum Test Procedure Requirements

The minimum test procedures are that the LN2 level will have been stabilized at atmospheric pressure before insertion of the 3-sensor set. The exhaust vent shall be set to relieve pressure from LN2 boil-off at the 15 psig level.

2.9 Special Technical and Engineering Support Requirements

None.

3.0 TEST PROCEDURES

3.1 Scope and Description of the Tests

The tests shall be the measurements of the response of the 3-sensor set during immersion into and withdrawal from the LN2 bath. The static and transient response behavior of the instruments will be measured up to 15 psig.

3.2 Safety Precautions

The test personnel will insure that the 15 psig pressure relief vent is in working order as the test proceeds. Furthermore, the pressure gauge shall be monitored at all times to insure that the pressure does not exceed 15 psig in the Dewar; a manual relief vent is available to override the automatic vent if necessary to drop the pressure.

3.3 Test Preparation and Checkout Instructions

The Dewar shall be filled with LN2 to one-half to two-thirds full, and maintained for a time period to insure a quiesent liquid surface as determined by visual inspection with the instrument mounting system and Dewar cap removed. Before installation of the instrument mounting system in the Dewar, the electronic subsystems shall be checked to insure proper light source operation and optical continuity through the fiber bundles and connectors.

3.4 Test Procedure

After filling and equilibration of the LN2 Dewar as per the Test Preparation instructions in item 3.3 above, the instrument assembly shall be mounted in the Dewar with the sensors in the "up" position, above and not immersed in the LN2. Monitoring of the sensor output signals shall proceed at this time to determine behavior during the cool down period.

After temperature equilibration of the sensors and mounting box assembly in the non-immersed position, as determined by stable output signals, the sensor outputs shall be monitored during a controlled rate of insertion into the LN2, so as to determine immersion time response characteristics.

After insertion of the sensors in the LN2 and further temperature equilibration in the immersed position, static response characteristics shall be measured to determine the required calibrations. Quasi-static response of the pressure sensor shall be obtained by relating the sensor output to the pressure in the Dewar as determined from the reference pressure gauge which monitors the Dewar tank pressure. Temperature calibration shall be obtained from the known temperature-pressure characteristics of LN2 (77^{o}K at 1 atm) plus a reference thermocouple attached to the sensor holder. Static response of the level sensor is determined by the on-off characteristics when above or immersed in the LN2.

After static, immersed response measurements have been obtained, the sensors shall be removed from the LN2 at a controlled rate to determine the transient response characteristics for this mode of operation.

The capability of the sensors to undergo a lifetime of 200 cycles shall be determined by cycling the sensors in and out of the LN2 200 times with the immersion device.

3.5 Emergency Shutdown or Special Hazardous Security Procedures

The manual vent relief value shall be opened if the Dewar tank pressure exceeds 15 psig.

3.6 Requirements of Quality Assurance of Compliance with Mandatory Procedural Instructions

None.

4.0 DESIGN OF SPECIAL TEST EQUIPMENT, FACILITY EQUIPMENT, AND TEST INSTALLATIONS

The Dewar test tank is the only item of equipment constructed especially for the tests described herein. This tank was designed and fabricated by Andonian Cryogenics, Inc. of Newtonville, MA, to operate down to liquid helium temperatures ($4.2^{o}K$) and up to 300 psi (20 atm) pressure; the tank is a high pressure version of Andonian Model number SCSM-3-1/2 with a capacity of 3.3 liters at 50% full. Figure 1 is a sketch illustrating the Dewar construction.

5.0 LIST OF REFERENCES

1. R. Watson "Sensor Recommendations for Fiber Optic Instrumentation", 31262-6001-RU-00, TRW DSSG, 31 March 1978.

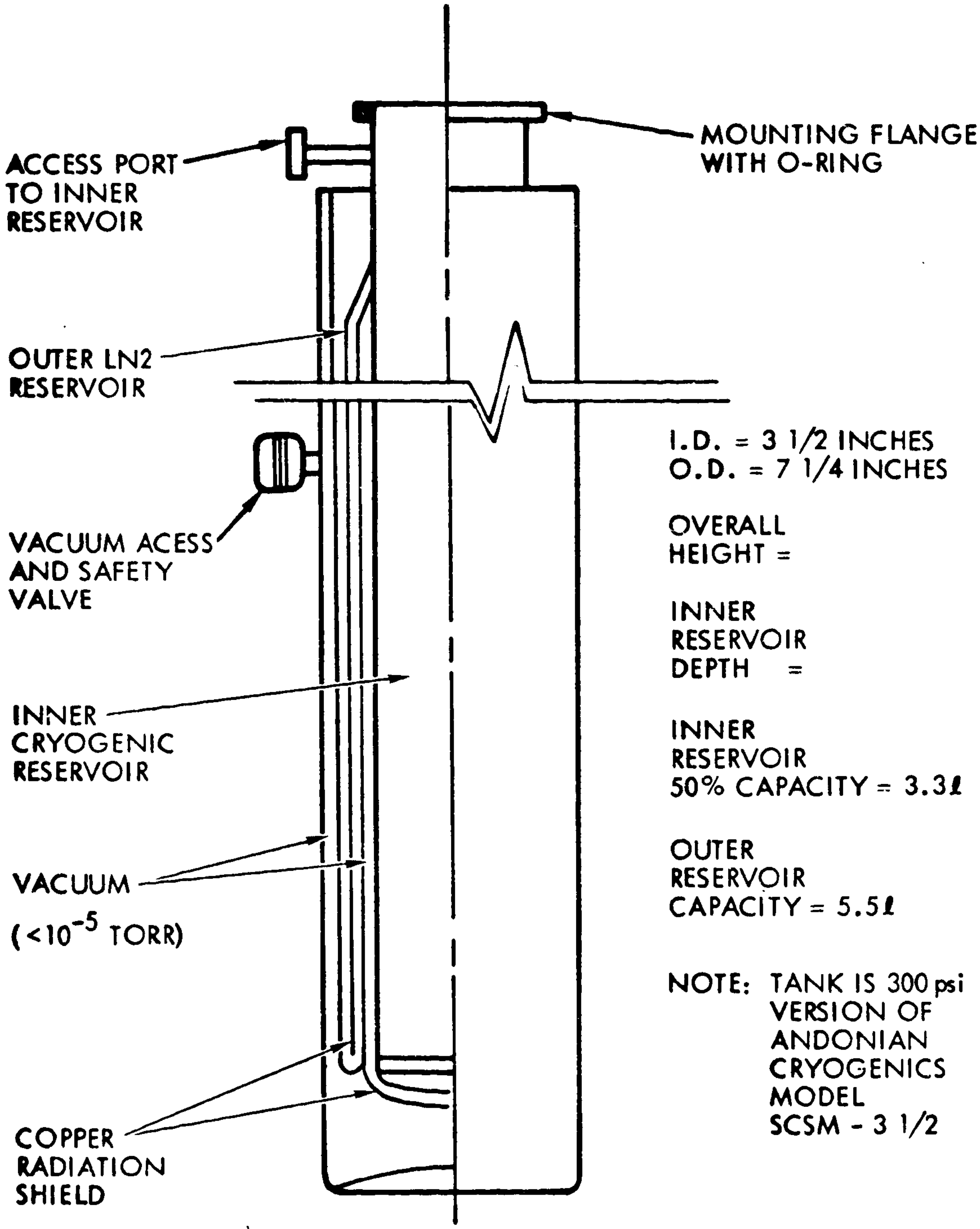

Figure 1. Special Stainless Steel Dewar Tank

INTEROFFICE CORRESPONDENCE

78.4351.2-021

TO: R. Brooks
M. Sharma
R. Watson
R. Witte

CC:

DATE: 10 February 1978

SUBJECT: The Bandgap and the Temperature Coefficient of the Bandgap of GaAs Between 0 and 300°K.

FROM: W. Von der Ohe

BLDG	MAIL STA.	EXT.
R1	1062	61816

REFERENCE: J. Pankove, Optical Processes in Semiconductors, Prentice Hall, Englewood Cliffs, New Jersey, 1971, p. 27:

The temperature dependence of the gap for many semiconductors has been fitted by the following empirical relation:[17]

$$E_g(T) = E_g(0) - \frac{\alpha T^2}{T + \beta} \qquad (2\text{-}2)$$

where $E_g(0)$ is the value of the energy gap at 0°K and α and β are constants. Table 2-3 lists these values for several semiconductors.

Table 2-3[17]

Values of the parameters in Eq. (2-2)

Substance	*Type of gap*	$E_g(0)$ (eV)	α ($\times 10^{-4}$)	β
diamond	E_{gi}	5.4125	−1.979	−1437
Si	E_{gi}	1.1557	7.021	1108
Ge	E_{gi}	0.7412	4.561	210
Ge	E_{gd}	0.8893	6.842	398
6H SiC	E_{gi}	3.024	0.3055	−311
GaAs	E_{gd}	1.5216	8.871	572
InP	E_{gd}	1.4206	4.906	327
InAs	E_{gd}	0.426	3.158	93

E_{gi} = indirect gap E_{gd} = direct gap

[17]Y. P. Varshni, *Physica* 34, 149 (1967).

The bandgap (Å versus °K) and the temperature coefficient of the bandgap (Å/°K versus °K) of GaAs between 0 and 300°K are shown in the attached figures.

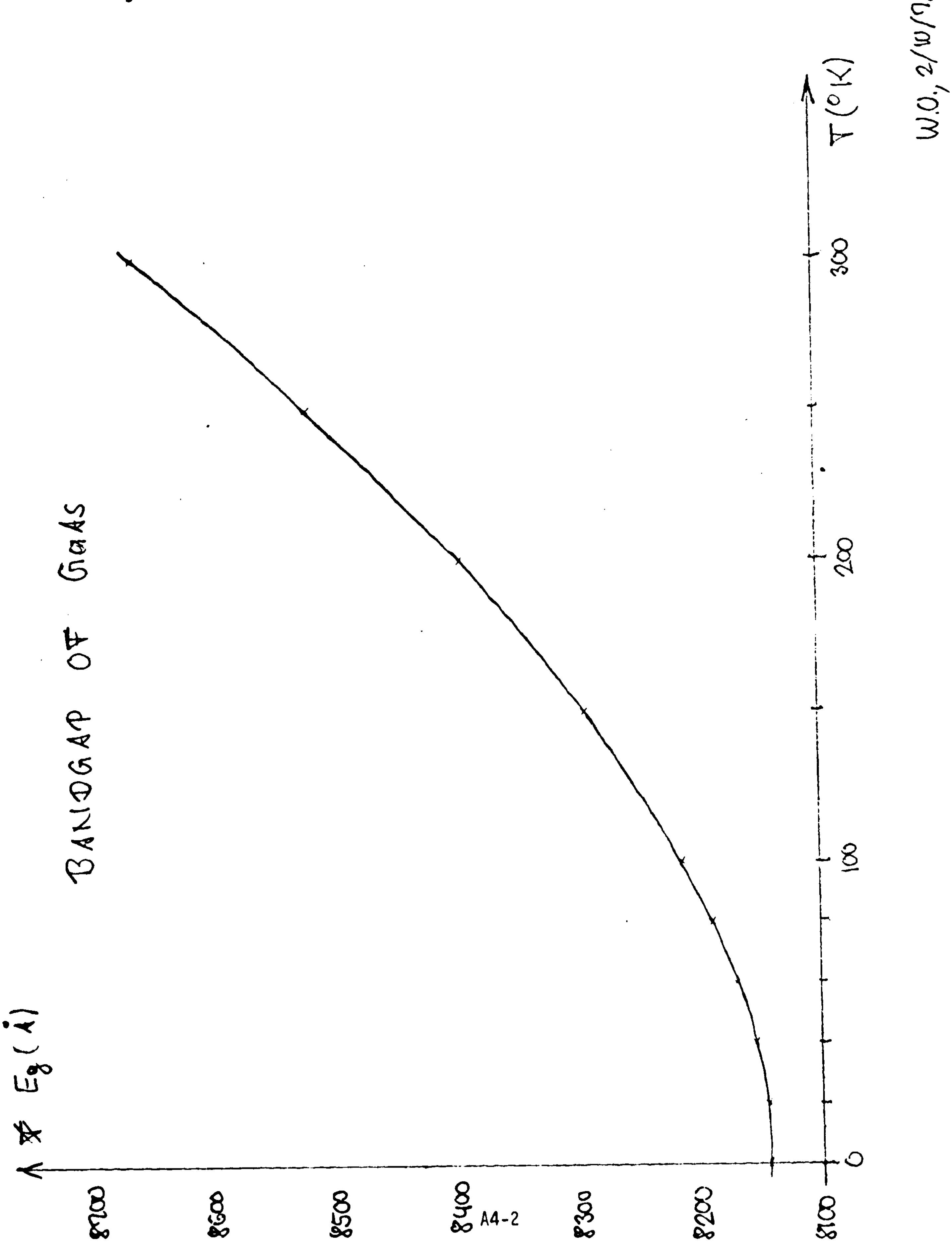
BANDGAP OF GaAs
Eg (Å)
T (°K)
W.O., 2/10/78
0
100
200
300
8100
8200
8300
8400
8500
8600
8700

W.O., 2/10/78

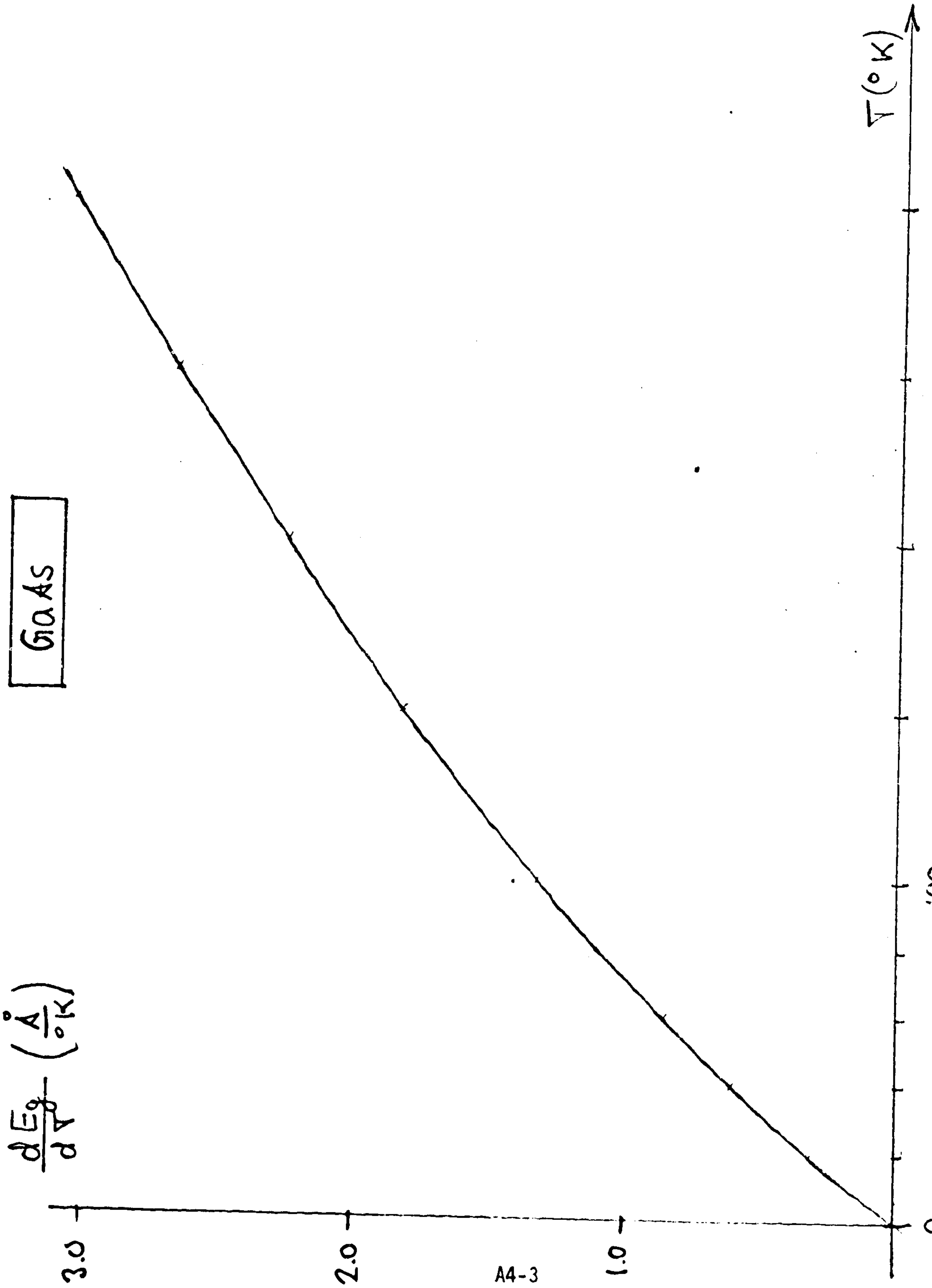
GaAs
$\frac{dE_g}{dT}$ $\left(\frac{\text{Å}}{°K}\right)$
3.0
2.0
1.0
0
100
200
300
T (°K)

GaAs (Pankove data)

T (°K)	E_g (eV)	E_g (Å)	$\frac{dE_g}{dT}$ $\left(\frac{eV}{°K}\right)$	$\frac{dE_g}{dT}$ $\left(\frac{Å}{°K}\right)$
0	1.5216	8142.7	0.0 $\times 10^{-4}$	0.0
10	1.5214	8143.5	0.3	0.162
20	1.5210	8145.9	0.6	0.315
40	1.5193	8155.2	1.12	0.60
60	1.516	8170.0	1.60	0.86
80	1.513	8189.6	2.04	1.11
100	1.508	8214.0	2.44	1.33
150	1.494	8293.4	3.30	1.83
200	1.476	8396.4	4.00	2.27
250	1.454	8520	4.57	2.68
300	1.430	8664.1	5.05	3.06
400	1.375	9007	5.80	3.80

TRW
DEFENSE AND SPACE SYSTEMS GROUP
ONE SPACE PARK · REDONDO BEACH · CALIFORNIA 90278

INTEROFFICE CORRESPONDENCE

78.4351.8-013

TO R. Watson CC·

DATE 9 February 1978

SUBJECT Swept Spectrum Temperature Gauge

FROM M. Sharma

BLDG	MAIL STA.	EXT.
R1	1070	61105

Problem

- The temperature-dependent bandedge shift in the crystal is the basis of the optical temperature gauge. Measuring this shift is really the key issue in the design of the temperature gauging.
- There are two methods that have been suggested for measuring the shift. One depends upon measuring the transmitted light intensity through the sensing crystal and the other measures the spectrum of the transmitted light using gratings, monochromators, prisms, etc.
- There are several problems associated with these approaches:
  - Extraneous drift
  - Limited temperature range.
  - Transmitted intensity output versus temperature is not a linear function. Some sort of nonlinear scaling factors will be required.
  - Complexity and very low-signal-level electronics required--electronics becomes a critical technology.

Objectives

- To study and incorporate methods that will alleviate the above problems.

Approach

- The new approach draws an analogy from the electronics measurement system where a bandpass of electronic filters can be measured by a sweep frequency generator.
- In the case of the optical temperature gauge, the spectral content of the light source is made to vary as a function of time; this is equivalent to a sweep generator. If time were to be measured from a reference to the time when the spectral characteristics of the light source and the sensing crystal match, the time interval would indicate the temperature.

- To employ this concept for temperature gauging, the spectrum of the light source must be varied in time; this can be done several ways:

  - The spectral response of an LED is dependent upon the bandedge; therefore upon the temperature of the LED chip. The chip temperature can be varied by applying power to the LED. To do this, known power is applied to the LED. If the chip is thermally isolated (has no heat sink), its temperature will rise with time linearly. The rate of rise will be a function of the mass of the chip, thermal capacity, and density, and will be controlled by the amount of power applied to it. This approach is a simple means to chirp the spectral output of the LED.

  - A similar approach can be applied to a laser diode since lasing wavelengths are close to the bandedge. The spectral width of laser diodes is very narrow, therefore, a high degree of resolution can be obtained.

  - Similar to the swept LED and the swept laser diode, a crystal can be made to perform the sweeping function. This would be advantageous in the case where the bandedge of the LED falls outside the range of measurement or other than LED light source is more desirable.

  - A sweeping monochromator in front of the light source can be employed where high resolution is needed. This monochromator can be simple since it is close to the light source and enough optical power is available.

Progress

- Sketches of 4 conceptual arrangements are shown.

- A dummy temperature gauge has been made for show-and-tell.

- Functional diagram is as shown.

- Pertinent characteristics of candidate crystals have been tabulated.

MMS:bj

Attachments

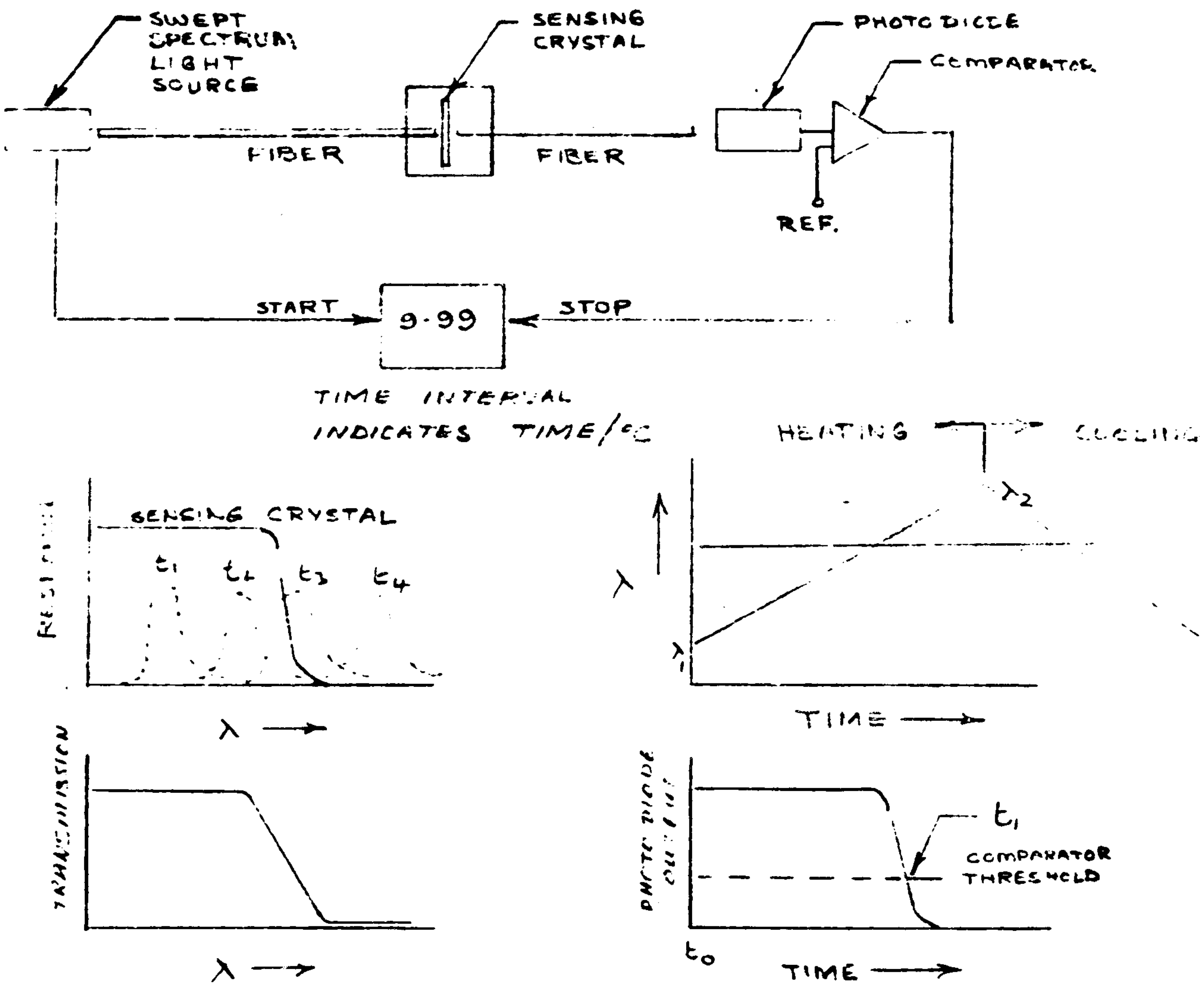

t_0 = START PULSE
t_1 = STOP PULSE

FIG-1 FUNCTIONAL DIAGRAM
SWEPT SPECTRUM TEMP. GAUGE

M.S. FEB 8,78

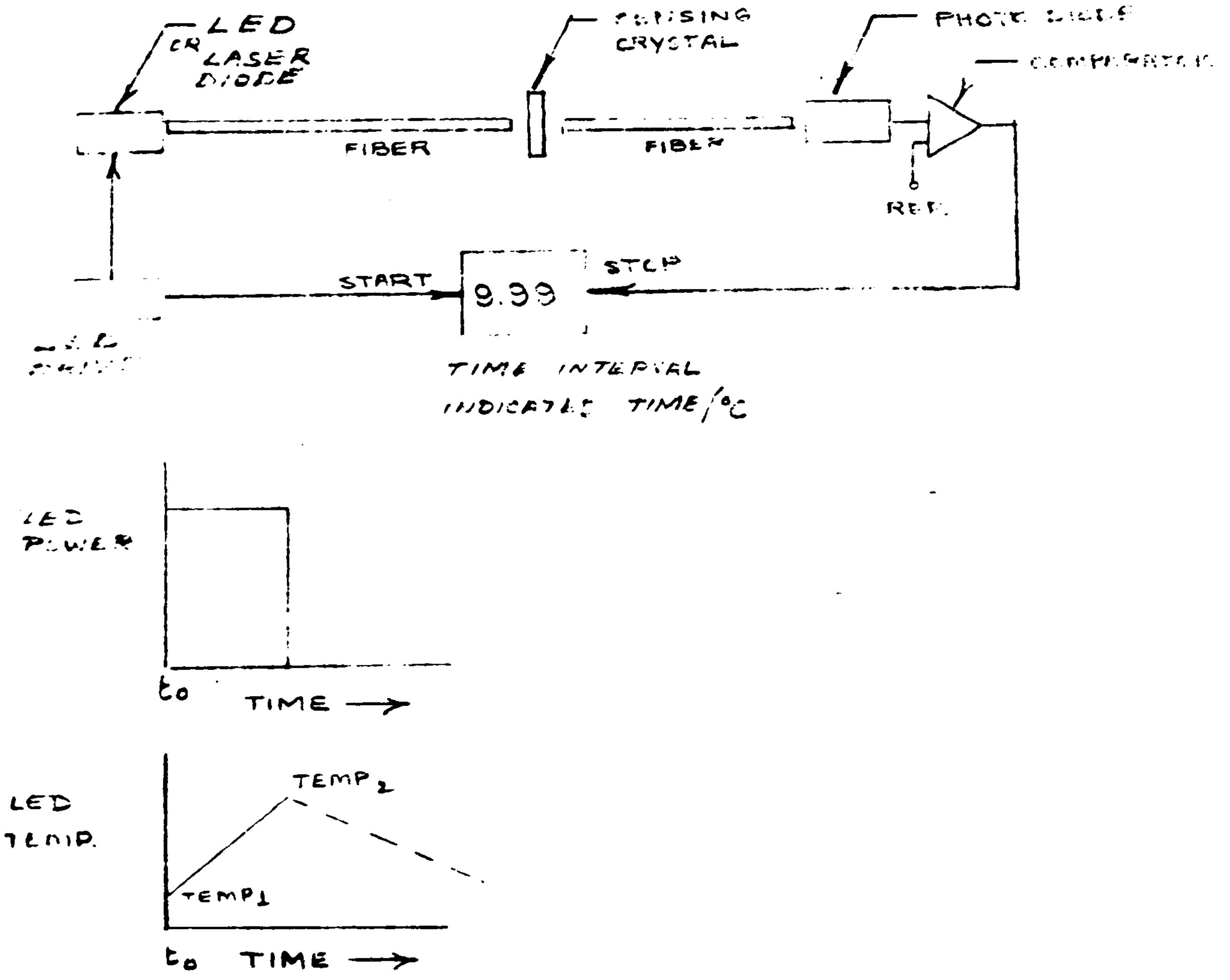

FIG. 2 INCORPORATES LED OR LASER DIODE
SWEPT SPECTRUM TEMP. GAUGE

M.S. FEB 8 78

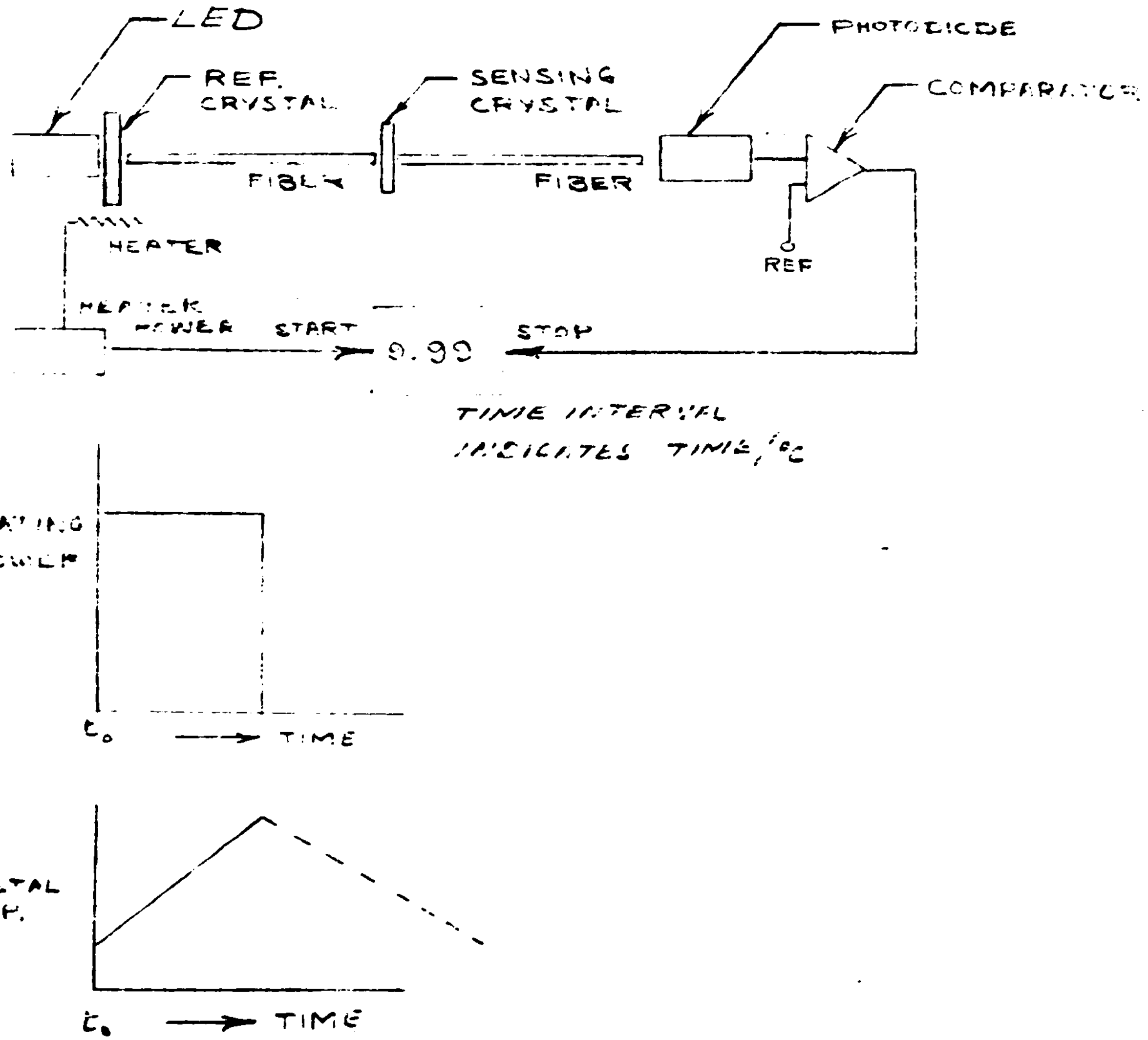

FIG 3 USES REF CRYSTAL
SWEPT SPECTRUM TEMP. GAUGE

M.S. FEB 8 '78

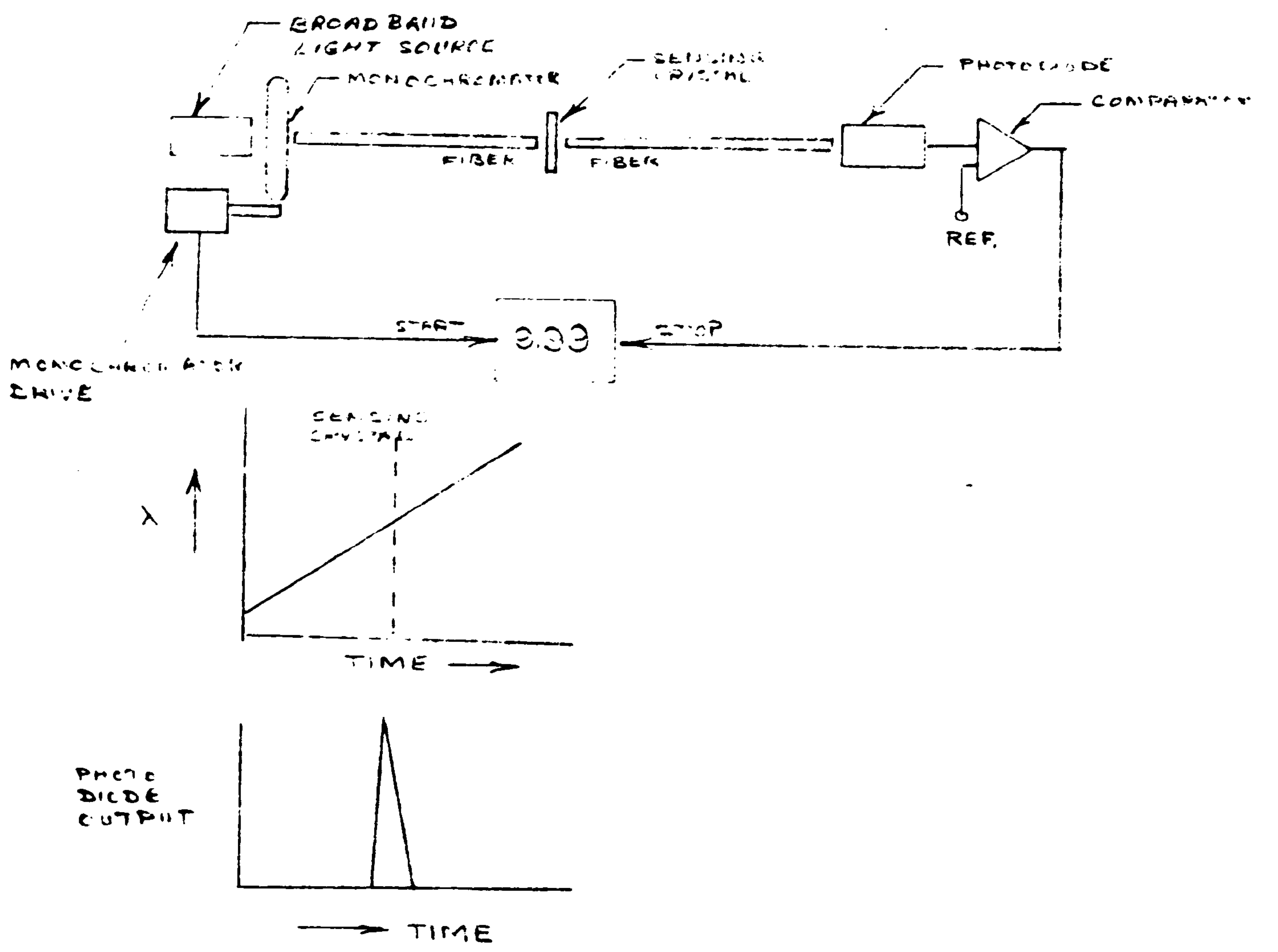

FIG. 4 INCOHERENT MONOCHROMATOR SWEPT SPECTRUM TEMP. GAUGE

M.S FEB 8, 78

REPRODUCIBILITY OF THE ORIGINAL PAGE IS POOR

SEMICONDUCTOR TABLE

	Type	D, Direct I, Indirect	E_G(eV) 300°K	E_G(eV) 0°K	Melting Temperature (°K)	Electron Affinity (eV)	Lattice Constants (Å)	Expansion Coefficient at 300°K ($\times 10^{-6}$ °C^{-1})	Mobility at 300°K (cm^2/Vsec) Electrons	Mobility at 300°K (cm^2/Vsec) Holes	Effective Mass m^*/m Electrons	Effective Mass m^*/m Holes	Dielectric Constant
IV	C	-	5.47	5.51	-	-	3.567	-	1800	1600 [1200]	0.2	0.25	5.5
	Si	I	1.12	1.16	-	4.01	5.431	2.33	1500 [1900]	600 [480]	m_l^*=0.97 m_t^*=0.19	m_{lh}^*=0.16 m_{hh}^*=0.5	11.8
	Ge	I	0.66	0.75	937	4.13	5.658	5.7	3900	1900	m_l^*=1.6 m_t^*=0.082	m_{lh}^*=0.04 m_{hh}^*=0.3	16
	Sn		0.08	0.08	1420		6.47		2500	2400			
IV-IV	SiC		3.0	3.1			4.35		400 [60]	50 [8]	0.6	1.0	10
III-V	AlAs	I	2.15		2013	3.5	5.66	5.2	1200	200			
	AlP	I	2.4		2823		5.451						
	AlSb	I	1.63	1.75	1323	3.65	6.135	3.7	200 [400]	420 [150]	0.3	0.4	11
	GaAs	D	1.43	1.52	1511	4.07	5.654	5.8	8500	400	0.068	0.5	10.9
	GaN		3.5	-							-	-	-
	GaP	I	2.24	2.40	1738	4.3	5.451	5.3	110 [80]	75 [17]	0.5	0.5	10
	GaSb	D	0.67	0.80	985	4.06	6.095	6.9	4000	650 [1400]	0.047	0.5	15
	InAs	D	0.33	0.46	1210	4.9	6.058	4.5(5.3)	33000	460 [240]	0.02	0.41	14.5
	InP	D	1.29	1.34	1343		5.869	4.5	4600	150 [700]	0.07	0.4	14
	InSb	D	0.16	0.26	803	4.59	6.479	4.9	78000	750 [1000]	0.013	0.6	17
V-VI	Bi_2Te_3		0.15				10.48		1250	515			
II-VI	CdS	D	2.42	2.56			4.137		300	50	0.17	0.6	10
	CdSe	D	1.7	1.85		4.95	6.05 [4.298]	-	800 [600]	-	0.13	0.45	10
	CdTe	D	1.44	-		4.28	6.477	-	700	45			
	HgS	I	2.5				5.852		?				
	HgSe	D	0.3				6.08		19500				
	HgTe	D	0.2				6.429		22000	160			
	ZnO		3.2	-					200	-	0.27	-	9
	ZnS	D	3.58	3.7			3.814		165 [120]	-	1.1	-	8
	ZnSe	D	2.67			4.09	5.667	7.0	530 [100]	16			
	ZnTe	D	2.26	-		3.5	6.103	8.2	530				
IV-VI	PbS	I	0.41	0.34			7.5		600 [800]	700 [1000]	0.66	0.5	17
	PbSe	D	0.26				6.14		1500	1500			
	PbTe	D,I†	0.32	0.24		-	6.45		6000 [1620]	4000 [750]	0.22	0.29	30

† Disparity in classification.

Note: Numbers in brackets ([ ]) are alternate values of the first value given above, obtained from another source.

m_l^* = longitudinal effective mass; m_t^* = transverse effective mass; m_{lh}^* = light hole effective mass; m_{hh}^* = heavy hole effective mass.

Reference: S. M. Sze, Physics of Semiconductor Devices, John Wiley & Sons, New York, 1969.

PROPERTIES OF SEMICONDUCTORS[1]

II

		Energy gap E_g (0 K) eV	Energy gap E_g (300 K) eV	Lowest conduction-band minimum, direct or indirect	$\left(\frac{dE_g}{dT}\right)$ × 10⁴ (300 K) eV/K	$\left(\frac{dE_g}{dP}\right)_T$ × 10⁶ eV/bar	Effective mass m_e^*	Effective mass m_h^*	Refractive index n	Static dielectric constant ϵ	Lattice constant a Å	Mobility μ_e cm²/V·sec	Mobility μ_h cm²/V·sec
IV	Si	1.166	1.11	ind 100	−2.3	1.5	m_l 0.98 m_t 0.19	0.52	3.44	11.7	5.43	1,350	480
IV	Ge	0.74	0.67	ind 111	−3.7	5.0	m_l 1.58 m_t 0.08	0.3	4.00	16.3	5.66	3,900	1,900
IV	α-Sn	−0.2‡		dir 000		5.0	0.02				6.489	2,000	1,000
IV-IV	SiC α	3.0 (6H)	2.8–3.2†	ind	−3.3				2.69 ⊥c 2.65 ∥c	10.2	a 3.0817 c 15.1123	400	
IV-IV	SiC β	2.68	2.2	ind							4.359		
VI	Se	1.95	1.74	dir 0001	−14	−20		0.12	5.56 ⊥c 3.72 ∥c	8.5		1	
VI	Te	0.334	0.32	dir 0001	0.3	−19	0.038 ∥	0.26 0.10 ∥	3.07 ⊥c 2.68 ∥c	5.0 ⊥c 2.2 ∥c		1,100	
III-V	BP		2	ind					2.6	6.9	4.538		
III-V	AlP	2.5	2.43	ind 100	−3.5		0.13‡		3.0	9.8	5.462	80	
III-V	AlAs	2.24	2.16	ind			0.5	m_l 1.06 m_t 0.49		12	5.66	1,000	~100
III-V	AlSb	1.6	1.6	ind 100	4	1.6	0.11	0.39	3.4	11	6.135	50	400
III-V	GaN	3.6	3.5	dir 0000	−3.9	3.7			2.4		a 3.18 c 5.16	150	
III-V	GaP	2.4	2.25	ind 100	−5.4	1.7	0.13	0.8‡	3.37	10	5.450	120	120
III-V	GaAs	1.520	1.43	dir 000	−5.0	11	0.07	0.5	3.4	12	5.653	8,600	400
III-V	GaSb	0.81	0.69	dir 000	−4.1	12	0.045	0.39	3.9	15	6.095	4,000	650
III-V	InP	1.42	1.28	dir 000	4.6	4.6	0.07	0.40	3.37	12.1	5.8687	4,000	650
III-V	InAs	0.43	0.36	dir 000	3.3	5	0.028	0.33	3.42	12.5	6.058	30,000	240
III-V	InSb	0.235	0.17	dir 000	−2.9	15	0.0133	0.18	3.75	18	6.4787	76,000	5,000 (78°K)
II-VI	ZnO		3.2	dir 0000	−9.5	0.6	0.32	0.27	2.2	7.9	a 3.2496 c 5.2065	180	
II-VI	ZnS α		3.8	dir 0000	−3.8	9	0.28	⊥1 0.5 ∥	2.4	8.3	a 3.814 c 6.257		
II-VI	ZnS β		3.6	dir 000	−5.3	5.7	0.39		2.4	8.3	5.406		
II-VI	ZnSe	2.80	2.58	dir 000	−7.2	6	0.17		2.89	8.1	5.667	100	
II-VI	ZnTe	2.39	2.28	dir 000	−5	6	0.15		3.56	9.7	6.101		7
II-VI	CdS	2.58	2.53	dir 0000	−5	3.3	0.20	0.7 ⊥c 5 ∥c	2.5	8.9	a 4.136 c 6.713	210	
II-VI	CdSe	1.85	1.74	dir 0000	4.6		0.13	2.5 ‡ 0.4 ∥		10.6	a 4.299 c 7.010	500	
II-VI	CdTe	1.60	1.50	dir 000	4.1	1.5	0.11	0.35	2.75	10.9	6.477	600	
II-VI	HgS		2.5										
II-VI	HgSe	−0.24	−0.15	dir 000			0.045			25	6.085	5,500	
II-VI	HgTe	−0.28	0.15 0.14	dir 000	+5.6		0.029	~0.3	3.7	20	6.42	22,000	100 (20 K)
IV-VI	PbS	0.29	0.37	dir 111	+4	−7	0.1	0.1	3.7	170	5.936	550	600
IV-VI	PbSe	0.15	0.26	dir 111	+4	−8	m_l 0.07 m_t 0.039	m_l 0.06 m_t 0.03		250	6.124	1,020	930
IV-VI	PbTe	0.19	0.29	dir 111	+4	−9	m_l 0.24 m_t 0.02	m_l 0.3 m_t 0.02	3.8	412	6.460	1,620	750
IV-VI	SnTe	0.3	0.18	dir 111							6.328		

[1]The data was gathered from many sources, primarily the following: C. Benoit-à-la-Guillaume et al., *Selected Constants Relative to Semiconductors*, Pergamon (1961); *Solids Under Pressure*, ed. W. Paul and D. M. Warschauer, McGraw-Hill (1963), p. 226; J. Tauc, *Progress in Semiconductors*, 9, 120 (1965); D. Long, *Energy Bands in Semiconductors*, Wiley (1968); S. Shionoya, "Luminescence of Lattices of the ZnS Type," *Luminescence of Organic Solids*, ed. P. Goldberg, Academic Press (1966), p. 206; G. Giesecke, "Lattice Constants," *Semiconductors and Semimetals*, Academic Press 2, 73 (1966); and a number of more recent papers. Where conflicting values appeared, the most recent data was use. Many parameters which depend on the purity of the semiconductor are subject to change as material technology improves.

†Depends on polytype.

‡Calculated value.

table 3-1 ***Ideal-work requirements for the liquefaction of gases beginning at 70°F and 1 atm***

Gas	*Normal boiling point, °R*		*Ideal work of liquefaction $-\dot{W}_i/\dot{m}$, Btu/lb$_m$*
Helium, He[4]	7.60		2870
Hydrogen, H_2	36.7		5002
Neon, Ne	48.8		557.5
Nitrogen, N_2	139.2	77°K	321.0
Air	141.8	78.7	308.6
Carbon monoxide, CO	146.9	81.5	320.7
Fluorine, F_2	153.6	85.4	206.6
Argon, A	157.1	87.5	200.9
Oxygen, O_2	162.4	90.2	204.7
Methane, CH_4	201.0	112.2	452.7
Carbon tetrafluoride, CF_4	261.3	145	73.9
Ethane, C_2H_6	332.1		142.4
Ammonia, NH_3	431.6		100.2

TABLE XI — **COPPER vs. COPPER-NICKEL** (Copper-Constantan) — TYPE T

Temperature in Degrees F — **Reference Junction at 32°F**

THERMOELECTRIC VOLTAGE IN ABSOLUTE MILLIVOLTS

DEG F	0	1	2	3	4	5	6	7	8	9	10	DEG F
-190	-4.009	-4.023	-4.037	-4.051	-4.065	-4.079	-4.093	-4.107	-4.121	-4.135	-4.149	-190
-180	-3.866	-3.879	-3.894	-3.908	-3.923	-3.937	-3.951	-3.966	-3.980	-3.994	-4.009	-180
-170	-3.717	-3.732	-3.746	-3.761	-3.776	-3.791	-3.806	-3.820	-3.835	-3.850	-3.864	-170
-160	-3.565	-3.580	-3.596	-3.611	-3.626	-3.641	-3.656	-3.671	-3.687	-3.702	-3.717	-160
-150	-3.410	-3.425	-3.441	-3.457	-3.472	-3.488	-3.503	-3.519	-3.534	-3.550	-3.565	-150
-140	-3.251	-3.267	-3.283	-3.299	-3.315	-3.331	-3.347	-3.362	-3.378	-3.394	-3.410	-140
-130	-3.089	-3.105	-3.121	-3.138	-3.154	-3.170	-3.186	-3.203	-3.219	-3.235	-3.251	-130
-120	-2.923	-2.939	-2.956	-2.973	-2.989	-3.006	-3.023	-3.039	-3.056	-3.072	-3.089	-120
-110	-2.755	-2.771	-2.788	-2.805	-2.822	-2.838	-2.855	-2.872	-2.889	-2.906	-2.923	-110
-100	-2.581	-2.598	-2.616	-2.633	-2.650	-2.667	-2.685	-2.702	-2.719	-2.736	-2.753	-100
-90	-2.405	-2.422	-2.440	-2.458	-2.475	-2.493	-2.511	-2.528	-2.546	-2.563	-2.581	-90
-80	-2.225	-2.243	-2.261	-2.279	-2.297	-2.315	-2.333	-2.351	-2.369	-2.387	-2.405	-80
-70	-2.042	-2.061	-2.079	-2.098	-2.116	-2.134	-2.152	-2.171	-2.189	-2.207	-2.225	-70
-60	-1.856	-1.875	-1.894	-1.912	-1.931	-1.950	-1.968	-1.987	-2.005	-2.024	-2.042	-60
-50	-1.667	-1.686	-1.705	-1.724	-1.743	-1.762	-1.781	-1.800	-1.819	-1.838	-1.856	-50
-40	-1.475	-1.494	-1.513	-1.533	-1.552	-1.571	-1.591	-1.610	-1.629	-1.648	-1.667	-40
-30	-1.279	-1.299	-1.319	-1.338	-1.358	-1.377	-1.397	-1.416	-1.436	-1.455	-1.475	-30
-20	-1.081	-1.101	-1.121	-1.141	-1.160	-1.180	-1.200	-1.220	-1.240	-1.260	-1.279	-20
-10	-0.879	-0.899	-0.920	-0.940	-0.960	-0.980	-1.000	-1.021	-1.041	-1.061	-1.081	-10
0	-0.674	-0.695	-0.716	-0.736	-0.757	-0.777	-0.798	-0.818	-0.838	-0.859	-0.879	0
DEG F	0	1	2	3	4	5	6	7	8	9	10	DEG F
0	-0.674	-0.654	-0.633	-0.613	-0.592	-0.571	-0.550	-0.529	-0.509	-0.488	-0.467	0
10	-0.467	-0.446	-0.425	-0.404	-0.383	-0.362	-0.341	-0.320	-0.299	-0.277	-0.256	10
20	-0.256	-0.235	-0.214	-0.193	-0.171	-0.150	-0.129	-0.107	-0.086	-0.064	-0.043	20
30	-0.043	-0.022	0.000	0.022	0.043	0.065	0.086	0.108	0.130	0.151	0.173	30
40	0.173	0.195	0.216	0.238	0.260	0.282	0.303	0.325	0.347	0.369	0.391	40
50	0.391	0.413	0.435	0.457	0.479	*0.501	0.523	0.545	0.567	0.589	0.611	50
60	0.611	0.634	0.656	0.678	0.700	0.722	0.745	0.767	0.789	0.812	0.834	60
70	0.834	0.857	0.879	0.902	0.924	0.947	0.969	0.992	1.014	1.037	1.060	70
80	1.060	1.082	1.105	1.128	1.151	1.173	1.196	1.219	1.242	1.265	1.288	80
90	1.288	1.311	1.334	1.357	1.380	1.403	1.426	1.449	1.472	1.495	1.518	90
100	1.518	1.542	1.565	1.588	1.611	1.635	1.658	1.681	1.705	1.728	1.752	100
110	1.752	1.775	1.799	1.822	1.846	1.869	1.893	1.917	1.940	1.964	1.988	110
120	1.988	2.011	2.035	2.059	2.083	2.107	2.131	2.154	2.178	2.202	2.226	120
130	2.226	2.250	2.274	2.298	2.322	2.347	2.371	2.395	2.419	2.443	2.467	130
140	2.467	2.492	2.516	2.540	2.565	2.589	2.613	2.638	2.662	2.687	2.711	140
150	2.711	2.736	2.760	2.785	2.809	2.834	2.859	2.883	2.908	2.933	2.958	150
160	2.958	2.982	3.007	3.032	3.057	3.082	3.107	3.131	3.156	3.181	3.206	160
170	3.206	3.231	3.256	3.281	3.307	3.332	3.357	3.382	3.407	3.432	3.458	170
180	3.458	3.483	3.508	3.533	3.559	3.584	3.609	3.635	3.660	3.686	3.711	180
190	3.711	3.737	3.762	3.788	3.813	3.839	3.864	3.890	3.916	3.941	3.967	190
200	3.967	3.993	4.019	4.044	4.070	4.096	4.122	4.148	4.174	4.199	4.225	200
210	4.225	4.251	4.277	4.303	4.329	4.355	4.381	4.408	4.434	4.460	4.486	210
220	4.486	4.512	4.538	4.565	4.591	4.617	4.643	4.670	4.696	4.722	4.749	220
230	4.749	4.775	4.801	4.828	4.854	4.881	4.907	4.934	4.960	4.987	5.014	230
240	5.014	5.040	5.067	5.093	5.120	5.147	5.174	5.200	5.227	5.254	5.281	240
250	5.281	5.307	5.334	5.361	5.388	5.415	5.442	5.469	5.496	5.523	5.550	250
260	5.550	5.577	5.604	5.631	5.658	5.685	5.712	5.739	5.767	5.794	5.821	260
270	5.821	5.848	5.875	5.903	5.930	5.957	5.985	6.012	6.039	6.067	6.094	270
280	6.094	6.122	6.149	6.177	6.204	6.232	6.259	6.287	6.314	6.342	6.369	280
290	6.369	6.397	6.425	6.452	6.480	6.508	6.536	6.563	6.591	6.619	6.647	290
300	6.647	6.675	6.702	6.730	6.758	6.786	6.814	6.842	6.870	6.898	6.926	300
310	6.926	6.954	6.982	7.010	7.038	7.066	7.094	7.122	7.151	7.179	7.207	310
320	7.207	7.235	7.263	7.292	7.320	7.348	7.377	7.405	7.433	7.462	7.490	320
330	7.490	7.518	7.547	7.575	7.604	7.632	7.661	7.689	7.718	7.746	7.775	330
340	7.775	7.804	7.832	7.861	7.889	7.918	7.947	7.975	8.004	8.033	8.062	340
350	8.062	8.090	8.119	8.148	8.177	8.206	8.235	8.264	8.292	8.321	8.350	350
360	8.350	8.379	8.408	8.437	8.466	8.495	8.524	8.553	8.583	8.612	8.641	360
370	8.641	8.670	8.699	8.728	8.757	8.787	8.816	8.845	8.874	8.904	8.933	370
380	8.933	8.962	8.992	9.021	9.050	9.080	9.109	9.139	9.168	9.198	9.227	380
390	9.227	9.257	9.286	9.316	9.345	9.375	9.404	9.434	9.464	9.493	9.523	390
400	9.523	9.553	9.582	9.612	9.642	9.671	9.701	9.731	9.761	9.791	9.820	400
410	9.820	9.850	9.880	9.910	9.940	9.970	10.000	10.030	10.060	10.090	10.120	410
420	10.120	10.150	10.180	10.210	10.240	10.270	10.300	10.330	10.360	10.390	10.420	420
430	10.420	10.451	10.481	10.511	10.541	10.572	10.602	10.632	10.662	10.693	10.723	430
440	10.723	10.753	10.784	10.814	10.845	10.875	10.905	10.936	10.966	10.997	11.027	440
450	11.027	11.058	11.088	11.119	11.149	11.180	11.211	11.241	11.272	11.302	11.333	450
460	11.333	11.364	11.394	11.425	11.456	11.487	11.517	11.548	11.579	11.610	11.640	460
470	11.640	11.671	11.702	11.733	11.764	11.795	11.826	11.856	11.887	11.918	11.949	470
480	11.949	11.980	12.011	12.042	12.073	12.104	12.135	12.166	12.198	12.229	12.260	480
490	12.260	12.291	12.322	12.353	12.384	12.416	12.447	12.478	12.509	12.540	12.572	490
500	12.572	12.603	12.634	12.666	12.697	12.728	12.760	12.791	12.822	12.854	12.885	500
510	12.885	12.917	12.948	12.979	13.011	13.042	13.074	13.105	13.137	13.168	13.200	510
520	13.200	13.232	13.263	13.295	13.326	13.358	13.390	13.421	13.453	13.485	13.516	520
530	13.516	13.548	13.580	13.611	13.643	13.675	13.707	13.739	13.770	13.802	13.834	530
540	13.834	13.866	13.898	13.930	13.961	13.993	14.025	14.057	14.089	14.121	14.153	540
550	14.153	14.185	14.217	14.249	14.281	14.313	14.345	14.377	14.409	14.441	14.474	550
560	14.474	14.506	14.538	14.570	14.602	14.634	14.666	14.699	14.731	14.763	14.795	560
570	14.795	14.828	14.860	14.892	14.924	14.957	14.989	15.021	15.054	15.086	15.118	570
580	15.118	15.151	15.183	15.216	15.248	15.281	15.313	15.345	15.378	15.410	15.443	580
590	15.443	15.475	15.508	15.540	15.573	15.605	15.638	15.671	15.703	15.736	15.769	590
600	15.769	15.801	15.834	15.866	15.899	15.932	15.965	15.997	16.030	16.063	16.096	600
610	16.096	16.128	16.161	16.194	16.227	16.259	16.292	16.325	16.358	16.391	16.424	610
620	16.424	16.457	16.490	16.523	16.555	16.588	16.621	16.654	16.687	16.720	16.753	620
630	16.753	16.786	16.819	16.852	16.886	16.919	16.952	16.985	17.018	17.051	17.084	630
640	17.084	17.117	17.150	17.184	17.217	17.250	17.283	17.316	17.350	17.383	17.416	640
650	17.416	17.450	17.483	17.516	17.550	17.583	17.616	17.649	17.683	17.716	17.750	650
660	17.750	17.783	17.816	17.850	17.883	17.917	17.950	17.984	18.017	18.051	18.084	660
670	18.084	18.118	18.151	18.185	18.218	18.252	18.285	18.319	18.353	18.386	18.420	670
680	18.420	18.454	18.487	18.521	18.555	18.588	18.622	18.656	18.690	18.724	18.757	680
690	18.757	18.791	18.824	18.858	18.892	18.926	18.960	18.993	19.027	19.061	19.095	690
700	19.095	19.129	19.163	19.197	19.230	19.264	19.298	19.332	19.366	19.400	19.434	700
710	19.434	19.468	19.502	19.536	19.570	19.604	19.638	19.672	19.706	19.740	19.774	710
720	19.774	19.808	19.842	19.877	19.911	19.945	19.979	20.013	20.047	20.081	20.116	720
730	20.116	20.150	20.184	20.218	20.252	20.287	20.321	20.355	20.389	20.423	20.458	730
740	20.458	20.492	20.526	20.560	20.595	20.629	20.663	20.698	20.732	20.766	20.801	740
750	20.801	20.835	20.869									750
DEG F	0	1	2	3	4	5	6	7	8	9	10	DEG F

* CONVERTED FROM DEGREES CELSIUS (1968).

TYPE T

T (24B) °F

COPPER-CONSTANTAN THERMOCOUPLES

Degrees Fahrenheit (Int. 1948) Cold End at 75° F (EMF at 32° F = –0.944 mv)

EMF IN ABSOLUTE MILLIVOLTS

°F.	0	–5	–10	–15	–20	–25	–30	–35	–40	–45	–50	–55	–60	–65	–70	–75	–80	–85	–90	–95	°F.
–300	–6.228	–6.276	–6.323																		–300
–200	–5.055	–5.123	–5.190	–5.256	–5.321	–5.385	–5.448	–5.510	–5.571	–5.632	–5.691	–5.749	–5.807	–5.863	–5.918	–5.973	–6.025	–6.078	–6.129	–6.179	–200
–100	–3.503	–3.589	–3.674	–3.758	–3.841	–3.924	–4.006	–4.087	–4.167	–4.245	–4.324	–4.401	–4.477	–4.553	–4.628	–4.701	–4.773	–4.845	–4.916	–4.986	–100
0	–1.614	–1.715	–1.816	–1.917	–2.016	–2.115	–2.214	–2.311	–2.407	–2.503	–2.598	–2.692	–2.786	–2.878	–2.970	–3.061	–3.151	–3.240	–3.329	–3.416	– 0

°F.	0	5	10	15	20	25	30	35	40	45	50	55	60	65	70	75	80	85	90	95	°F.
0	–1.614	–1.511	–1.407	–1.303	–1.198	–1.093	–0.986	–0.880	–0.773	–0.664	–0.555	–0.445	–0.335	–0.224	–0.112	0.000	0.113	0.227	0.342	0.457	0
100	0.573	0.689	0.807	0.925	1.043	1.163	1.282	1.402	1.523	1.645	1.767	1.891	2.014	2.138	2.263	2.388	2.514	2.640	2.768	2.895	100
200	3.023	3.152	3.281	3.411	3.542	3.673	3.805	3.936	4.070	4.203	4.336	4.471	4.606	4.741	4.877	5.013	5.150	5.288	5.426	5.564	200
300	5.703	5.842	5.982	6.122	6.264	6.405	6.547	6.689	6.832	6.976	7.120	7.263	7.408	7.553	7.698	7.844	7.991	8.138	8.285	8.432	300
400	8.581	8.730	8.879	9.029	9.179	9.329	9.479	9.630	9.782	9.934	10.086	10.239	10.392	10.546	10.699	10.853	11.009	11.164	11.319	11.474	400
500	11.631	11.788	11.944	12.102	12.259	12.418	12.576	12.734	12.894	13.053	13.213	13.373	13.533	13.693	13.855	14.017	14.178	14.340	14.503	14.666	500
600	14.829	14.993	15.157	15.320	15.485	15.649	15.814	15.980	16.145	16.311	16.477	16.644	16.810	16.977	17.145	17.313	17.481	17.649	17.817	17.986	600
700	18.156	18.325	18.495	18.664	18.835	19.005	19.176	19.347	19.519	19.690	19.861										700

T (24B) °C

COPPER-CONSTANTAN THERMOCOUPLES

Degrees Celsius (Centigrade, Int. 1948) Cold End at 25° C (EMF at 0° C = –0.990 mv)

EMF IN ABSOLUTE MILLIVOLTS

°C.	0	–5	–10	–15	–20	–25	–30	–35	–40	–45	–50	–55	–60	–65	–70	–75	–80	–85	–90	–95	°C.
–100	–4.339	–4.478	–4.614	–4.747	–4.877	–5.004	–5.128	–5.249	–5.367	–5.482	–5.593	–5.702	–5.807	–5.909	–6.008	–6.103	–6.195	–6.284	–6.369		–100
0	–0.990	–1.181	–1.370	–1.557	–1.741	–1.923	–2.102	–2.279	–2.453	–2.625	–2.794	–2.961	–3.125	–3.286	–3.445	–3.601	–3.754	–3.904	–4.052	–4.197	0

°C.	0	5	10	15	20	25	30	35	40	45	50	55	60	65	70	75	80	85	90	95	°C.
0	–0.990	–0.797	–0.601	–0.403	–0.203	0.000	0.204	0.411	0.620	0.831	1.045	1.260	1.477	1.697	1.918	2.142	2.367	2.594	2.823	3.054	0
100	3.287	3.522	3.759	3.997	4.237	4.479	4.722	4.967	5.214	5.463	5.713	5.964	6.218	6.472	6.729	6.988	7.246	7.507	7.769	8.032	100
200	8.298	8.565	8.833	9.103	9.373	9.645	9.919	10.193	10.469	10.745	11.025	11.304	11.585	11.867	12.150	12.435	12.720	13.007	13.295	13.583	200
300	13.874	14.165	14.457	14.750	15.045	15.340	15.636	15.934	16.232	16.531	16.831	17.133	17.435	17.737	18.042	18.347	18.652	18.959	19.267	19.575	300
400	19.884																				400

T (24B)

END

DATE

FILMED

APR 7 1980